Infrared Behaviour Of QCD Observables

A thesis presented for the degree of

Doctor of Philosophy

by

David M. Howe

Institute for Particle Physics Phenomenology

University of Durham

September 2004

Abstract

The perturbation series created through the method of Feynman diagrams can be used to calculate experimental quantities to a good level of accuracy in many cases. The method of obtaining such a series and relating it to an observable for a QFT such as QCD is outlined. This is followed by an introduction into some of the complications of QFT's such as renormalisation, which leads to scale dependence for dimensionless quantities, and the factorial growth of perturbation series. The problem, due to the Landau pole, of defining the QCD perturbation series for the ratio $R_{e^+e^-}$ in the infrared is approached through a contour improved or analytic perturbation theory (CIPT or APT) series. For a fixed-order truncation such a series will smoothly freeze to the value $2/b$ where $b = (33 - 2N_f)/6$ is the first beta function coefficient. This is extended to considering all-orders perturbation theory through Borel summation which is used to evaluate the series factorial growth. This, along with the non-perturbative operator product expansion (OPE), is shown to be well-defined and finite for all values of the energy scale. The perturbative component again freezes to $2/b$. A phenomenological comparison with low energy data is performed using a smeared $R_{e^+e^-}$ and a good agreement is found.

A similar approach is developed for the ratio R_τ. This case has an added complication due to a non-freezing ambiguous term that arises when one tries to perform CIPT/APT. The apparent ambiguity is fixed through Borel summation. A comparison with experimental data allows the QCD parameter $\Lambda_{\overline{MS}}$ to be evaluated for three flavours of quark, with the result $\Lambda_{\overline{MS}} = 382^{+18}_{-20}$ MeV obtained from a fixed-order calculation and $\Lambda_{\overline{MS}} = 340^{+12}_{-13}$ MeV from an all-orders calculation.

Acknowledgements

My thanks to all those who have helped me through my time here. Special thanks must go to my supervisor Chris Maxwell, who has been friendly and helpful at all times.

I am happy to have worked in an environment where I have made many friends, in particular Peter Williams and Jonathan Levell, who spent their entire Ph.D's sharing the same office with me. Thanks also to Adam Millican-Slater, who along with Jonathan were excellent people to live with.

Thanks must also go to the many people I have enjoyed a few beers with, they are too many to mention, but in particular Ian, Anthony, Jessica, Kate, Ben, Steve, Fi, Stef, and Maria.

I gratefully acknowledge the support from PPARC.

Finally thanks to my family for their constant support and encouragement.

Declaration

I declare that no material in this thesis has been previously been submitted for a degree at this or any other university.
All the research in this thesis has been carried out in collaboration with Dr C.J. Maxwell, and with the exception of the research in chapter 6, has appeared in

1. D.M. Howe and C.J. Maxwell, Phys. Lett. **B541** (2002) 129.

2. D.M. Howe and C.J. Maxwell, Phys. Rev. **D70** (2004) 014002.

Contents

List of Figures

Outline

This thesis utilises the theory of Quantum Chromodynamics and outlines methods of performing perturbative calculations in conditions where it is often hard to make sense of such calculations, namely the low energy (infrared) limit, and for a series considered in all-orders of perturbation theory.

The first chapter introduces Quantum Chromodynamics as a Quantum field theory, showing how a field theory is defined through its Lagrangian and how physical quantities can be related to a Green's function that is calculated using Feynman diagrams determined by the Lagrangian.

Chapter 2 deals with the apparently infinite results that come from naively performing higher order calculations. The problem is shown to be solvable using renormalisation, where the divergences are removed by the rescaling of the parameters of the theory. The problem of scheme dependence is discussed, and the renormalisation group is introduced. The relation between the coupling and a full perturbation series with respect to certain energy scales is introduced.

Chapter 3 introduces the factorial growth found in perturbation series coefficients and outlines how to treat the series as asymptotic to a finite result via Borel summation. The leading factorial growth of some perturbation series is introduced and is evaluated.

Chapter 4 outlines a method of obtaining a finite series for in the low energy limit for a particular observable, the R-ratio, and then proceeds to discuss its divergent series, showing that such a series can be considered in the infrared limit. The fifth chapter uses the methods of chapter 4 to compare data with theory in the low energy region.

Chapter 6 continues the approach for the more complicated case of the hadronic branching fraction for the τ lepton. Finally the thesis is summarised in the conclusions.

Chapter 1

Quantum Field Theory

1.1 Introduction to quarks and gluons

Quantum field theory has been used to model the interactions of elementary particles with great success. This introductory section will briefly introduce Quantum Chromodynamics (QCD).

QCD is a theory of quarks and gluons; these are the two classes of particles that make up the protons and neutrons that form all the atomic nuclei. As well as forming the nucleons, these QCD particles make up a whole family of particles known as hadrons. The hadrons can all interact via the strong nuclear force, which is the residual effect of the interactions between the quarks and gluons of different hadrons. In fact this residual force is the force that holds all atomic nuclei together.

The quarks and gluons are always bound within hadrons, a solitary quark or gluon has never been observed.

Quarks have an electric charge and so they can be detected through electromagnetic interactions with other charged particles. If an electron is fired at a hadron it can interact with a quark. The way in which the electron behaves will then give information about the nature of the quark, e.g. the frequency with which interactions occur can tell how strong the electric charge of the quarks is.

The gluons are required to mediate the QCD interactions between quarks, so if the gluons were left out of the theory nuclei and hadrons would have no force holding them together. In electromagnetism particles with an electric charge can interact electromagnetically; similarly in QCD there is a colour charge which comes in three types often called red, green and blue. In electromagnetism the mediating particle, the photon, has no electric charge; however, in QCD the gluons have a colour charge which is a combination of the colour charges of the quarks. This leads to self interactions for the gluon, making the theory of QCD more complex than its electromagnetic counterpart Quantum Electrodynamics (QED).

The work presented in this thesis is concerned with relating results obtained from the theory (QCD) to measured observables from experiments. This tests QCD and makes it possible to calculate the strength of QCD interactions.

1.2 Gauge invariance and Noether's theorem

Quantum field theory (QFT) is used to describe all interactions except gravity between fundamental particles. There are many texts on this subject, including those in references [1], [2].

A field theory is partially defined by the type of value the field takes at every point in spacetime; for example classical electromagnetism has a vector field that takes the value of a vector everywhere. The action denoted by S completes the definition. The action is given as the integral of the Lagrangian density

$$S = \int \mathcal{L} d^4x \ . \tag{1.1}$$

This density, $\mathcal{L}$, is a function of the fields (ϕ_j), and their derivatives with respect to space and time ($\partial\phi_j/\partial x^\mu$)

$$\mathcal{L} = \mathcal{L}\left(\phi_j, \frac{\partial\phi_j}{\partial x^\mu}\right) \ . \tag{1.2}$$

The subscript j labels the different fields, and the x^μ are space-time co-ordinates, x^0 is time and x^1, x^2, x^3 are the three space co-ordinates. The theory is constrained by making the action stationary with respect to a change in the field(s); this leads to the Euler-Lagrange equations,

$$\partial_\mu \left(\frac{\partial \mathcal{L}}{\partial(\partial_\mu \phi_j)} \right) - \frac{\partial \mathcal{L}}{\partial \phi_j} = 0 \ , \tag{1.3}$$

where ∂_μ denotes the partial derivative with respect to x^μ, $\partial_\mu = (\partial/\partial t, -\underline{\nabla})$. The Euler-Lagrange equations can relate the field to relativistic quantum mechanics. For example the Lagrangian density

$$\mathcal{L} = \frac{1}{2}\partial_\mu \phi \partial^\mu \phi - \frac{1}{2}m^2\phi^2 \ , \tag{1.4}$$

has the Euler-Lagrange equation $(\Box + m^2)\phi = 0$, where $\Box = \partial_\mu \partial^\mu$. This is the Klein-Gordon wave equation for a free relativistic particle.

The Lagrangian density

$$\mathcal{L} = \bar{\psi}(i\gamma^\mu \partial_\mu - m)\psi \tag{1.5}$$

gives the Dirac equation and its conjugate, where the matrices γ^μ obey the anti-commutation relation $\{\gamma^\mu, \gamma^\nu\} = 2g^{\mu\nu}$, and $\bar{\psi} = \psi^\dagger \gamma^0$. In this case the field is a spinor field and can be represented by a 4×1 matrix when in four dimensions.

The electromagnetic field equations can be obtained from the Lagrangian density

$$\mathcal{L} = -\frac{1}{4}F^{\mu\nu}F_{\mu\nu} + j^\mu A_\mu \ , \tag{1.6}$$

where

$$F_{\mu\nu} = \partial_\mu A_\nu - \partial_\nu A_\mu \ , \tag{1.7}$$

is the field strength tensor, and j^μ is the electromagnetic current density. The field here is a vector field, and takes the value of a four-vector at every spacetime point.

Using the Euler-Lagrange equations a conserved current can be found provided there is a continuous global symmetry for the field, i.e. the transformation

$$\phi(x) \to \phi'(x') = \phi'(x) \tag{1.8}$$

does not alter the action. Noether's theorem states that there is a conserved current for every continuous global symmetry transformation. Consider the

Lagrangian density for complex scalar field theory

$$\mathcal{L} = \partial_\mu \phi^* \partial^\mu \phi - m^2 \phi^2 \; . \tag{1.9}$$

This is invariant under the transformation $\phi \to \phi' = \phi e^{i\alpha}$ for some constant α. For an infinitesimal α, $\phi' = \phi + i\alpha\phi$. For this transformation the Lagrangian density is changed by

$$\frac{\partial \mathcal{L}}{\partial \phi} i\alpha\phi + \frac{\partial \mathcal{L}}{\partial(\partial_\mu \phi)} i\alpha \partial_\mu \phi + \text{complex conjugate} \; . \tag{1.10}$$

This equals zero up to an α^2 term as $\mathcal{L}$ is invariant under the transformation. Using the Euler-Lagrange equation for the field the terms with α to the first power are

$$\alpha \partial_\mu \left(\frac{\partial \mathcal{L}}{\partial(\partial_\mu \phi)} i\phi \right) + \text{complex conjugate} = 0 \; . \tag{1.11}$$

This gives the conserved current density

$$\begin{aligned} j_\mu &= i(\phi \partial_\mu \phi^* - \phi^* \partial_\mu \phi) \; , \\ \partial_\mu j^\mu &= 0 \; . \end{aligned} \tag{1.12}$$

1.3 Local gauge transformations

Consider the Lagrangian density for a Dirac field

$$\mathcal{L} = \bar{\psi}(i\gamma_\mu \partial^\mu - m)\psi \; . \tag{1.13}$$

The Euler-Lagrange equation for the field ψ is the Dirac equation, which describes free fermions in relativistic quantum mechanics. This Lagrangian is almost invariant under the local transformation $\psi \to \psi e^{i\alpha(x)}$; this transformation produces the extra term $\bar{\psi}\gamma_\mu(\partial^\mu \alpha)\psi$ in $\mathcal{L}$. If ∂_μ is replaced by the term $\partial_\mu + ieA_\mu$ in Eq.(1.13), then the Lagrangian density is invariant under the transformation $\psi \to \psi e^{i\alpha(x)}$ provided that the new field obeys the transformation $A_\mu \to A_\mu - \frac{1}{e}\partial_\mu \alpha$. The field A_μ could be the electromagnetic field where for a free field

$$\begin{aligned}\mathcal{L} &= -\frac{1}{4}F^{\mu\nu}F_{\mu\nu} \\ F_{\mu\nu} &= \partial_\mu A_\nu - \partial_\nu A_\mu \ ,\end{aligned} \tag{1.14}$$

which is invariant under the transformation $A_\mu \rightarrow A_\mu - \frac{1}{e}\partial_\mu \alpha$. Combining the modified Eq.(1.13) and Eq.(1.14) the Euler-Lagrange equation for A_μ is

$$\begin{aligned}\partial_\mu F^{\mu\nu} &= ej^\nu \ , \\ j^\nu &= \bar{\psi}\gamma^\nu\psi \ .\end{aligned} \tag{1.15}$$

Eq.(1.15) gives Maxwell's inhomogeneous equations in the presence of a current. This current can be shown to be conserved through Noether's theorem. The magnitude of the charge is given by the constant e. If a different charge is desired, as might be the case for several Dirac fields, then the field's charge Q appears in the transformation for the Dirac field $\psi \rightarrow \psi e^{iQ\alpha(x)}$ and in the Lagrangian density $\partial_\mu + ieQA_\mu$. The electron for example will have a value of $Q = -1$.

The Euler-Lagrange equation for the Dirac field will now give

$$(iD_\mu\gamma^\mu - m)\psi = 0 \ , \tag{1.16}$$

where

$$D_\mu = \partial_\mu + ieQA_\mu \ . \tag{1.17}$$

The symbol D is known as the covariant derivative.

Changing from separate field theories of free fields, and demanding invariance under the local gauge transformation has introduced interactions given by a term proportional to $j^\mu A_\mu$ which appears in the Lagrangian density in addition to the free (non-interacting) field theory terms. This describes Quantum Electrodynamics (QED), the quantum field theory of electromagnetism,

$$\mathcal{L}_{QED} = -\frac{1}{4}F^{\mu\nu}F_{\mu\nu} + \bar{\psi}(i\gamma^\mu D_\mu - m)\psi \ . \tag{1.18}$$

The Lagrangian density in Eq.(1.14) shows that the electromagnetic field is invariant under the gauge transformation $A_\mu \rightarrow A_\mu - \frac{1}{e}\partial_\mu \alpha$. If the electromagnetic field is transformed in such a way with $\frac{1}{e}\Box\alpha = \partial_\mu A^\mu$, then after the transformation the field obeys $\partial_\mu A^\mu = 0$. This relation will hold under further transformations provided that $\Box\alpha = 0$. Choosing the field so that $\partial_\mu A^\mu = 0$ is known as the Lorentz gauge.

1.4 Particle states from field theory

A field operator can be represented by an inverse Fourier transform

$$\phi(\vec{x}, t) = \int \frac{d^3k}{(2\pi)^3} \tilde{\phi}(\vec{k}, t) e^{i\vec{k}\cdot\vec{x}} \; . \tag{1.19}$$

When the field is quantised the Fourier transform can be related to creation and annihilation operators. Using free real scalar field theory as an example

$$\tilde{\phi}(\vec{k}, t) = \frac{1}{2E_k}\left(a(k)e^{-iE_k t} + b(k)e^{iE_k t}\right) \; , \tag{1.20}$$

where $b(k_0, \vec{k}) = a^\dagger(k_0, -\vec{k})$ gives $\phi = \phi^*$. The Klein-Gordon equation sets $E_k^2 = \vec{k}^2 + m^2$. A state with particles of momenta $p_1 \cdots p_n$ is represented by

$$\begin{aligned} a^\dagger(p_1)\cdots a^\dagger(p_n)|0> &= |p_1 \cdots p_n> \\ <0|a(p_1)\cdots a(p_n) &= <p_1 \cdots p_n| \; . \end{aligned} \tag{1.21}$$

The state $|0>$ is the vacuum and is the state that is annihilated by the operator $a(p)$ for any momentum p. When acted upon by operators to determine the state's properties, such as the Hamiltonian to determine the state's energy, the states share the corresponding properties associated with the particles they represent. These states have the normalisation

$$\begin{aligned} &< p'_1 \cdots p'_n | p_1 \cdots p_n > \\ &\qquad = (2\pi)^{3n} 2E_{p_1} \cdots 2E_{p_n} \delta^{(3)}(\vec{p_1} - \vec{p'_1}) \cdots \delta^{(3)}(\vec{p_n} - \vec{p'_n}) \; . \end{aligned} \tag{1.22}$$

This normalisation comes from the commutation relations between the operators

$$[a(p), a^\dagger(p')] = (2\pi)^3 2E_p \delta^{(3)}(\vec{p} - \vec{p'}) \; . \tag{1.23}$$

For all fields that will be considered there are similar relations between the field operator and the creation and annihilation operators.

1.5 Incoming and Outgoing states

There exist cases where particles can be treated independently and have known momenta, such as incoming and outgoing particles in scattering experiments. In such cases those particles can be represented by states for free particles. In and out states are introduced

$$
\begin{aligned}
|p_1, p_2; in >&= a^{\dagger}_{in}(p_2)|p_1; in >= a^{\dagger}_{in}(p_2)a^{\dagger}_{in}(p_1)|0> \\
< p_1, p_2; in| &=< p_1; in|a_{in}(p_2) =< 0|a_{in}(p_1)a_{in}(p_2) \ ,
\end{aligned}
\tag{1.24}
$$

with the $a, a^{\dagger}$ operators defined through an inverse Fourier transform. In the case of real scalar field theory

$$
\begin{aligned}
a_{in}(k) &= \lim_{x^0 \to -\infty} \int d^3x [e^{ik\cdot x} i\partial_0 \phi(x) - \phi(x) i\partial_0 e^{ik\cdot x}] \\
a^{\dagger}_{in}(k) &= - \lim_{x^0 \to -\infty} \int d^3x [e^{-ik\cdot x} i\partial_0 \phi(x) - \phi(x) i\partial_0 e^{-ik\cdot x}] \ .
\end{aligned}
\tag{1.25}
$$

Equivalent expressions exist for outgoing states with the time limit taken to be $x^0 \to \infty$. The field used in the inverse transform is for the interacting theory but taken in the limit as time goes to $\pm\infty$.

1.6 Cross sections and decay rates

Matrix elements such as $< k_1 \cdots k_n; out|p_1, p_2; in >$ need to be calculated: evolving the in and out states to the same time introduces the S-matrix S

$$
< k_1 \cdots k_n; out|p_1, p_2; in >=< k_1 \cdots k_n|S|p_1 p_2 > \ , \tag{1.26}
$$

where the states on the right-hand side of the equation are evaluated at the same time.

The transition between initial and final states can be calculated using the S-matrix S. However, experimental interest is in measurable quantities such as decay rates and cross sections. A brief explanation of how one obtains such quantities now follows.

When a beam of particles passes through a static target the number of scattering events ΔN in time Δt in volume ΔV is

$$\Delta N = \sigma \rho \mathfrak{L} \Delta V \Delta t \ . \tag{1.27}$$

Where σ is the cross section, ρ is the particle density of the target, and $\mathfrak{L}$ is the particle luminosity of the beam passing through the volume.

The quantity ΔN is obtained from the S-matrix by summing over the final states one is interested in detecting. Absorbing the normalisation of the incoming states given by Eq.(1.22) into the target density and beam luminosity one obtains

$$\frac{\Delta N}{\rho \mathfrak{L}} = \sum_f \frac{|<f|S|p_1, p_2>|^2}{2m_1 2E_{p_2}|\vec{v}_2|} \ , \tag{1.28}$$

where m_i represents the rest mass of the particle with momentum p_i, and E_{p_i} is the energy of such a particle with velocity $\vec{v}_i$. The laboratory frame has been used, where $\vec{v}_1 = 0$. The normalisation of the initial states has been dealt with explicitly. The normalisation of the final states is dealt with by choosing the sum over all final states to give the total probability equal to one. If $|f>$ represents a possible final state, the unitarity condition $S^\dagger S = 1$ is obtained provided that $\sum_{\text{all } f} |f><f| = 1$. Choosing the outgoing states to be summed over all possible momenta and noting that

$$\int \left(\prod_{i=1}^{n} \frac{d^3 k_i}{(2\pi)^3 2E_{k_i}} \right) |k_1 \cdots k_n><k_1 \cdots k_n|q_1 \cdots q_n> = |q_1 \cdots q_n> \ , \tag{1.29}$$

one has the sum over final states that gives unitarity.

The cross section to be obtained from Eq.(1.27) is given by

$$\prod_{i=1}^{n} \int \frac{d^3 k_i}{(2\pi)^3 2E_{k_i}} \frac{|<k_1 \cdots k_n|S|p_1 p_2>|^2}{2m_1 2E_{p_2}|\vec{v}_2|} = \sigma \int d^4 x \ , \tag{1.30}$$

where $S^\dagger S = 1$.

Eq.(1.30) is invariant to boosts along the direction of the beam of particles, with the $2m_1 2E_{p_2}|\vec{v}_2|$ term replaced with the more general $2E_{p_1} 2E_{p_2}|\vec{v}_2 - \vec{v}_1|$.

Boosts perpendicular to the beam direction will transform the cross section like an area.

Writing $S = 1 + iT$ we can separate out the case where the incoming and outgoing states are the same, which does not correspond to scattering. Using iT in place of S in Eq.(1.30) gives the desired cross-section. Momentum must be conserved, and it is convenient to write the matrix element in terms of the invariant amplitude M defined to be

$$< k_1 \cdots k_n|T|p_1 p_2 > (2\pi)^4 \delta^{(4)}(p_1 + p_2 - k_1 \cdots - k_n) \\ = M(p_1 p_2 \rightarrow k_1 \cdots k_n) \ . \tag{1.31}$$

This recasts Eq.(1.30) as

$$\sigma = \prod_{i=1}^{n} \int \frac{d^3 k_i}{(2\pi)^3 2E_{k_i}} \\ (2\pi)^4 \delta^{(4)}(p_1 + p_2 - k_1 \cdots - k_n) \frac{|M(p_1 p_2 \rightarrow k_1 \cdots k_n)|^2}{2m_1 2E_{p_2}|\vec{p}_2|/m_2} \ . \tag{1.32}$$

The momentum conservation has now been inserted into the integration over the final state momenta.

With decay rates it is much simpler. Working in the rest frame of the decaying particles, the number of decays is given by an expression analogous to Eq.(1.27)

$$\Delta N = \rho \Gamma \Delta t \Delta V \ . \tag{1.33}$$

The decay rate Γ is the inverse of the mean particle lifetime. Proceeding as for the cross section one obtains

$$\prod_{i=1}^{n} \int \frac{d^3 k}{(2\pi)^3 2E_k} \frac{| < k_1 \cdots k_n|S|p_1 > |^2}{2m_1} = \Gamma \int d^4 x \ . \tag{1.34}$$

1.7 LSZ reduction formula

For a two-particle scattering process the quantity $< k_1 \cdots k_n; out|p_1, p_2; in >$ must be calculated. To calculate this the LSZ reduction formula is used [3]; this relates the matrix element to a Green's function.

Consider two-to-two particle scattering. For simplicity the particles will be the same type of scalar particle represented by a real field. The matrix element is represented by $< p_3, p_4; out|p_1, p_2; in >$, where p_1, p_2 are the 4-momenta of the incoming particles, and p_3, p_4 are 4-momenta for the outgoing particles. We now take these external states to be free fields in the limit where the time is the far future (past) for the outgoing (incoming) particles. For free real scalar field theory the field operator $\phi(x)$ can be expressed as a Fourier transform of the creation and annihilation operators,

$$\phi(x) = \int \frac{d^3k}{(2\pi)^3 2E_k}\left(a(k)e^{-ik\cdot x} + a^{\dagger}(k)e^{ik\cdot x}\right) , \tag{1.35}$$

with the inverse transform

$$a^{(\dagger)}(k) = (-)\int d^3x \left[e^{(-)ik\cdot x} i\partial_0\phi(x) - i\partial_0 e^{(-)ik\cdot x}\phi(x)\right] . \tag{1.36}$$

The final state can be represented as $< p_4|a_{\text{out}}(p_3)$ where the subscript "out" represents an outgoing state. We can re-write the matrix element as

$$\begin{aligned}&< p_4; out|a_{\text{in}}(p_3)|p_1, p_2; in > \\ &\qquad + < p_4; out|(a_{\text{out}}(p_3) - a_{\text{in}}(p_3))|p_1, p_2; in > ,\end{aligned} \tag{1.37}$$

the first term is zero unless one of the incoming states is identical to the outgoing state with momentum p_3; this is ignored, as it does not represent any scattering. In a free field theory the second term would vanish; however, we now take the annihilation operator to be the inverse Fourier transform of an interacting field. In the limit of the far past and the far future the particles will effectively become free and the inverse Fourier transforms give creation and annihilation operators for a free field theory.

Inserting the inverse Fourier transform into the scattering part of the matrix element,

$$\begin{aligned}&\int d^3x e^{ik\cdot x} < p_4; out|(k_0 + i\partial_0\phi(x))|p_1, p_2; in > |_{x^0=-\infty}^{x^0=\infty} \\ &= \int d^4x \partial_0\left(e^{ik\cdot x} < p_4; out|(k_0 + i\partial_0)\phi(x)|p_1, p_2; in >\right) \\ &= i\int d^4x e^{ik\cdot x} < p_4; out|((k_0)^2 + (\partial_0)^2)\phi(x)|p_1, p_2; in > .\end{aligned} \tag{1.38}$$

To avoid an excess of subscripts we have replaced p_3 with k. Using $(k_0)^2 = \vec{k}^2 + m^2$, where m is the mass of the particle with momentum p_3 we can integrate by parts to obtain the following expression for the matrix element

$$\begin{aligned} < p_3, p_4; out|p_1, p_2; in > &=< p_4; out|a_{\text{in}}(p_3)|p_1, p_2; in > \\ &+ i \int d^4x e^{ip_3 \cdot x} < p_4; out|(\Box + m^2)\phi(x)|p_1, p_2; in > \ . \end{aligned} \tag{1.39}$$

Repeating the procedure again for the incoming state with momentum p_1 is analogous to using $a_{\text{out}}(p_3) = a_{\text{in}}(p_3) + a_{\text{out}}(p_3) - a_{\text{in}}(p_3)$ in Eq.(1.37) and leads to the expression,

$$\phi(x)a^{\dagger}_{\text{in}}(p_1) = a^{\dagger}_{\text{out}}(p_1)\phi(x) + \phi(x)a^{\dagger}_{\text{in}}(p_1) - a^{\dagger}_{\text{out}}(p_1)\phi(x) \ . \tag{1.40}$$

The important thing to note here is that in order to extract the part that has no scattering, the "out" operator is on the left and the "in" operator is on the right. When the procedure to express the element in terms of fields is applied the fields must be time ordered, that is the time ordered product of two fields $T[\phi(x)\phi(y)]$ is equal to $\phi(x)\phi(y)$ when $x^0 > y^0$ and $\phi(y)\phi(x)$ when $y^0 > x^0$.

Repeating the procedure one obtains

$$\begin{aligned} &< p_3, p_4; out|p_1, p_2; in >= \text{non-scattering}+ \\ &i^4 \int d^4x_1 d^4x_2 d^4x_3 d^4x_4 e^{-ip_1\cdot x_1 - ip_2\cdot x_2 + ip_3\cdot x_3 + ip_4\cdot x_4}(\Box_{x_1} + m^2)(\Box_{x_2} + m^2) \\ &(\Box_{x_3} + m^2)(\Box_{x_4} + m^2) < 0|T[\phi(x_1)\phi(x_2)\phi(x_3)\phi(x_4)]|0 > , \end{aligned} \tag{1.41}$$

where "non-scattering" refers to those terms that do not have every particle involved in the scattering and so do not contribute to the calculation of two-to-two scattering. The term $< 0|T[\phi(x_1)\phi(x_2)\phi(x_3)\phi(x_4)]|0 >$ is the Green's function mentioned earlier.

This is the LSZ reduction formula for two-to-two particle scattering for a real scalar field theory. In QCD fields that represent the quarks and gluons are of interest. Also an arbitrary number of particles in the final state is required.

In Eq.(1.41) the matrix element of momenta $p_1 \to p_4$ is related to a Green's function of space-time co-ordinates $x_1 \to x_4$.

1.8 Path integrals and interactions

In order to calculate various quantities in QFT, functions of the form

$$< 0|T\phi(x_1)\cdots\phi(x_n)|0 > , \tag{1.42}$$

need to be calculated. This can be related to a path integral Z_ϕ [4]

$$Z_\phi = \int \mathfrak{D}\phi \; e^{iS_\phi} , \tag{1.43}$$

S_ϕ is the action for the field ϕ, and $\mathfrak{D}\phi$ integrates over all values of the field ϕ at every point in space and time.

The relation between Eq.(1.42) and the path integral can be determined by considering the quantity

$$< \phi_f|T\phi(x_1)\cdots\phi(x_n)|\phi_i > \; . \tag{1.44}$$

The states $|\phi_i >$ and $< \phi_f|$ are the initial and final states of the field ϕ, i.e. the field at times $t \to \pm\infty$. Considering the state of the field at each point in space and time separately one obtains

$$< \phi_f|T\phi(x_1)\cdots\phi(x_n)|\phi_i >= \mathcal{C} \int \mathfrak{D}\phi \; \phi(x_1)\cdots\phi(x_n)e^{iS_\phi} \; . \tag{1.45}$$

This is analogous to quantum mechanics, except that there the integral is over all spatial dimensions as opposed to the field at every point in space-time. The constant $\mathcal{C}$ is removed when relating the initial and final states to the energy eigenstates of the Hamiltonian

$$\begin{aligned} |\phi_i >= \sum_n |E_n >< E_n|\phi_i, t = 0 > e^{iE_n t} , \\ \text{where} \qquad H|E_n > = E_n|E_n > \; . \end{aligned} \tag{1.46}$$

Making the substitution $t \to t' = t(1-i\epsilon)$, the initial state exists in the limit as $t \to -\infty$. The extra imaginary exponent damps out all energy states with the exception of the lowest, namely the vacuum. Repeating this procedure for the final state allows Eq.(1.45) to be re-written as

$$< 0|T\phi(x_1)\cdots\phi(x_n)|0 >= \frac{\int \mathfrak{D}\phi\ \phi(x_1)\cdots\phi(x_n)e^{iS_\phi}}{\int \mathfrak{D}\phi\ e^{iS_\phi}} \ . \tag{1.47}$$

The only remaining complication is that the time associated with fields in Eq.(1.47) is a real number multiplied by the complex factor $(1-i\epsilon)$. Taking ϵ to be vanishingly small this leaves Eq.(1.47) unchanged.

To simplify the expression in Eq.(1.47) the functional derivative is introduced

$$\frac{\boldsymbol{\delta}}{\boldsymbol{\delta}J(x)}F[J(y)] = \lim_{\epsilon\to 0}\frac{F[J(y)+\epsilon\delta^{(4)}(x-y)]-F[J(y)]}{\epsilon} \ . \tag{1.48}$$

This defines the functional derivative with respect to $J(x)$, where x is the 4-dimensional space-time co-ordinate.

Introducing a new path integral

$$Z_\phi[J] = \int \mathfrak{D}\phi\ e^{iS_\phi + i\int d^4x J(x)\phi(x)} \ , \tag{1.49}$$

$J(x)\phi(x)$ is a new source term added to the Lagrangian. Taking the functional derivative with respect to $J(x_1)$ gives

$$\frac{\boldsymbol{\delta}}{\boldsymbol{\delta}J(x_1)}Z_\phi[J] = \int \mathfrak{D}\phi\ i\phi(x_1)e^{iS_\phi + i\int d^4x J(x)\phi(x)} \ . \tag{1.50}$$

Eq.(1.47) can now be written as

$$\begin{aligned} &< 0|T\phi(x_1)\cdots\phi(x_n)|0 > \\ &\qquad = \left\{\frac{1}{Z_\phi[J]}(-i)^n\frac{\boldsymbol{\delta}}{\boldsymbol{\delta}J(x_1)}\cdots\frac{\boldsymbol{\delta}}{\boldsymbol{\delta}J(x_n)}Z_\phi[J]\right\}\Bigg|_{J=0} \ . \end{aligned} \tag{1.51}$$

Splitting the Lagrangian density into an interacting $\mathcal{L}_I$ and a non-interacting part $\mathcal{L}_0$, the exponential for the interacting part can be expanded

$$\begin{aligned} Z_\phi[J] &= \int \mathcal{D}\phi\; e^{i\int d^4x \mathcal{L}_I(\phi(x))} e^{iS_0 + i\int d^4x J(x)\phi(x)} \\ &= \int \mathcal{D}\phi\; \left[1 + \sum_{n=1}^{\infty} \frac{1}{n!}\left(i\int d^4x \mathcal{L}_I(\phi(x))\right)^n\right] e^{iS_0 + i\int d^4x J(x)\phi(x)} . \end{aligned} \tag{1.52}$$

Where S_0 is the action for the non-interacting theory.

The interacting Lagrangian is a function of the field, e.g. in ϕ^4 theory it is the field to the fourth power multiplied by a constant. We can then replace $\phi(x)$ in the interacting Lagrangian with $-i\frac{\boldsymbol{\delta}}{\boldsymbol{\delta} J(x)}$

$$\begin{aligned} & Z_\phi[J] \\ &= \left[1 + \sum_{n=1}^{\infty} \frac{1}{n!}\left(i\int d^4x \mathcal{L}_I(-i\frac{\boldsymbol{\delta}}{\boldsymbol{\delta} J(x)})\right)^n\right] \int \mathcal{D}\phi\; e^{iS_0 + i\int d^4x J(x)\phi(x)} . \end{aligned} \tag{1.53}$$

To progress further the free field is chosen to come from a real scalar field theory where it obeys the Klein-Gordon equation. This is chosen as it gives a simple example. Using integration by parts on the action rewrites the path integral in Eq.(1.53) as

$$\int \mathfrak{D}\phi\; \exp\left[-\frac{i}{2}\int d^4x \phi(x)(\Box + m^2)\phi(x) - 2J(x)\phi(x)\right] . \tag{1.54}$$

Defining the function $f(x,y)$ to have the property

$$(\Box_x + m^2)\int d^4y f(x,y)A(y) = A(x) , \tag{1.55}$$

where $A(x)$ is an arbitrary function of x, and making the substitution $\phi(x) = \phi'(x) + \int d^4y f(x,y)J(y)$, one can re-express Eq.(1.54) as

$$\begin{aligned} & \int \mathfrak{D}\phi\; \exp\left[-\frac{i}{2}\int d^4x \phi(x)(\Box + m^2)\phi(x) - 2J(x)\phi(x)\right] \\ &= \int \mathfrak{D}\phi'\; \exp\left[-\frac{i}{2}\int d^4x\; \phi'(x)(\Box + m^2)\phi'(x)\right. \\ &\qquad\qquad \left. - \int d^4x d^4y f(x,y)J(x)J(y)\right] . \end{aligned} \tag{1.56}$$

The ϕ'-dependent part is a constant that will be eliminated when Eq.(1.51) is applied. Combining Eqs.(1.51,1.53,1.56) gives the result

$$
\begin{aligned}
&< 0|T\phi(x_1)\cdots\phi(x_n)|0 > \\
&\quad = \left.\frac{(-i)^n \frac{\boldsymbol{\delta}}{\boldsymbol{\delta} J(x_1)}\cdots\frac{\boldsymbol{\delta}}{\boldsymbol{\delta} J(x_n)}\left[\sum_{n=0}^{\infty}\frac{1}{n!}\left(i\int d^4z\mathcal{L}_I(-i\frac{\boldsymbol{\delta}}{\boldsymbol{\delta} J(z)})\right)^n\right]F[J]}{\left[\sum_{n=0}^{\infty}\frac{1}{n!}\left(i\int d^4z\mathfrak{L}_I(-i\frac{\boldsymbol{\delta}}{\boldsymbol{\delta} J(z)})\right)^n\right]F[J]}\right|_{J=0}, \\
&\text{where}\quad F[J] = \exp\left[\frac{i}{2}\int d^4x d^4y f(x,y)J(x)J(y)\right]. \qquad (1.57)
\end{aligned}
$$

This gives the desired term in Eq.(1.42) as a function of its co-ordinates, the function $f(x,y)$, and the parameters of the interacting Lagrangian.

In order to proceed further the function $f(x,y)$ needs to be explicitly obtained. Eq.(1.55) still holds if $f(x+a,y+a)$ is used in place of $f(x,y)$, $f(x,y)$ is just a function of the difference of its arguments i.e. $f(x-y)$. Relating $f(x-y)$ to its Fourier transform

$$
f(x-y) = \int\frac{d^4p}{(2\pi)^4}\tilde{f}(p)e^{-ip\cdot(x-y)}\,, \qquad (1.58)
$$

and using Eq.(1.55) gives $f(x-y)$ as an integral over momentum

$$
f(x-y) = \int\frac{d^4p}{(2\pi)^4}\frac{1}{m^2-p^2}e^{-ip\cdot(x-y)}\,. \qquad (1.59)
$$

The integral over p^0 runs over all real values of p^0 divided by $1-i\epsilon$, this is due to moving time off the real axis so that Eq.(1.47) could be obtained. Alternatively the displacement off the real axis can be moved into the integrand

$$
f(x-y) = \int\frac{d^4p}{(2\pi)^4}\frac{1}{m^2-p^2-i\epsilon}e^{-ip\cdot(x-y)}\,, \qquad (1.60)
$$

again ϵ is arbitrarily small. It is useful to note that $f(x-y) = f(y-x)$, as its Fourier transform is invariant under $p\to -p$.

At this point the calculation is better understood if Feynman diagrams are used. For this the interacting Lagrangian needs to be chosen: for an example ϕ^4 theory is chosen. Here $\mathfrak{L}_I(\phi) = -\lambda\phi^4/4!$, where λ is a dimensionless parameter of the theory. This means that the calculation for

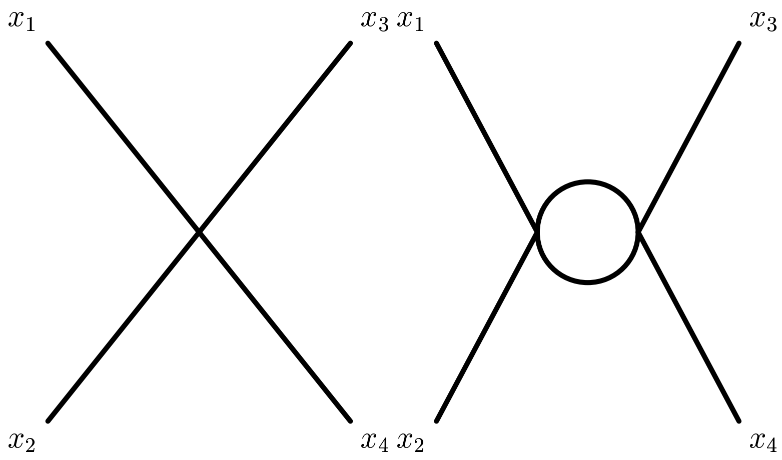

Figure 1.1: Examples of Feynman diagrams with four external lines.

$< 0|T\phi(x_1)\cdots\phi(x_n)|0 >$ will consist of the function $f(x-y)$, the parameter λ and integrals over the dummy co-ordinates. The Feynman diagrams represent all the contributions to the calculation in Eq.(1.57) as diagrams. In this case $-if(x-y)$ is represented as a line connecting the points x and y, and $-i\lambda\int d^4z$ is represented as a vertex of four lines at a point z. Lines between vertices are known as propagators, the propagator is then the two point Green's function. The mathematical expressions for propagators and vertices of various theories can be found in [1]. Contributions to $< 0|T\phi(x_1)\phi(x_2)\phi(x_3)\phi(x_4)|0 >$ include the two diagrams in figure 1.1. The free ends of the external lines represent the co-ordinates $x_1\cdots x_4$. Each diagram should be multiplied by a symmetry factor, it is clear that a vertex with four lines that do not end at the same place has 4! ways of being arranged. However, when the diagrams have loops this will no longer be the case and each diagram will be divided by its symmetry factor.

If the parameter λ is small then only diagrams with a few vertices need to be considered in order to obtain a good approximation.

The diagrams from the denominator in Eq.(1.57) can be cancelled out: the denominator corresponds to all the diagrams with no external legs. The numerator will have a diagram with the desired external legs and nothing else, also it will have diagrams consisting of that same diagram and a separate part which is the same as one of the diagrams for the denominator. As an example consider the first diagram in figure 1.1. This diagram appears in the numer-

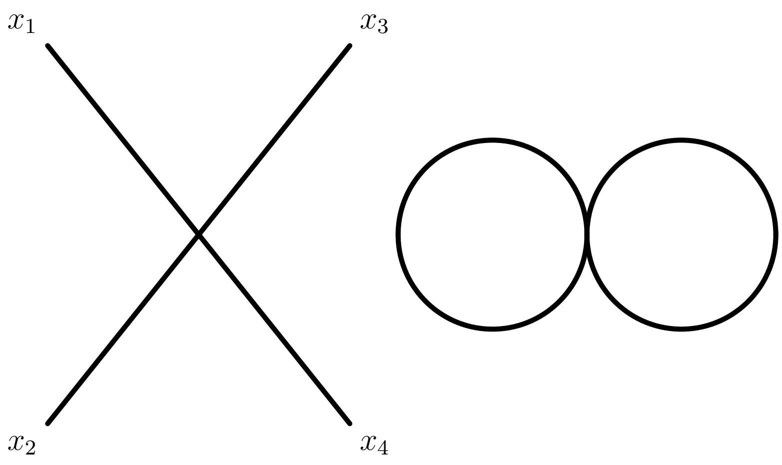

Figure 1.2: Diagram eliminated by the denominator of Eq.(1.57).

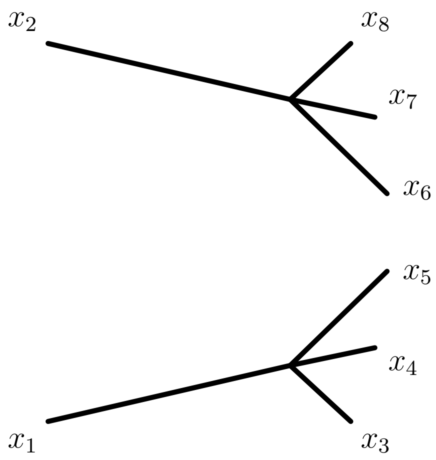

Figure 1.3: Diagram that contributes to $< 0|T\phi(x_1)\cdots\phi(x_8)|0 >$ but not to 2 $\rightarrow$ 6 scattering.

ator along with the diagram in figure 1.2. These extra diagrams enhance the one in figure 1.1 by a factor of: 1+contribution of all diagrams with no external legs.

This factor is the contribution from the denominator, so in order to cancel out the denominator in Eq.(1.57) all diagrams with parts that are unconnected to the external legs are ignored.

Furthermore, diagrams where all the external lines are not connected are also removed, as they will not correspond to the physical processes that are of interest. For example 2 $\rightarrow$ 6 scattering would require $< 0|T\phi(x_1)\cdots\phi(x_8)|0 >$ to be calculated, but the diagram in figure 1.3 does not have any scattering between the initial state particles.

As the transition amplitude of states with known momentum is of interest it is nice to have a set of rules to calculate the diagrams in terms of momentum. Eq.(1.41) has the factor $i \int d^4 x e^{-ik\cdot x}(\Box_x + m^2)$ for an external leg at point x, where k ($-k$) is the momentum of an incoming (outgoing) particle. The $-if(x-y)$ links the external leg to some vertex at the point y that has the integral $\int d^4 y$ associated with it. The operator $i(\Box_x + m^2)$ acting on this integral will remove the $-if(x-y)$ and replace any function of y with an equivalent function of x, as required by Eq.(1.55). With the x-integral added the term introduced from Eq.(1.57) effectively removes the function $-if(x-y)$ for the external leg and changes the vertex integral so that it includes an extra exponential, i.e.

$$i \int d^4 x e^{-ik\cdot x}(\Box_x + m^2) \int d^4 y(-if(x-y))A(y) = \int d^4 x e^{-ik\cdot x} A(x) \ , \quad (1.61)$$

for some arbitrary function A.

After all the external legs are dealt with, the co-ordinates are eliminated by performing the integrals for all the vertices: as the space-time dependence for the propagators is just an exponential this integration leaves behind a momentum delta function. The Feynman diagrams now have momentum conservation at each vertex, and each propagator gives the Fourier transform of the propagator $\int d^4 x e^{ip\cdot x} < 0|T\phi(x)\phi(0)|0 >= i/(p^2 - m^2 + i\epsilon)$. There are also some momentum integrals which are removed by the delta functions, leaving only unfixed momenta to be integrated over, and a delta function for momentum conservation of the external momenta. The delta function is then removed if $M(p_1 p_2 \to k_1 \cdots k_n)$, introduced in Eq.(1.31), is calculated.

One important piece of terminology is that the diagrams that contain no loops in some calculation are known as the tree-level diagrams for that calculation. The diagrams with one loop (or one unconstrained momentum to integrate) are known as the one-loop diagrams, two loops known as two-loop diagrams, etc.

The diagrams with the lowest power of the coupling (λ) are known as the leading order (LO) part of a calculation. Those with the next lowest power are known as next to leading order (NLO), then next to next to leading order

(NNLO), etc.

1.9 Feynman rules in QCD/QED

QCD is a theory of quarks and gluons, and deriving its Feynman rules is more complex than for an interacting scalar field theory. Many different texts including [1], derive the rules for QCD (and QED) Feynman diagrams.

1.9.1 QED Feynman rules

The QCD Lagrangian is similar to the QED Lagrangian, and so before the QCD rules are introduced the QED rules will be covered. The QED Lagrangian is given in Eq.(1.18), and the Feynman rules for QED are shown in figures 1.4 to 1.6.

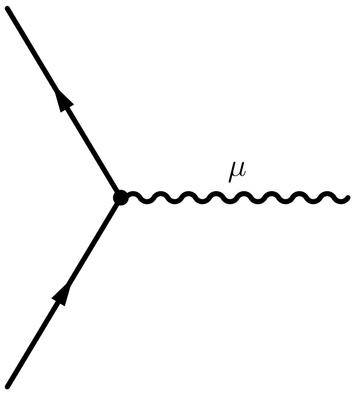

$$-ieQ\gamma_\mu$$

Figure 1.4: QED vertex

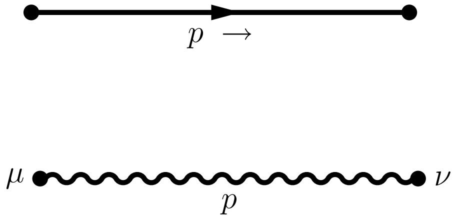

$$\frac{(i\not{p}+m)}{p^2-m^2+i\epsilon}$$

$$\frac{-id^{\mu\nu}(p)}{p^2+i\epsilon}$$

Figure 1.5: QED propagators

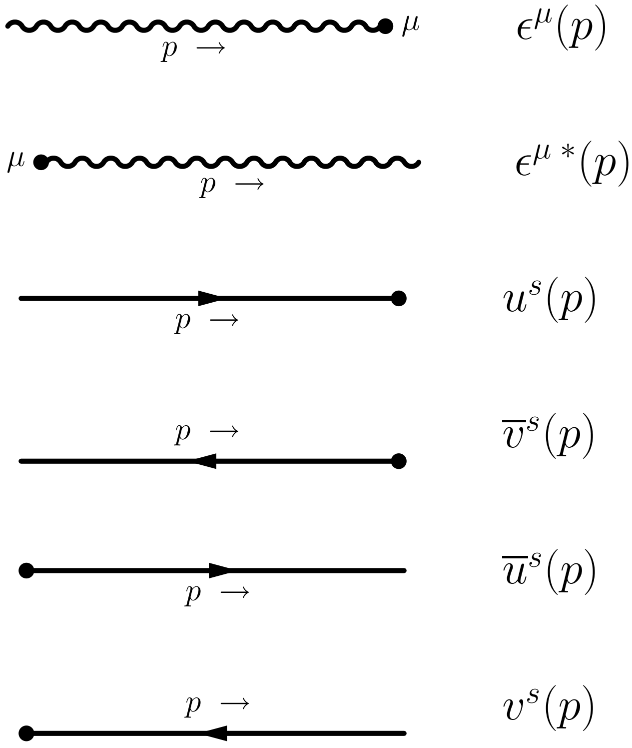

Figure 1.6: QED external particles

The external fermion lines introduce the spinors $u(p)$, $v(p)$, and their conjugates. External vector bosons introduce the polarisation vector $\epsilon_\mu(p)$ and its conjugate. The notation of a slash through a vector denotes the sum $\not{k} = k_\mu \gamma^\mu$. The spinors and their conjugates obey the equations

$$\begin{aligned} (\not{p} - m)u(p) = (\not{p} + m)v(p) = 0 \\ \overline{u}(p)(\not{p} - m) = \overline{v}(p)(\not{p} + m) = 0 \ . \end{aligned} \tag{1.62}$$

The function $u(p)$ obeys the Fourier transform of the Dirac equation, as does $v(-p)$.

$\epsilon_\mu(p)$ is the polarisation vector for an initial state vector boson. This polarisation vector is transverse to the momentum for massless vector particles such as the photon, i.e. $p \cdot \epsilon = 0$

In addition to these rules any unconstrained momenta k caused by loops in the diagrams will be integrated by $\int d^4k/(2\pi)^4$. The diagram will be multiplied by a minus sign for every fermion loop.

It should be noted that the fermion components of the diagrams have an arrow associated with them. For the external particles this determines whether they are fermions or antifermions. The QED vertex has an arrow going in and one going out, which keeps the number of fermions minus the number of antifermions the same.

One complication with the rules for QED is that the photon propagator is not easily defined. The photon propagator will need to be the solution for the function $D_{\mu\rho}(x,y)$ where

$$(\Box g^{\mu\nu} - \partial^\mu\partial^\nu)\int d^4y D_{\mu\rho}(x,y)A(y) = ig^\nu_\rho A(x) \ , \tag{1.63}$$

for some arbitrary function $A(x)$. Eq.(1.63) has no solution, as will be demonstrated shortly.

Adding a term proportional to $(\partial^\mu A_\mu)^2$ to the Lagrangian will make no difference if the Lorentz gauge is chosen. Adding the term

$$-\frac{1}{2\xi}(\partial^\mu A_\mu)^2 \tag{1.64}$$

to the Lagrangian will alter Eq.(1.63) to the solvable equation

$$(\Box g^{\mu\nu} - (1-1/\xi)\partial^\mu\partial^\nu)\int d^4y D_{\mu\rho}(x,y)A(y) = ig^\nu_\rho A(x) \ , \tag{1.65}$$

the solution to which is

$$\begin{aligned} D_{\mu\nu}(x,y) &= \int \frac{d^4k}{(2\pi)^4}\frac{-id_{\mu\nu}(k)}{k^2+i\epsilon}e^{-ik\cdot(x-y)} \\ \text{where} \quad d_{\mu\nu}(k) &= g_{\mu\nu} - (1-\xi)\frac{k_\mu k_\nu}{k^2} \ . \end{aligned} \tag{1.66}$$

As $\xi \to \infty$ as the extra term vanishes showing that Eq.(1.63) has no solution. The parameter ξ is chosen arbitrarily, and so results obtained from QED calculations should not depend upon this parameter.

The QED Lagrangian will now become

$$\mathcal{L}_{QED} = -\frac{1}{4}F_{\mu\nu}F^{\mu\nu} - \frac{1}{2\xi}(\partial^\mu A_\mu)^2 + \bar{\psi}(i\gamma_\mu D^\mu - m)\psi \ . \tag{1.67}$$

1.9.2 QCD Feynman rules

Moving on to QCD, the Lagrangian must first be obtained, which turns out to be similar to the QED Lagrangian.

Due to the colour charges the free quark part of the Lagrangian has three fermion fields

$$\mathcal{L} = \sum_{j=1}^{3} \bar{\psi}_j (i\partial_\mu \gamma^\mu - m)\psi_j \; . \tag{1.68}$$

The local transformation for the quark field that will leave the Lagrangian invariant will be of the form

$$\psi_i(x) \to \sum_{i=1}^{3} U_{ij}(x)\psi_j(x) \; . \tag{1.69}$$

In QCD the quark field transforms in the fundamental representation of the continuous group of $SU(3)$ transformations, that is the transformations $U_{ij}(x)$ are

$$U_{ij}(x) = \exp\left(i \sum_{a=1}^{8} \alpha_a(x) T^a_{ij} \right) \; , \tag{1.70}$$

and $U^\dagger = U^{-1}$, $det(U) = 1$. These constraints leave transformations with 8 parameters. The T^a are the generators of $SU(3)$, and for $SU(N)$ they are Hermitian $N \times N$ matrices with the following properties

$$\begin{aligned} tr(T^a T^b) &= \frac{1}{2}\delta^{ab} \; , \\ \sum_{a,j} T^a_{ij} T^a_{jk} = C_F \delta_{ik} &= \frac{N^2-1}{2N}\delta_{ik} \; . \end{aligned} \tag{1.71}$$

The commutator of these matrices is

$$[T_a, T_b] = i f^{abc} T^c \; , \tag{1.72}$$

the f^{abc} are real and antisymmetric. They are known as structure constants and obey the relation

$$\sum_{b,c} f^{abc} f^{dbc} = C_A \delta_{ad} = N \delta_{ad} \; . \tag{1.73}$$

In order to make the Lagrangian of Eq.(1.68) invariant under the $SU(3)$ transformation the derivative ∂_μ must again be replaced by a covariant derivative D_μ. In this case the covariant derivative must obey the transformation

$$\begin{aligned} D^\mu_{ij} &\rightarrow U_{ik}(x) D^\mu_{kl} U^\dagger_{lj}(x) \;, \\ D^\mu_{ij}\psi_j(x) &\rightarrow U_{ik}(x) D^\mu_{kj}\psi_j(x) \;, \end{aligned} \tag{1.74}$$

where a summation convention over colours is now assumed. Taking the form of the covariant derivative to be $D^\mu_{ij} = \partial^\mu \delta_{ij} - iA^\mu_{ij}$ requires the new field $A^\mu(x)$ to have the transformation

$$A^\mu_{ij}(x) \rightarrow U_{ik}(x) \left(A^\mu_{kl}(x) + i\partial^\mu \delta_{kl} \right) U^\dagger_{lj}(x) \;, \tag{1.75}$$

where

$$A^\mu = g \sum_{a=1}^{8} A^\mu_a T^a \;, \tag{1.76}$$

and g is the QCD coupling constant. This field transforms in the adjoint representation of the group.

Using the 8 fields in the covariant derivative to describe the gluons of QCD the free gluon Lagrangian, in analogy with QED, is

$$\mathcal{L} = -\frac{1}{4} \sum_{a=1}^{8} (\partial_\mu A^a_\nu - \partial_\nu A^a_\mu)(\partial^\mu A^{a\nu} - \partial^\nu A^{a\mu}) \;. \tag{1.77}$$

Defining a new field strength tensor with the covariant derivative in place of the partial derivative gives

$$\begin{aligned} F_{\mu\nu} = D_\mu A_\nu - D_\nu A_\mu = g \sum_a T^a \left(\partial_\mu A^a_\nu - \partial_\nu A^a_\mu + g f^{abc} A^b_\mu A^c_\nu \right) \;, \\ F_{\mu\nu} \rightarrow U(x) F_{\mu\nu} U^\dagger(x) \;, \end{aligned} \tag{1.78}$$

and a summation convention for the gluon colours is now assumed. Taking the trace can then create a Lagrangian that is invariant under the transformation in Eq.(1.75)

$$\mathcal{L} = -\frac{1}{2g^2} tr(F_{\mu\nu} F^{\mu\nu}) \;. \tag{1.79}$$

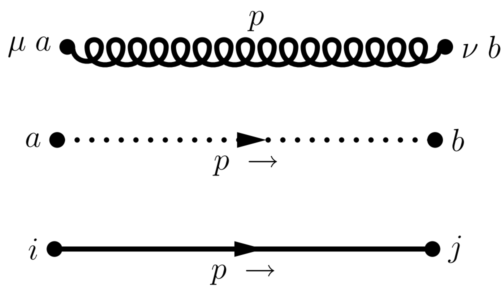

$$\frac{-i\delta_{ab}d^{\mu\nu}(p)}{p^2+i\epsilon}$$

$$\frac{i\delta_{ab}}{p^2+i\epsilon}$$

$$\frac{(i\not{p}+m)\delta^{ij}}{p^2-m^2+i\epsilon}$$

Figure 1.7: QCD propagators

This can be written as

$$-\frac{1}{4}F^a_{\mu\nu}F^{a\mu\nu}\ , \tag{1.80}$$

where

$$F^a_{\mu\nu} = \partial_\mu A^a_\nu - \partial_\nu A^a_\mu + gf^{abc}A^a_\mu A^b_\nu\ . \tag{1.81}$$

Clearly when the coupling is set to zero the Lagrangian returns to the free Lagrangian in Eq.(1.77)

Including the extra gauge-fixing part to obtain a propagator, the Lagrangian for QCD is

$$\mathcal{L}_{QCD} = -\frac{1}{4}F^a_{\mu\nu}F^{a\mu\nu} + \frac{1}{2\xi}(\partial^\mu A^a_\mu)^2 + \bar{\psi}_i(i\gamma_\mu D^\mu_{ij} - m\delta_{ij})\psi_j \tag{1.82}$$

One way in which the gluon field in QCD differs from the photon field in QED is that photon field commutes with itself, which makes QED an Abelian theory. However, the gluon field has a non-zero commutator due to the commutation relations for the generators of $SU(3)$, and so QCD is a non-Abelian theory.

For the work presented in this thesis it is sufficient to know that QCD Feynman rules can be used to calculate a transition amplitude as a series in the QCD coupling. The extra Feynman rules needed for QCD are shown in figures 1.7 and 1.8.

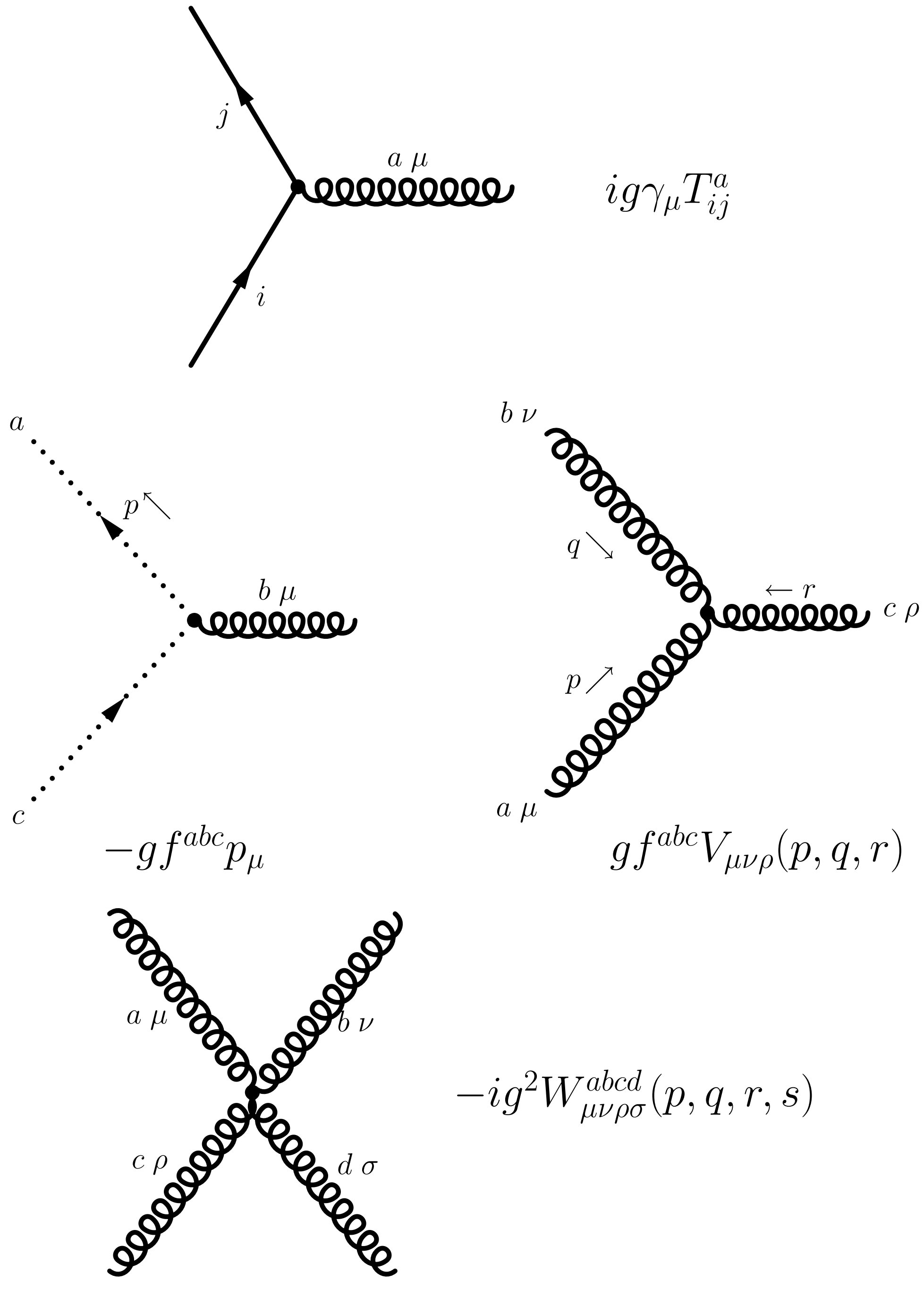

Figure 1.8: QCD vertices

The vertex terms for the gluons are

$$\begin{aligned} V_{\mu\nu\rho}(p,q,r) &= g_{\mu\nu}(p-q)_\rho + g_{\mu\rho}(r-p)_\nu + g_{\nu\rho}(q-r)_\mu \ , \\ W^{abcd}_{\mu\nu\rho\sigma} &= f^{abe}f^{cde}(g_{\mu\rho}g_{\nu\sigma} - g_{\mu\sigma}g_{\nu\rho}) + f^{ace}f^{bde}(g_{\mu\nu}g_{\rho\sigma} - g_{\mu\sigma}g_{\rho\nu}) \\ &\quad + f^{ade}f^{bce}(g_{\mu\nu}g_{\sigma\rho} - g_{\mu\rho}g_{\sigma\nu}) \ . \end{aligned} \tag{1.83}$$

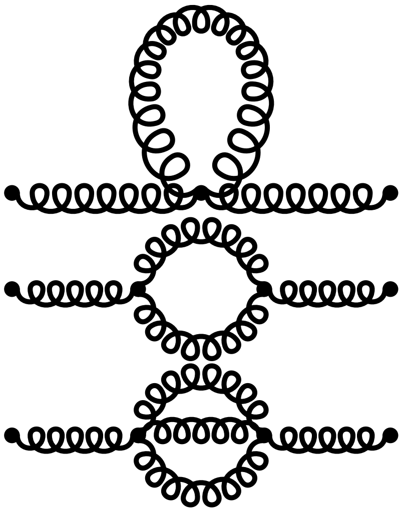

Figure 1.9: Parts of QCD Feynman diagrams that give a symmetry factor

There are symmetry factors for gluon loops shown in figure 1.9. The first two diagrams have a symmetry factor of 1/2!, and the third has a symmetry factor of 1/3!.

There are some unexpected inclusions to the QCD Feynman rules: the dotted lines are the contributions from Faddeev-Popov ghosts [5]. The gauge transformations for the gluon field give physically equivalent field configurations. Factoring out all the equivalent field configurations from the path integral leads to the extra Feynman rules shown. If there is a ghost loop, then just as with fermion loops, the diagram will gain an extra minus sign.

The ghost-gluon vertex involve the structure constants of $SU(3)$. For an Abelian theory such as QED the structure constants are zero and it is unsurprising that there is no ghost contribution.

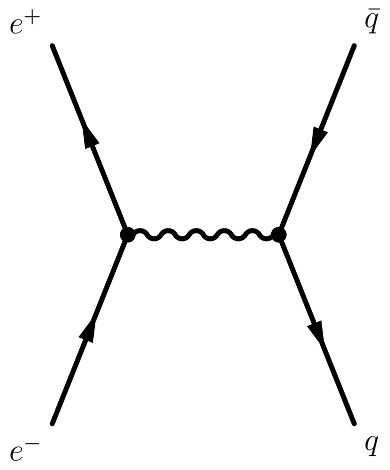

Figure 1.10: Leading order QED diagram for the R-ratio

1.10 $R_{e^+e^-}$

The hadronic cross section from electron-positron annihilation depends upon the strong force and can be used to test QCD and determine its coupling. First the R-ratio is defined:

$$R_{e^+e^-} = \frac{\sigma(e^+e^- \rightarrow \text{hadrons})}{\sigma(e^+e^- \rightarrow \mu^+\mu^-)} \; . \tag{1.84}$$

Assuming leading-order QED, the hadrons are produced from a quark anti-quark pair. The only difference between the two processes is the charge on the outgoing particles. The R-ratio can then be simply calculated from the square of the ratio of the electric charges of the quark and the muon. As there is more than one type of quark, the ratio must be summed over all the possible types of quark.

$$R_{e^+e^-} = N \sum_f Q_f^2 \tag{1.85}$$

Here $N = 3$ is the number of different colours a quark can take, Q_f is the electric charge of a quark of flavour f and the sum is over the different flavours of quark.

Massless quarks and muons have been assumed in this argument. This is a valid assumption if the particle rest masses are negligible when compared with their energies. The sum is over those flavours of quark whose mass is less than half the centre of mass energy, otherwise there would not be enough energy to produce the quark antiquark pair.

Taking the sum to be over the u,d,s,c,b quarks, the approximation of Eq.(1.85) gives the R-ratio to be 11/3. In actual fact the R-ratio is found to be larger than this. Reference [7] gives the R-ratio to be 4.11 ± 0.16 when the centre of mass energy of the collision is 22 GeV.

This discrepancy can be used to measure the contribution from higher order diagrams. The correction from the leading order QCD calculation is an enhancement by the factor $1 + a$ where $a = (g/2\pi)^2$ [8]. The discrepancy found from experiment can then be used to obtain a value for the QCD coupling.

1.11 Optical Theorem

The QCD contribution to the R-ratio can be related to the vacuum polarisation. In order to see this the optical theorem needs to be applied. Consider an element of the S-matrix

$$M(p_1p_2 \to p_3p_4) =< p_3p_4|T|p_1p_2 > (2\pi)^4\delta^{(4)}(p_1 + p_2 - p_3 - p_4) \ , \qquad (1.86)$$

where the S-matrix $S = 1 + iT$. Eq.(1.86) is the matrix element for a two-to-two-body scattering process: particles with momenta p_1p_2 scattering to particles with momenta p_3p_4. Using the unitarity of the S-matrix, $i(T^\dagger - T) = T^\dagger T$, and inserting $T^\dagger T$ between the initial and final states one obtains

$$\begin{aligned} < p_3p_4|T^\dagger T|p_1p_2 >= i[M^*(p_3p_4 \to p_1p_2) - M(p_1p_2 \to p_3p_4)] \\ (2\pi)^4\delta^{(4)}(p_1 + p_2 - p_3 - p_4) \ . \end{aligned} \qquad (1.87)$$

Combining this with the completeness of states gives

$$\begin{aligned} i[M^*(p_3p_4 \to p_1p_2) - M(p_1p_2 \to p_3p_4)](2\pi)^4\delta^{(4)}(p_1 + p_2 - p_3 - p_4) \\ = \sum \int \prod_i^n \frac{d^3q_i}{(2\pi)^3 2E_{q_i}} < p_3p_4|T^\dagger|q >< q|T|p_1p_2 > \ . \end{aligned} \qquad (1.88)$$

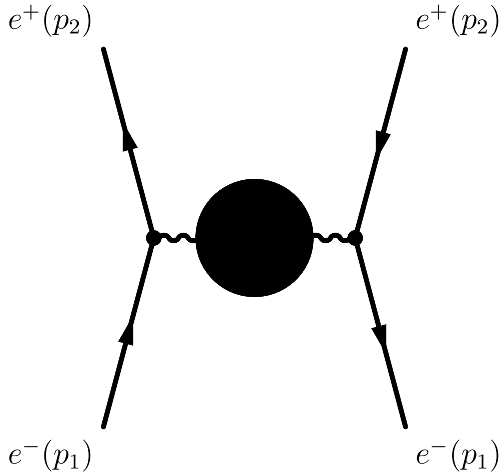

Figure 1.11: Hadronic correction to electron positron scattering

We represent the intermediate state with particles of momenta $q_1 \cdots q_n$ by $|q>$; the sum is over all possible intermediate states. If we take the initial and final states to be identical, the right hand side of Eq.(1.88) is proportional to the cross section of two particles scattering into anything:

$$2E_{cm}p_{cm}\sigma(p_1p_2 \to q) = Im(M(p_1p_2 \to p_1p_2)) \ , \tag{1.89}$$

where $E_{cm} = E_{p_1} + E_{p_2}$, and $p_{cm} = |\vec{p}_1 - \vec{p}_2|$.

The optical theorem can be used in order to obtain $\sigma(e^+e^- \to hadrons)$. Working in leading order QED the intermediate states inserted in Eq.(1.88) become hadronic states, so to calculate the hadronic cross section we need the invariant amplitude $M(e^+(p_1)e^-(p_2) \to e^+(p_1)e^-(p_2))$ calculated using QCD and leading order QED.

For massless electrons the hadronic cross section is given by $2s\sigma(e^+e^- \to \text{hadrons}) = Im[M(e^+(p_1)e^-(p_2) \to e^+(p_1)e^-(p_2))]$, with $s = (p_1 + p_2)^2$. The Feynman diagrams required to calculate the cross section are represented by figure 1.11 The photon propagator has the hadronic vacuum polarisation, represented by the dark circle in figure 1.11, inserted in order to obtain the QCD contribution. This covers all the QCD intermediate states that can be inserted into the propagator. The vacuum polarisation is due to the propagator interacting with a quark current that is created and annihilated at two points, and so the vacuum polarisation is the correlation between two quark currents,

$$i\Pi^{\mu\nu}(q) = \int d^4x e^{iq\cdot x} < 0|Tj^\mu(x)j^\nu(0)|0 > \ . \tag{1.90}$$

$\Pi^{\mu\nu}(q)$ represents the vacuum polarisation, and $j^\mu(x)$ is a quark current.

From current conservation it is clear that $q^\mu\Pi^{\mu\nu}(q) = q^\nu\Pi^{\mu\nu}(q) = 0$. The only rank-2 tensors that $\Pi^{\mu\nu}(q)$ can depend on are the metric $g^{\mu\nu}$, and $q^\mu q^\nu$. From these facts $\Pi^{\mu\nu}(q)$ can be related to a scalar function

$$\Pi^{\mu\nu}(q) = (g^{\mu\nu}q^2 - q^\mu q^\nu)\Pi(q^2) \ . \tag{1.91}$$

Using the Feynman rules for QED at leading order, the relation between the vacuum polarisation and the cross-section is

$$\sigma(e^+e^- \to \text{hadrons}) = \frac{16\pi^2\alpha^2}{s} Im(\Pi(s+i\epsilon)) \ . \tag{1.92}$$

Due to the $q^2 + i\epsilon$ prescription for the propagator demonstrated in Eq.(1.60) the imaginary part of $\Pi(s+i\epsilon)$ is taken; this is an analytical function and so

$$\sigma(e^+e^- \to \text{hadrons}) = \frac{8\pi^2\alpha^2}{is}(\Pi(s+i\epsilon) - \Pi(s-i\epsilon)) \ . \tag{1.93}$$

To leading-order QED the result for muon scattering is

$$\sigma(e^+e^- \to \mu^+\mu^-) = \frac{4\pi\alpha^2}{3s} \ . \tag{1.94}$$

The relation between the vacuum polarisation and the R-ratio is

$$R_{e^+e^-} = 12\pi Im(\Pi(s+i\epsilon)) = -6\pi i(\Pi(s+i\epsilon) - \Pi(s-i\epsilon)) \ , \tag{1.95}$$

with $\Pi(q^2)$ given by Eqs.(1.90,1.91). Leading-order QED has been used here due to the relatively small size of the QED coupling: corrections due to higher order QED effects are taken to be negligible.

It is convenient to define the Adler D-function:

$$D(s) = -12\pi^2 s \frac{d}{ds}\Pi(-s) \ . \tag{1.96}$$

Using Eq.(1.95) the following relation can be obtained

$$R_{e^+e^-} = R(s) = \frac{1}{2\pi i}\int_{-s-i\epsilon}^{-s+i\epsilon} dt \frac{D(t)}{t} \ . \tag{1.97}$$

This relation will become important later on in this thesis.

1.12 Operator product expansion

If it is assumed that short-distance ($x \to 0$) effects dominate Eq.(1.90), then the operator product expansion (OPE) can be applied [6]. This expansion replaces the product of the two currents with a series of suitable single operators evaluated locally

$$T[j^\mu(x)j^\nu(0)] \to \sum_n C_n^{\mu\nu}(x)O_n(0) \ . \tag{1.98}$$

The dimension of the coefficients $C_n^{\mu\nu}(x)$ depends upon the operator. Placing the operators in order of their mass dimension, the first coefficient, which has the most singular behaviour in x, is for the operator $O_1 = 1$. The first coefficient will be of order x^{-6}, while the next coefficients are of order x^{-2} and come from operators such as the product of two field strength tensors $F_a^{\alpha\beta}(0)F^a_{\alpha\beta}(0)$. Using the same arguments used to obtain Eq.(1.91), $\Pi(q^2)$ can be written as

$$\begin{aligned} i\Pi(q^2) &= c_1(q^2) + (\cdots)(q^2)^{-2} + \cdots \\ c_1(q^2)(g^{\mu\nu}q^2 - q^\mu q^\nu) &= \int d^4x e^{iq\cdot x} C_1^{\mu\nu}(x) \ . \end{aligned} \tag{1.99}$$

The q^2-dependence has come from the OPE coefficients only, and so the series can be ordered in terms of the q^2-dependence of each part. The first coefficient is of order $(q^2)^0$ and the next coefficients are of order $(q^2)^{-2}$. The calculation from perturbative QCD gives the contribution from $c_1(q^2)$ whereas the other coefficients are non-perturbative in nature. Assuming that short-distance (high energy) effects dominate, the perturbative part from c_1 should be sufficient.

1.13 Summary

The theory behind the quarks and gluons that make up hadrons is Quantum Chromodynamics. QCD is a quantum field theory that is described by a Lagrangian density that is a function of the theory's fields and their derivatives.

The field's Fourier transform can be expressed in terms of creation and annihilation operators. These operators when acting upon the vacuum produce states corresponding to a certain number of particles, each particle has a momentum associated with it.

Physical observables such as the cross section can be calculated from the S-matrix, whose elements are the overlap of the incoming and outgoing states.

Taking the limit of the far future and far past for outgoing and incoming states will allow these states to be described by a non-interacting theory, then through the Euler-Lagrange equations for the free fields the states can be related to the corresponding field. The LSZ reduction formula then relates the chosen S-matrix element to a Green's function dependent upon the fields from the interacting theory.

The Green's function produced from the LSZ reduction formula can be computed from a path integral by considering all possible values of the field at every point in space and time. Expanding the result from the path integral as a series in some coupling constant that determines the size of the interacting part of the Lagrangian gives a result in terms of simple mathematical constructs. The rules for Feynman diagrams give a simple way of expressing the calculation required for a particular S-matrix element.

The Lagrangian for QCD is similar to the QED Lagrangian. The QED Lagrangian has a vector (photon) field, and fermion fields. The interactions in QED are introduced when invariance under a local gauge transformation is demanded. The QED Feynman rules include propagators for the photon and fermions, and a vertex for a photon and two fermions. There is no vertex consisting of just fermions or photons, as the interaction part of the Lagrangian has no terms consisting of a single type of field.

For QCD the local gauge transformations are given by the group $SU(3)$. This amongst other things gives the theory 8 vector (gluon) fields, as opposed to the solitary photon field of QED. The interaction Lagrangian does have parts that consist entirely of the gluon fields, giving vertices that have only gluon fields.

There is also the added complication of ghosts in QCD which come from integrating out the physically equivalent field configurations in the path integral.

The ratio of hadron production to muon production from electron positron annihilation, $R_{e^+e^-}$ was considered. This ratio can be computed using the optical theorem which links a cross section to the imaginary part of a matrix element. The matrix element contains the product of two currents, which through the operator product expansion is a series of operators of increasing mass dimension multiplied by some coefficient function. The first such coefficient function can be calculated from perturbative QCD.

Chapter 2

Renormalisation

2.1 Introduction

Higher order calculations in a QFT have integrals over the unfixed momentum flowing through a loop in a Feynman diagram. These integrals are not necessarily finite. For example the QED Feynman diagram in figure 2.1 is in fact divergent, and for a fermion with unit charge this diagram gives

$$\bar{v}(k_2)\gamma^\mu u(k_1)\frac{1}{q^2}e^4$$
$$\int \frac{d^4k}{(2\pi)^4} tr\left[\gamma_\mu \frac{i(\not{k}+m)}{k^2-m^2}\gamma_\nu \frac{i((\not{k}+\not{q})+m)}{(k+q)^2-m^2}\right]\frac{1}{q^2}\bar{u}(k_3)\gamma^\nu v(k_4)\ , \qquad (2.1)$$

with $k_1 + k_2 = q = k_3 + k_4$. The d^4k integral in Eq.(2.1) is the source of the divergence; the large k part of the integral is proportional to $\int d^4k 1/k^2$. Setting the upper limit of the magnitude of k in the integral to be K the large k part of the integral will produce something proportional to K^2, the upper limit of the integral is infinite and so the integral diverges.

The solution to this problem is the renormalisation of the theory. When a theory is renormalised the integrals have their divergent behaviour isolated by some mechanism. This is known as regularisation. One method of regularisation is dimensional regularisation [9], which is often used in QED and QCD. Dimensional regularisation re-writes the theory with D space-time dimensions, the divergences then becoming poles in $1/(4-D)$.

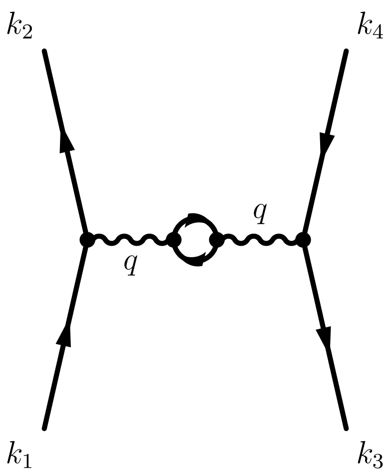

Figure 2.1: 1-loop diagram in QED

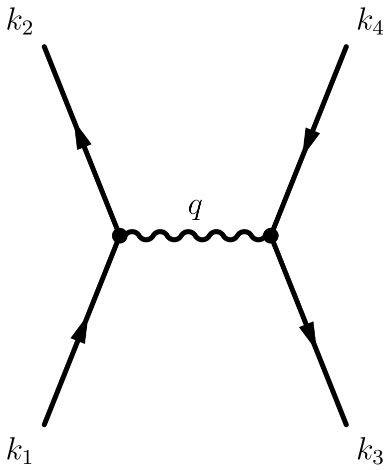

Figure 2.2: Tree level diagram for the same process

The next step of renormalisation is to rescale the parameters of the theory, the fields, masses and couplings, so that the divergences are eliminated. The rescaling leads to higher-order terms associated with the components of Feynman diagrams. For example the diagram in figure 2.2 contributes to the same process as figure 2.1 does. This diagram is of order e^2, but when the theory is renormalised the diagram has higher-order terms associated with it. The e^4 term from these extra terms will have a part that cancels out the divergence from Eq.(2.1). If the theory is renormalised so that just the $1/(4-D)$ pole is removed from the divergent integrals like Eq.(2.1) then the minimal subtraction (MS) scheme has been used [10]. If the quantity

$1/(4-D)-\gamma_E+\ln(4\pi)$ is removed for every $1/(4-D)$ pole, then the modified minimal subtraction ($\overline{\mathrm{MS}}$) scheme has been used. γ_E is Euler's constant, defined to be

$$\gamma_E = \lim_{N\to\infty}\sum_{n=1}^{N}\frac{1}{n} - \ln(N+1) = 0.5722\ldots \ . \tag{2.2}$$

Unless otherwise stated the, $\overline{\mathrm{MS}}$-scheme will be used throughout this thesis.

When the theory is regularised a new parameter with a mass dimension is introduced. For example in dimensional regularisation an extra parameter in the Lagrangian must appear. Consider the QED interaction in four dimensions: the action will have the term

$$\int d^4x \left(-eQ\bar{\psi}(x)A_\mu(x)\gamma^\mu\psi(x)\right) \ . \tag{2.3}$$

From Eqs.(1.13,1.14) the mass dimensions of the vector and fermion fields are $(D-2)/2$ and $(D-1)/2$ respectively. In D dimensions the interaction term must then become

$$\int d^Dx \left(-eQ\bar{\psi}(x)A_\alpha(x)\gamma^\alpha\psi(x)\mu^{(4-D)/2}\right) \ , \tag{2.4}$$

μ is a new parameter with a mass dimension of one. The Lagrangian can be written in terms of non-renormalised or bare fields and parameters as in Eq.(2.4), or in terms of renormalised fields and parameters with renormalisation constants when the theory gets rescaled

$$\int d^Dx \left(-Z_e e_r Q Z_\psi^{1/2}\bar{\psi}_r(x) Z_A^{1/2} A_{r\,\alpha}(x)\gamma^\alpha Z_\psi^{1/2}\psi_r(x)\mu_r^{(4-D)/2}\right) \ . \tag{2.5}$$

The subscript r signifies renormalised quantities. The relation between the bare and renormalised coupling is

$$e_r = eZ_e^{-1}\left(\frac{\mu}{\mu_r}\right)^{(D-4)/2} \ . \tag{2.6}$$

The renormalisation constant Z_e depends on μ_r, giving a non-zero $de_r/d\mu_r$ as $D\to 4$. This leads to the beta function equation. Dropping the r subscript

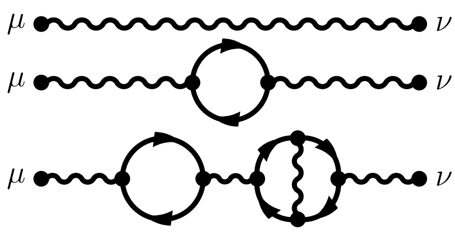

Figure 2.3: Feynman diagrams contributing to Eq.(2.8)

and taking $\alpha = e^2/4\pi$

$$\mu \frac{d\alpha}{d\mu} = \beta_0 \alpha^2 + \beta_1 \alpha^3 + \beta_2 \alpha^4 + \cdots \ . \tag{2.7}$$

The coefficients β_i can be calculated for QED. $\beta_0 = \frac{2}{3\pi} \sum_f Q_f^2$, where the sum is over all the fermions that have electromagnetic charges.

2.2 Example: Renormalised photon propagator

For an example of renormalisation consider the photon propagator and its higher-order terms in momentum space

$$\int e^{iq.x} < 0|T A_\mu(x) A_\nu(0)|0 > d^4x \ . \tag{2.8}$$

The physical photon field is related to the bare photon field via some renormalisation constant

$$A_0^\mu = Z_A^{1/2} A^\mu \ . \tag{2.9}$$

The bare fields of the Lagrangian are identified by the 0 subscript.

Examples of the diagrams corresponding to Eq.(2.8) are given in figure 2.3 These diagrams can be divided into two sorts, those that can be split into two individual diagrams by the removal of a single propagator and those that cannot. The third diagram in figure 2.3 can be split up in this way whereas the second diagram cannot. The diagrams that cannot be split up by the removal of a single propagator are referred to as one-particle-irreducible diagrams (1PI diagrams). If the sum of all 1PI diagrams is represented by

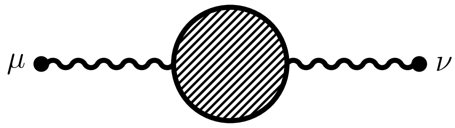

Figure 2.4: One particle irreducible diagrams represented as single diagram

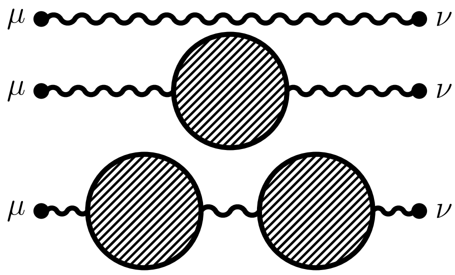

Figure 2.5: Feynman diagrams contributing to Eq.(2.8) using 1PI notation

a single diagram as in figure 2.4, then the Feynman diagrams for Eq.(2.8) can be represented as the sum of diagrams which have a photon propagator interspersed with a number of 1PI diagrams.

These diagrams are then just combinations of the photon propagator and the two-point correlator of the electromagnetic current. The second diagram of figure 2.5 is

$$\frac{-id^{\mu\alpha}}{q^2+i\epsilon} i\tilde{\Pi}_{\alpha\beta}(q) \frac{-id^{\beta\nu}}{q^2+i\epsilon} \ , \tag{2.10}$$

where q is the momentum flowing through the photon propagators. The function $\tilde{\Pi}_{\alpha\beta}(q)$ is

$$i\tilde{\Pi}_{\alpha\beta}(q) = -e^2 \int d^4x e^{iq\cdot x} < 0|Tj_\alpha(x)j_\beta(0)|0> \ . \tag{2.11}$$

Eq.(2.11) combined with current conservation can relate $\tilde{\Pi}_{\alpha\beta}(q)$ to a scalar, in analogy with Eq.(1.91):

$$\tilde{\Pi}_{\alpha\beta} = (g_{\alpha\beta} - q_\alpha q_\beta/q^2)q^2\tilde{\Pi}(q^2) \ . \tag{2.12}$$

Noting that $d_{\mu\nu}(g^\nu_\rho - q^\nu q_\rho/q^2) = (g_{\mu\rho} - q_\mu q_\rho/q^2)$ a diagram where the photon propagator is split by n 1PI parts is equal to

$$-i\frac{g^{\mu\nu} - q^{\mu}q^{\nu}/q^2}{q^2 + i\epsilon}(\tilde{\Pi}(q^2))^n \ . \tag{2.13}$$

The ξ-dependent part has been ignored, as all ξ dependence vanishes when calculating a physical process.

The part of $\tilde{\Pi}_{\alpha\beta}(q)$ with the lowest power of the coupling is given by a single fermion loop, and is

$$\tilde{\Pi}_{\alpha\beta}(q) = -ie^2 \int \frac{d^4k}{2\pi^4} tr\left(\gamma_\alpha \frac{i(\not{k} + m)}{k^2 - m^2}\gamma_\beta \frac{i((\not{k}+\not{q}) + m)}{(k+q)^2 - m^2}\right) \ . \tag{2.14}$$

The integral in Eq.(2.14) when dimensional regularisation is used takes the form

$$\begin{aligned}&\tilde{\Pi}_{\alpha\beta}(q)\\ &= (q^2 g_{\alpha\beta} - q_\alpha q_\beta)\frac{e^2}{12\pi^2}\left[\frac{2}{D-4} + \gamma_E - \ln(4\pi) + \text{finite terms}\right] \ .\end{aligned} \tag{2.15}$$

The details of this calculation have been left out, and can be found in [1].

The sum of all the diagrams in figure 2.5 is

$$\frac{-i(g^{\mu\nu} - q^{\mu}q^{\nu}/q^2)}{q^2 + i\epsilon}\sum_{n=0}^{\infty}\left(\tilde{\Pi}(q^2)\right)^n \ . \tag{2.16}$$

The perturbation series in the coupling for the summation in Eq.(2.16) is the same as that for $\frac{1}{1-\tilde{\Pi}(q^2)}$. Returning to Eqs.(2.8,2.9), it can be seen that in order to make Eq.(2.8) finite the renormalisation constant Z_A will have to be chosen so that it cancels out the divergence given by $\tilde{\Pi}(q^2)$. If the convention of the $\overline{\text{MS}}$ scheme is used then

$$Z_A = 1 + \frac{e^2}{12\pi^2}\left(\frac{2}{D-4} + \gamma_E - \ln(4\pi)\right) + \mathcal{O}(e^4) \ . \tag{2.17}$$

The finite $\gamma_E - \ln(4\pi)$ part is removed due to the choice of renormalisation scheme.

QCD is a renormalisable theory, as was shown in [11]. This results in a renormalised QCD coupling that has a dependence on some arbitrary renormalisation scale. Furthermore, renormalising QCD in different ways with different renormalisation scales leads to a truncated perturbation series which is scheme dependent. This scheme dependence renders calculations in QCD perturbation theory ambiguous.

However, in a QCD perturbation series there is often a logarithm taken to a power that increases with the order of the series. This logarithm contains the ratio of the renormalisation scale to some physical scale, and if the renormalisation scale is taken to be close to this physical scale then the series will converge faster to the full perturbation series. Often such physical scales are used for choices of the QCD renormalisation scale, else the series may not converge well.

2.3 Renormalisation group

There are an infinite number of ways of removing the divergences through renormalisation. The use of different renormalisation schemes for the same Green's function will yield different finite results. The finite renormalisation between different procedures constitutes the renormalisation group [12]. Consider a renormalised Green's function G. This is related to the bare Green's function G_B

$$G_B = ZG \; . \tag{2.18}$$

In another renormalisation scheme one has

$$G_B = \bar{Z}\bar{G} \; . \tag{2.19}$$

From the ratio of the two renormalised Green's functions one obtains a finite renormalisation

$$z = \frac{\bar{G}}{G} = \frac{Z}{\bar{Z}} \; . \tag{2.20}$$

A physical process must have a unique solution, and so cannot depend upon the choice of scheme. It was shown earlier that a physical process calculated using a QFT will be obtained from a Green's function. A physical observable

R can be calculated in the two schemes

$$R(Q, g, m, \mu) = \bar{R}(Q, \bar{g}, \bar{m}\bar{\mu}) \ , \tag{2.21}$$

Q represents the physical scale(s) that R depends upon: the renormalised coupling, mass and the renormalisation scale change when moving from one scheme to another. Calculated from different renormalisation schemes the functional form of R and $\bar{R}$ will differ, but leave a result that is scheme invariant.

Varying the renormalisation scale should not alter the result for any physical measurement

$$\mu \frac{dR}{d\mu} = 0 \ . \tag{2.22}$$

Taking a generic physical quantity calculated from a theory with no mass terms in the Lagrangian this becomes

$$\left(\mu \frac{\partial}{\partial \mu} + \beta(g) \frac{\partial}{\partial g} \right) R(Q, g, \mu) = 0 \ , \tag{2.23}$$

where $\beta(g)$ is the beta function for the renormalised coupling g.

$$\beta(g) = \mu \frac{dg}{d\mu} \ . \tag{2.24}$$

If R has zero mass dimension and depends upon only one physical scale then if the coupling is held fixed the only dependence on μ must be of the form μ/Q, and so

$$\left(-Q \frac{\partial}{\partial Q} + \beta(g) \frac{\partial}{\partial g} \right) R \left(\frac{Q}{\mu}, g \right) = 0 \ . \tag{2.25}$$

This shows that the observable has a scale dependence determined by the coupling's beta function, and the observable's dependence on the coupling i.e. its perturbation series.

2.4 QCD beta function and scale dependence

From now on any dependence on the QCD coupling will be given in terms of $a = (g/2\pi)^2$, and that will also be called the coupling.

The beta function for a is

$$\mu \frac{\partial a}{\partial \mu} = \beta(a) = -ba^2(1 + ca + c_2 a^2 + \cdots) \,, \tag{2.26}$$

in which the coefficients b and c are renormalisation scheme invariant. These coefficients have been calculated [13] as

$$\begin{aligned} b &= \frac{11N - 2N_f}{6} = \frac{33 - 2N_f}{6} \,, \\ c &= \frac{34N^3 - N_f(13N^2 - 3)}{24bN} = \frac{153 - 19N_f}{12b} \,, \end{aligned} \tag{2.27}$$

N and N_f are the numbers of colours and flavours of quark respectively. c_2, and c_3 have been calculated in the $\overline{MS}$ scheme [14]

$$\begin{aligned} c_2^{\overline{MS}} &= \frac{5714N^5 + N_f(-3418N^4 + 561N^2 + 27) + N_f^2(224N^3 - 66N)}{3456bN^2} \\ &= \frac{77139 - 15099N_f + 325N_f^2}{1728b} \,, \\ c_3^{\overline{MS}} &= [5196312\zeta_3 + 36389979 - (351432\zeta_3 + 9705249)N_f \\ &\quad + (116532\zeta_3 + 450585)N_f^2 + 2186N_f^3\big] /(373248b) \,. \end{aligned} \tag{2.28}$$

The function ζ_n is the Riemann zeta function, defined as

$$\zeta_n = \sum_{l=1}^{\infty} \frac{1}{l^n} \,. \tag{2.29}$$

If the beta function equation is integrated then one obtains

$$\int_0^a \frac{dx}{\beta(x)} = k + \ln\left(\frac{\mu}{\Lambda}\right) \,, \tag{2.30}$$

where the constant of integration has had its infinite part isolated in k, leaving the massive constant Λ finite. If the choice $k = \int_0^\infty \frac{1}{-bx^2(1+cx)}\, dx$ used in [15] is made, then Λ will be represented by $\tilde{\Lambda}$. This choice Λ in the $\overline{MS}$ scheme can be related to the standard convention for $\Lambda_{\overline{MS}}$ defined in [16] by

$$\Lambda_{\overline{MS}} = \left(\frac{2c}{b}\right)^{c/b} \tilde{\Lambda}_{\overline{MS}} \,. \tag{2.31}$$

Using this choice for k and Λ

$$\ln\left(\frac{\mu}{\tilde{\Lambda}}\right) = \int_a^\infty \frac{1}{bx^2(1+cx)}\,dx + \int_0^a \left[\frac{1}{bx^2(1+cx)} + \frac{1}{\beta(x)}\right]\,dx\ . \tag{2.32}$$

The second integral vanishes as $a \to 0$. This can be seen because

$$\begin{aligned}\frac{1}{\beta(a)} + \frac{1}{ba^2(1+ca)} &= \frac{-(1+ca)+1+ca+c_2a^2+\cdots}{ba^2(1+ca)(1+ca+c_2a^2+\cdots)} \\ &= \frac{c_2+c_3a+\cdots}{b(1+ca)(1+ca+c_2a^2+\cdots)}\ .\end{aligned} \tag{2.33}$$

This means that the second integral in Eq.(2.32) for small a is $c_2a + \mathcal{O}(a^2)$, which vanishes when the limit $a \to 0$ is taken.

Solving the first integral in Eq.(2.32) gives

$$b\ln\left(\frac{\mu}{\tilde{\Lambda}}\right) = \frac{1}{a} + c\ln\left(\frac{ca}{1+ca}\right) + \mathcal{O}(a)\ . \tag{2.34}$$

This equation shows the property of the QCD coupling known as asymptotic freedom, where the coupling vanishes in the limit where the renormalisation scale becomes infinite. Asymptotic freedom from Eq.(2.34) requires that the beta function coefficient b be positive.

An equivalent approach can be used for a QCD perturbation series dependent on a physical energy scale [17, 18].

$$R(Q) = a(\mu) + r_1(Q,\mu)a^2(\mu) + r_2(Q,\mu)a^3(\mu) + \cdots\ , \tag{2.35}$$

where Q is the physical energy scale. If this series corresponds to something measurable it does not depend on the arbitrary renormalisation scale, i.e. $\mu\frac{dR(Q)}{d\mu} = 0$. For a dimensionless $R(Q)$ the series coefficients $r_n(Q,\mu)$ are dimensionless and so depend on the Q and μ through the ratio Q/μ. Note that this applies to a theory with only one physical energy scale, otherwise R would depend upon the ratios of such scales and μ. Making use of the fact that a physical quantity is independent of the choice of renormalisation scale,

$$\mu\frac{dR(Q)}{d\mu} = \beta(a)\frac{\partial R(Q)}{\partial a} + \mu\frac{\partial R(Q)}{\partial \mu}\bigg|_a = 0\ , \tag{2.36}$$

so

$$\beta(a)\left(1+2r_1(Q,\mu)a(\mu)+\cdots\right)+\mu\frac{\partial r_1(Q,\mu)}{\partial\mu}a^2(\mu)+\mu\frac{\partial r_2(Q,\mu)}{\partial\mu}a^3(\mu)+\cdots$$
$$=\beta(a)\left(1+2r_1(Q,\mu)a(\mu)+\cdots\right)$$
$$-Q\frac{\partial r_1(Q,\mu)}{\partial Q}a^2(\mu)-Q\frac{\partial r_2(Q,\mu)}{\partial Q}a^3(\mu)+\cdots=0\,. \quad (2.37)$$

Rearranging Eq.(2.37) gives

$$Q\frac{\partial R(Q)}{\partial Q}=\beta(a)\left(1+2r_1(Q,\mu)a(\mu)+3r_2(Q,\mu)a^2(\mu)+\cdots\right)\,. \quad (2.38)$$

This can be converted into the Effective Charge beta function [19, 20] by considering the series inversion of Eq.(2.35), $a(R)$

$$Q\frac{\partial R(Q)}{\partial Q}=-bR^2(Q)\left(1+cR(Q)+\rho_2R^2(Q)+\cdots\right)\,, \quad (2.39)$$

where ρ_2 is the scheme-invariant combination $\rho_2=c_2+r_2-r_1^2-r_1c$.

The same approach can now be applied to $R(Q)$ as was applied to $a(\mu)$, leading to

$$b\ln\left(\frac{Q}{\Lambda_R}\right)=\frac{1}{R}+c\ln\left(\frac{cR}{1+cR}\right)+\mathcal{O}(R)\,. \quad (2.40)$$

Asymptotic freedom can be seen to be exhibited by the perturbation series. Just as the coupling vanishes as the scale μ becomes infinite, the series R vanishes as $Q\to\infty$.

Inserting the perturbation series back into Eq.(2.40) relates Λ_R to $\tilde{\Lambda}$

$$b\ln\left(\frac{Q}{\Lambda_R}\right)=\frac{1}{a}-r_1+c\ln\left(\frac{ca}{1+ca}\right)+\mathcal{O}(a)=b\ln\left(\frac{\mu}{\tilde{\Lambda}}\right)-r_1+\mathcal{O}(a)\,. \quad (2.41)$$

Setting $\mu=Q$ and taking the limit $Q\to\infty$ gives

$$\Lambda_R=\tilde{\Lambda}e^{r_1(\mu=Q)/b}\,. \quad (2.42)$$

Eq.(2.41) and Eq.(2.42) relate the ratio $\tilde{\Lambda}/Q$ to the coupling $a(Q)$:

$$\frac{\tilde{\Lambda}}{Q}=e^{-1/ba}\left(\frac{ca}{1+ca}\right)^{-c/b}\left(1+\mathcal{O}(a)\right)\,. \quad (2.43)$$

Eq.(2.43) shows that terms of the form $\left(\tilde{\Lambda}/Q\right)^n$ that appear in the OPE are non-perturbative in nature. The right hand side of Eq.(2.43) has a vanishing power series expansion in a due to the $e^{-1/ba}$ term.

2.5 CORGI

Complete Renormalisation Group Improvement, or CORGI, is the summation of all physical ultraviolet logarithms of a perturbation series [21]. Some results from CORGI will be used in this thesis, and so an introduction is required.

Starting with the perturbation series for a QCD observable of zero mass dimension, which depends upon a single energy scale $\mathcal{R}(Q)$,

$$\begin{aligned}\mathcal{R}(Q) &= a(\mu) + r_1(Q,\mu)a^2(\mu) + r_2(Q,\mu)a^3(\mu) + \cdots \\ &= a(\mu) + \sum_{n=1}^{\infty} r_n(Q,\mu)a^{n+1}(\mu) \qquad (2.44)\end{aligned}$$

The choice of renormalisation scheme (RS) fixes the values of the beta function coefficients, and so it is conceivable that the choice of RS can be identified through the choice of these coefficients. In fact it has been shown [15] that the RS-dependence can be parametrised through the choice of $\tau = b\ln(\mu/\tilde{\Lambda})$ and the scheme-dependent beta function coefficients $c_2, c_3, \cdots$, allowing the RS dependence of the r_n to be obtained through their derivatives with respect to $\tau, c_2, c_3, \cdots$. It was shown in [15] that a series truncated above the a^{n+1} term has a scheme dependence from $\tau, c_2, c_3, \cdots$ of order a^{n+2} which is cancelled by higher order terms. If there was some extra parameter determining the RS dependence of the series coefficients then the scheme dependence of the truncated series would no longer be of order a^{n+2}, and the cancellation with the scheme dependence of higher order terms would be lost.

Because $\mathcal{R}$ must be RS independent we know that if the sum in Eq.(2.44) is truncated so that we set $r_n = 0$, $n \geq m$, then the sum we are left with can only have an RS dependence of order a^{m+1} or higher. If we vary one of the RS parameters but keep the others constant we can obtain the partial derivatives with respect to that parameter.

Consider the solution to the beta function equation

$$\int_0^a \frac{dx}{\beta(x)} + k = \ln(\mu/\Lambda) \ , \tag{2.45}$$

where k and Λ are constants. Partially differentiating this with respect to the RS parameters will tell us how a depends on the RS parameters [43].

$$\begin{aligned} \frac{\partial a}{\partial \tau} &= \frac{\beta(a)}{b} \\ \frac{\partial a}{\partial c_n} &= -b\beta(a)\int_0^a \frac{x^{n+2}}{(\beta(x))^2}\, dx \ . \end{aligned} \tag{2.46}$$

Expanding these in powers of a and demanding that the RS dependence of $\mathcal{R}(Q)$ cancels order by order we first arrive at the following equations for r_1

$$\begin{aligned} \frac{\partial r_1}{\partial \tau} &= 1 \ , \\ \frac{\partial r_1}{\partial c_n} &= 0 \ , \end{aligned} \tag{2.47}$$

solving these equations one obtains

$$r_1 = \tau - \rho_0 \ . \tag{2.48}$$

The constant ρ_0 is an RS-invariant constant of integration [15]. Finding the partial derivatives for the other r_n with r_1 replacing τ gives [15]

$$\begin{aligned} \frac{\partial r_2}{\partial r_1} &= 2r_1 + c, \ \frac{\partial r_2}{\partial c_2} = -1, \\ \frac{\partial r_3}{\partial r_1} &= 3r_2 + 2cr_1 + c_2, \ \frac{\partial r_3}{\partial c_2} = -2r_1, \ \frac{\partial r_3}{\partial c_3} = -1/2 \ . \end{aligned} \tag{2.49}$$

Note that for each r_n we have $\partial r_n/\partial c_{m>n} = 0$. Integrating the partial derivatives we arrive at [22]

$$\begin{aligned} r_2 &= r_1^2 + r_1 c - c_2 + X_2, \\ r_3 &= r_1^3 + 5/2cr_1^2 + 3X_2 r_1 - 2r_1 c_2 - c_3/2 + X_3 \\ r_n &= f_n(r_1, c_2, \cdots, c_n) + X_n. \end{aligned} \tag{2.50}$$

The function f_n represents the renormalisation group (RG) predictable parts obtained from all the previous parts of the perturbation series. That is, if we have a RS-independent series then the $r_n a^{n+1}$ part of the series will have a part that cancels the a^{n+1} part of the RS-dependence of the previous parts of the series. This part of r_n is represented above by the function f_n. The X_n are Q-independent constants of integration; they cannot depend on the choice of RS, as the RS dependence is contained in the integration.

Next we express our quantity $\mathcal{R}(Q)$ in terms of RG-predictable parts and the X_n

$$\begin{aligned}\mathcal{R}(Q) &= a + r_1 a^2 + [(r_1^2 + r_1 c - c_2) + X_2]a^3 \\ &\quad + [(r_1^3 + 5/2 c r_1^2 - 2 r_1 c_2 - c_3/2) + X_2(3r_1) + X_3]a^4 + \cdots \,. \end{aligned} \tag{2.51}$$

All the parts not containing the RS invariant X_n when summed up will themselves be RS invariant. Similarly all the terms with an X_2 will sum to something RS invariant, and those with an X_3, etc. What CORGI does is to include this summing up of the RS dependence in the coupling [22]. Looking at the parts that do not include the X_n we can sum these up into a new CORGI coupling a_0

$$a_0 = a + r_1 a^2 + (r_1^2 + r_1 c - c_2)a^3 + (r_1^3 + 5/2 c r_1^2 - 2 r_1 c_2 - c_3/2)a^4 + \cdots \,. \tag{2.52}$$

This CORGI coupling is equivalent to the choice of RS where $r_1 = c_2 = c_3 = c_n = 0$ [22]. Realising that, we see from Eq.(2.51) that our perturbation series for $\mathcal{R}(Q)$ becomes

$$\mathcal{R}(Q) = a_0(Q) + X_2 a_0^3(Q) + X_3 a_0^4(Q) + \cdots \,. \tag{2.53}$$

By considering the equivalent choice of RS and substituting the above series into Eq.(2.39), relations between the X_n and the ρ_n can be obtained, for example $X_2 = \rho_2$, $X_3 = \rho_3/2$.

The coupling $a_0(Q)$ now depends on the physical scale Q; this comes from the Q-dependence of the RS dependent parts of the r_n. The μ dependence cancels out: to illustrate this consider taking the derivative with respect to

$\ln \mu$

$$\mu \frac{\partial a_0}{\partial \mu} = \beta(a) + 2a\beta(a)r_1 + ba^2 + 3a^2\beta(a)(r_1^2 + cr_1 - c_2) + (2br_1 + cb)a^3 + \mathcal{O}(a^4) \; . \tag{2.54}$$

The a^2 and the a^3 terms are zero in this expression, and if we included the higher order terms we would see that this is also true for those terms with a^4, a^5, etc.

The CORGI approach is equivalent to the effective charge approach at NLO [19,20]. In the Effective Charge approach the beta function of the renormalisation scheme that sets all the perturbation series coefficients ($r_1, r_2,$ etc) to zero is chosen. This means that the observable itself has a beta function, and the ρ_n of Eq.(2.39) are the same as the beta function coefficients c_n. Solving Eq.(2.39) at NLO gives $R(Q)$ in the same form as the CORGI series at NLO.

2.6 Summary

Higher-order corrections in perturbative QFT's can diverge due to the integration over unfixed loop momenta. The solution to this problem is to renormalise the parameters of the theory in the Lagrangian.

The divergences are first regularised through some mechanism such as dimensional regularisation. This isolates the divergences, and the relevant rescaling of the parameters in the Lagrangian, through the renormalisation constants, will then cancel out the unwanted divergences.

A problem with renormalisation is that there are an infinite number of ways (schemes) of renormalising a theory, and different schemes of renormalisation can lead to different results for calculations such as a truncated perturbation series. The finite renormalisations that move from one scheme to another make up the renormalisation group. Any physical observable should be invariant under a transformation of the renormalisation group, as renormalisation is just a way of making sense of a calculation and different schemes do not have direct physical significance.

When renormalising, a new parameter appears that has a mass dimension. The renormalised coupling depends upon such a scale, the scale dependence being given via the coupling's beta function. Although an observable does not depend upon this scale a similar dependence upon some physical scale can be found from the coupling's beta function and the observable's dependence on the coupling. The Effective Charge beta function determines the dependence of an observable on the physical energy scale, Q, much in the same way as the beta function determines the renormalisation scale dependence of the coupling.

The scale dependence of both the coupling and an observable are characterised by the ratio of the scale to some parameter that comes from the constant of integration when the beta function is solved.

A truncated perturbation series depends upon the choice of renormalisation scheme. In order for the whole series to be independent of the method of renormalisation there is a renormalisation-group-predictable part in each series coefficient that is required to cancel out the scheme dependence from the coefficients at lower orders in the series. Complete Renormalisation Group Improvement (CORGI) sums these predictable parts into the scheme-invariant CORGI coupling, leaving behind a series with scheme-invariant coefficients.

Chapter 3

Divergent Series And Renormalons

3.1 Introduction to divergent series

In this chapter we give a short introduction to renormalons. A review of this aspect of QFT can be found in reference [22].

We would like perturbation theory to be convergent, as this would allow us to reach any level of accuracy for a calculation provided we calculate to a high enough order. However, it turns out that the perturbation series diverge for any case of interest to this thesis.

A simple explanation of why a perturbation series will diverge in QED was given by Dyson [23]. Consider a perturbation series for a measurable quantity $R(\alpha)$

$$R(\alpha) = r_0\alpha + r_1\alpha^2 + r_2\alpha^3 + \cdots \ , \tag{3.1}$$

this is a standard QED perturbation series that would be obtained from Feynman diagrams. Assuming that for a small enough value of α this series will converge it follows that $R(\alpha)$ is an analytic function at $\alpha = 0$. For a small enough value of $|\alpha|$ the quantity $R(-|\alpha|)$ will be an analytic function with a convergent series.

However, having a well-behaved theory for negative values of α leads to problems. Consider a system of N charged particles: the energy of such a system is given by

$$E \approx NT + \frac{1}{2}\alpha V N^2 \tag{3.2}$$

where T is the mean kinetic energy of a particle, and αV is the mean potential energy associated with a pair of particles. For a positive value of α Eq.(3.2) rises monotonically with N, whereas for a negative value of α there is a maximum value for the energy for some value of N. Beyond this critical value of N the energy will always decrease with increasing N, and for a high enough value of N the energy of Eq.(3.2) will drop below the energy of the vacuum. In the case of negative α the vacuum is unstable and will, through quantum tunnelling effects, eventually decay into regions of charged particles of the same sign of charge. With an unstable vacuum $R(\alpha)$ would not be an analytic function for negative α, and so by the argument given above, the perturbation series of Eq.(3.1) cannot be convergent for any non-zero α.

This means that we deal with a divergent series and the level of accuracy is now determined by the size of the coupling. Consider a simple perturbation series F for an observable dependent on a single coupling α

$$F = f_0\alpha + f_1\alpha^2 + f_2\alpha^3 + \cdots \ , \tag{3.3}$$

with $f_n = A\kappa^n n!$. Here A and κ are just constants. The series has zero radius of convergence about $\alpha = 0$. As we calculate each partial sum starting with f_0, then f_1 etc, the series will appear to converge until we reach the f_n such that $|f_n|/|f_{n-1}| \geq 1/\alpha$. For the series given above this occurs when $n \geq 1/(\kappa\alpha)$, so the size of the coupling clearly limits how accurately we can evaluate this series.

Although this series is not convergent, it may be asymptotic. That is for a region in the complex α-plane we can state how closely the observable is approximated by the series when it is truncated to any order. To be more specific there exist a set of numbers K_N, which for a region in the complex α-plane obey

$$\left| F' - \sum_{n=0}^{N} f_n \alpha^{n+1} \right| < K_N |\alpha^{N+1}| \ . \tag{3.4}$$

Here F' is the quantity to which the series F is asymptotic. The K_N reveal where to truncate to obtain the most accurate result from the perturbation series. In QCD there is no non-perturbative definition of our quantity and so we can't say if our series is asymptotic or not.

3.2 Borel integral and renormalons

We would like to be able to evaluate the series in Eq.(3.3). The method we employ throughout this thesis to evaluate such series will be Borel summation. We evaluate this series through the Borel Integral

$$F = \int_0^\infty B[F](z) \exp(-z/\alpha) \, dz \, , \tag{3.5}$$

where $B[F](z)$ is the Borel transform defined by

$$B[F](z) = \sum_{k=0}^{\infty} \frac{f_k z^k}{k!} \, . \tag{3.6}$$

This is based upon the integral

$$\int_0^\infty \exp(-z/\alpha) z^n \, dz = n! \alpha^{n+1} \, . \tag{3.7}$$

Considering the coefficients $f_n = A(-\kappa)^n$, the Borel transform is

$$B[F](z) = A \sum_{k=0}^{\infty} \frac{(-\kappa z)^k}{k!} = A \exp(-\kappa z) \, , \tag{3.8}$$

Evaluating the integral we arrive at

$$\int_0^\infty \exp(-z/\alpha) A \exp(-\kappa z) \, dz = \frac{A\alpha}{1+\alpha\kappa} \, . \tag{3.9}$$

This result has the same perturbation series in α as the series given by the f_n. In general if the series in α has a finite radius of convergence the Borel sum defined from the integral will equal the conventional sum of the series. Such summation methods are said to be regular. In such a case the Borel transform will have a series in z that is convergent for any value of z. This convergent series is then summed up inside the Borel integral, and the integral will return the result for the perturbation series. If the original series has zero radius of convergence in α, then the Borel transform has a finite radius of convergence and must be analytically continued beyond its radius of convergence to define the Borel integral.

The technique of using a perturbation series and evaluating it with the Borel integral does not give the value of its corresponding observable. Consider the quantity $\tilde{F} = \frac{A\alpha}{1+\kappa\alpha} + \exp(-1/\alpha)$: this differs in value from F but has the same perturbation series. Using the Borel integral $\tilde{F}$ is evaluated to be the same as F. Non-perturbative terms like $\exp(-1/\alpha)$ are invisible to this technique.

Cases where the perturbation series has zero radius of convergence are of interest, and so one can try to use the Borel integral to obtain a result. For example the series with coefficients $f_n = A(-\kappa)^n n!$ has zero radius of convergence, but it does have a Borel transform

$$B[F](z) = A\sum_{k=0}^{\infty}(-\kappa z)^k = \frac{A}{1+\kappa z} \; . \tag{3.10}$$

The Borel integral is then

$$\int_0^{\infty} \exp(-z/\alpha)\frac{A}{1+\kappa z} = -\frac{A}{\kappa}\exp(1/(\kappa\alpha))Ei(-1/(\kappa\alpha)) \; . \tag{3.11}$$

Where $Ei(x)$ is the exponential integral function

$$Ei(x) = -\int_{-x}^{\infty} \frac{\exp(-t)}{t}\, dt \; . \tag{3.12}$$

The Borel integral here is unambiguous, but in the next example we shall see a Borel integral that is ambiguous.

Consider the coefficients $f_n = A\kappa^n n!$. In this case the Borel transform is

$$B[F](z) = A\sum_{k=0}^{\infty}(\kappa z)^k = \frac{A}{1-\kappa z} \; , \tag{3.13}$$

Evaluating the integral we arrive at

$$\int_0^{\infty} \exp(-z/\alpha)\frac{A}{1-\kappa z}\, dz = \frac{A}{\kappa}\exp(-1/(\kappa\alpha))Ei(1/(\kappa\alpha)) \; . \tag{3.14}$$

The integrand has a simple pole at $z = 1/\kappa$, which leads to the Borel integral not being exactly defined if $\kappa > 0$. Poles in the Borel plane arising from factorial divergence in a perturbation series are known as renormalons.

Analytically continuing $Ei(x)$ off the negative x-axis leaves us with an ambiguity that depends upon how we integrate around the pole at $t = 0$. This leaves us with an ambiguous term in our evaluation of the series proportional to the residue, $A/\kappa \exp(-1/(\kappa\alpha))$. This ambiguous term is non-perturbative in nature, and it is thought that ambiguities in non-perturbative contributions to an observable will cancel with this renormalon ambiguity. This is indeed the case in the O(N) σ-model [24, 25].

In QFT one expects branch point singularities in the Borel plane [26, 27], giving a Borel transform of the form

$$B[F](z) = \frac{A}{(1-\kappa z)^{1+\gamma}} \ . \tag{3.15}$$

The Borel transform above corresponds to a series with the coefficients $f_n = A\kappa^n (n+\gamma)!/\gamma!$. In the limit of large n where the factorial divergence dominates these coefficients are approximately $f_n \approx A\kappa^n n^\gamma n!/\gamma!$. Note that $\gamma!$ for a non-integer γ is evaluated using the gamma function

$$\gamma! = \Gamma(\gamma+1) = \int_0^\infty e^{-t} t^\gamma \, dt \ . \tag{3.16}$$

The ambiguity in the Borel integral is the difference between integrating above and below the branch point.

3.3 QED example

Diagrams like those in figure 3.1 give rise to factorial divergences in QED. The diagrams have a chain of fermion loops inserted into an internal photon propagator. Because of the $2n$ fermion photon vertices these diagrams have an α^n contribution. Taking the propagator and inserting n loops into it leads to a factorial divergence [28, 29].

These diagrams are part of the photon vacuum polarisation in QED and so taking the derivative of the logarithm of the momentum of the external

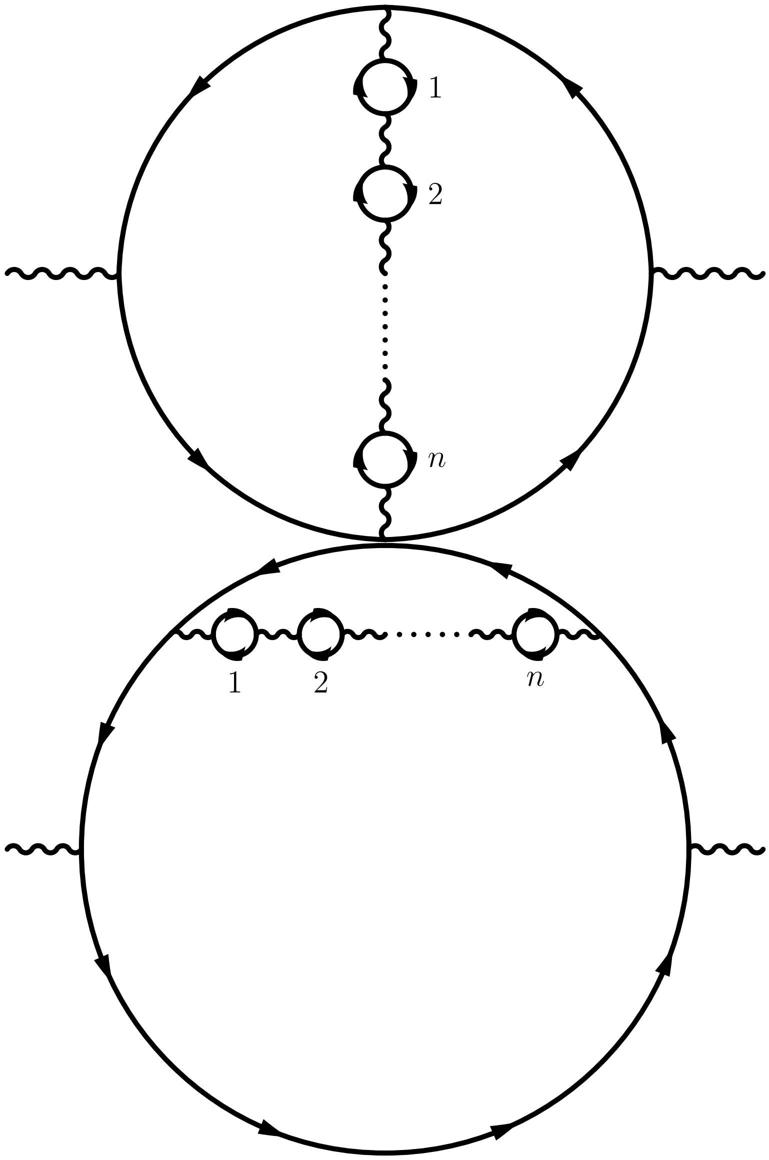

Figure 3.1: Contributions to divergent series in QED

photons will produce a term that contributes to the Adler D-function when shifting from QED to QCD. The logarithmic derivative of these diagrams is then of interest.

The contribution from the logarithmic derivative of the n-chain diagrams is proportional to [22]

$$\int_0^\infty \frac{dk^2}{k^2} F(k^2) \left[\beta_0 \alpha \left(\ln \left(k^2 \frac{Q^2}{\mu^2} \right) + C \right) \right]^n , \tag{3.17}$$

where unit charges are assumed.

The term in the square brackets comes from the renormalised fermion loop, with the renormalisation scale μ. There are n loops, and that leads to the loop term being taken to the power of n. The scale Q^2 is related to the external momentum q, $Q^2 = -q^2$. The dimensionless scale k is the ratio $k^2 = \tilde{k}^2/Q^2$, $\tilde{k}$ is the momentum flowing through the photon chain. $F(k^2)$ is a function of the scale k^2. The constant C depends upon the choice of renormalisation scheme, and for the $\overline{MS}$ scheme $C = -5/3$.

Consider the case where n is large. Then for $Q^2 \sim \mu^2$ the fermion-loop part will cause the large and small k^2 parts of the integrand to dominate. The function $F(k^2)$ in the large and small k^2 limits is

$$\begin{aligned} F(k^2) &= Ak^4 + \mathcal{O}(k^6 \ln k^2) \quad \text{small } k^2 , \\ F(k^2) &= \frac{1}{k^2}\left(B \ln k^2 + B'\right) + \mathcal{O}(\frac{\ln k^2}{k^4}) \quad \text{large } k^2 , \end{aligned} \tag{3.18}$$

where A, B, and B' are constants [30]. Splitting the integral in Eq.(3.17) at the point where the fermion loop term vanishes, and inserting the small and large k^2 approximations for $F(k^2)$ gives the integral to be

$$\begin{aligned} &\frac{A}{2}\left(\frac{Q^2 e^C}{\mu^2}\right)^{-2} \left(-\frac{\beta_0 \alpha}{2}\right)^n n! \\ &\qquad + B\frac{Q^2 e^C}{\mu^2}(\beta_0\alpha)^n n! \left(n + 1 + \frac{B'}{B} - \ln\left(\frac{Q^2 e^C}{\mu^2}\right)\right) , \end{aligned} \tag{3.19}$$

For a large enough n factorial divergence takes over.

For diagrams with more than one chain it is not hard to see that the factorial growth will not be as strong for the same order in α.

When calculating the diagrams in figure 3.1 the momentum flowing through the chain of fermion loops is integrated over. The second term of (3.19) (the part proportional to B) comes from the region of that integration where the momentum is large; these contributions are known as ultraviolet (UV) renormalons. The other terms come from the region of integration where the momentum is small (the part proportional to A); these contributions are known as infrared (IR) renormalons. The term "renormalon" was introduced by 't Hooft in [29].

3.4 Renormalons in the Adler function

3.4.1 Perturbation series for $\mathcal{D}$

Moving to QCD, the photons are replaced by gluons and the fermions are quarks. Such diagrams contribute to the Adler D-function and are shown in figure 3.2.

The Adler D-function defined earlier in Eq.(1.96) can be related to a QCD quantity $\mathcal{D}$, as we shall see later:

$$D = N \sum_f Q_f^2 (1 + \mathcal{D}) + \left(\sum_f Q_f \right)^2 \tilde{\mathcal{D}} \; , \tag{3.20}$$

where f represents a flavour of quark with electric charge Q_f. The term $\tilde{\mathcal{D}}$ is "the light-by-light" contribution and will be introduced in the next chapter. $\mathcal{D}$ can be split into a perturbation series, $\mathcal{D}_{PT}(Q^2)$, and a non-perturbative Operator Product Expansion (OPE) part, $\mathcal{D}_{NP}(Q^2)$,

$$\mathcal{D}(Q^2) = \mathcal{D}_{PT}(Q^2) + \mathcal{D}_{NP}(Q^2) \; , \tag{3.21}$$

$\mathcal{D}_{PT}(Q^2)$ can be expressed as a power series in the QCD coupling.

$$\mathcal{D}_{PT}(s) = \sum_{n=0}^{\infty} d_n(s, \mu^2) a^{n+1}(\mu^2) \; . \tag{3.22}$$

Note that s is the physical scale associated with the Adler D-function, and

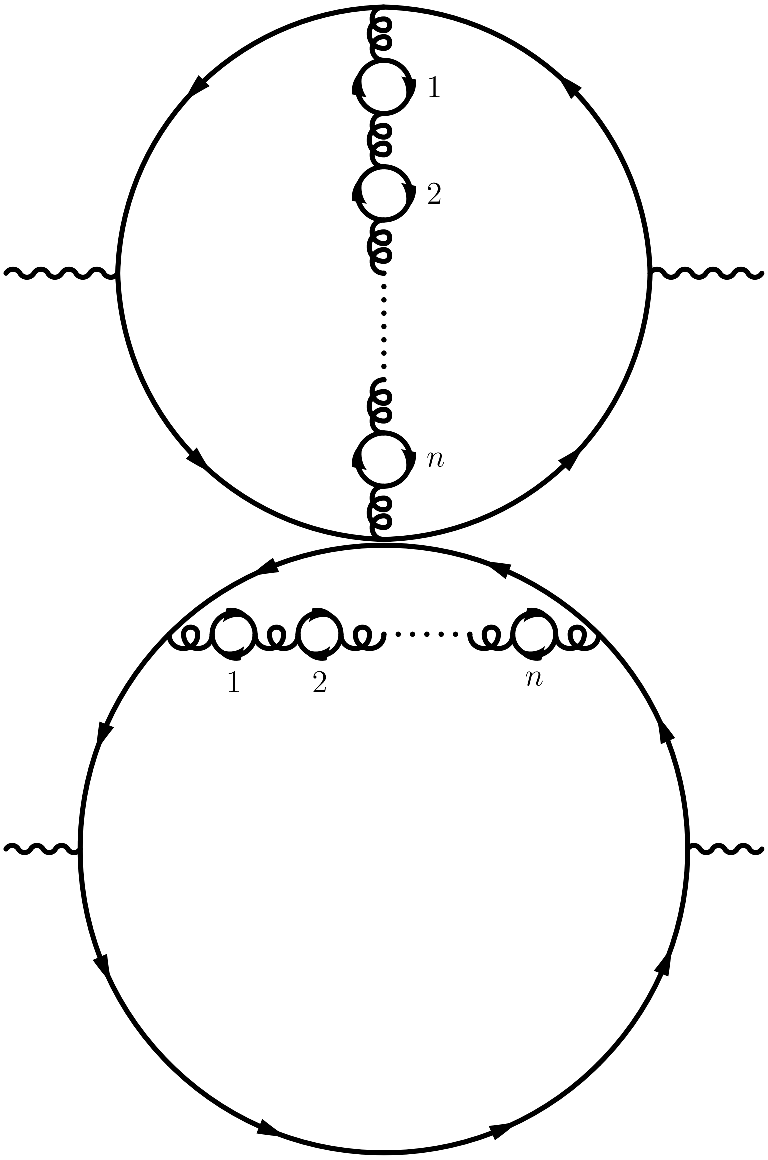

Figure 3.2: Contributions to divergent series in QCD

μ is the renormalisation scale. This perturbative part has the Borel integral

$$\mathcal{D}_{PT}(Q^2) = \int_0^\infty B[\mathcal{D}](z)e^{-z/a}\,dz\ . \tag{3.23}$$

In section 1.12 the OPE was introduced, the non-perturbative OPE contribution for $\mathcal{D}$ is

$$\mathcal{D}_{NP}(Q^2) = \sum_n \frac{C_n(Q^2,\tilde{\mu}^2) < O_n(\tilde{\mu}^2) >}{Q^{2n}}\ , \tag{3.24}$$

where the sum is over the relevant operators O_n of dimension $2n$. $\tilde{\mu}$ denotes the scale that factorises out the short-distance perturbative effects from the long-distance non-perturbative effects, and C_n is the coefficient function. For the Adler D-function the relevant operator of lowest dimension is the dimension four gluon condensate,

$$< 0|F^a_{\mu\nu}F^{\mu\nu}_a|0 >\ . \tag{3.25}$$

Factorising out the dimensionful scale $\tilde{\Lambda}^{2n}$ from the operator expectation value, and combining with the coefficient function, the $\mathcal{D}_{NP}(Q^2)$ component can be written as an expansion in $\tilde{\Lambda}^2/Q^2$ with overall coefficients $\mathcal{C}_n$

$$\mathcal{D}_{NP}(Q^2) = \sum_n \mathcal{C}_n\left(\frac{\tilde{\Lambda}^2}{Q^2}\right)^n\ . \tag{3.26}$$

These coefficients are themselves series expansions in the coupling a,

$$\mathcal{C}_n = Ka^{\delta_n}[1+\mathcal{O}(a)]\ , \tag{3.27}$$

where δ_n is related to the anomalous dimension of the operator O_n.

The n fermion loops in the chain give the dependence on the number of flavours of quarks to be N_f^n, where N_f is the number of flavours of quarks considered. Diagrams with extra chains will have a lower power of N_f at the same order in perturbation theory, and additional gluon propagators increase the power of the coupling, but not the power of N_f. The contribution to the Adler D-function from figure 3.2 gives the largest power contribution from N_f, and so in the large-N_f limit these diagrams give the coefficients in the perturbation series. In other words, if the series coefficients are written as

$$d_n = \sum_{k=0}^{n} d_n^{[k]} N_f^k \;, \tag{3.28}$$

then the diagrams of figure 3.2 give the value $d_n^{[n]}$.

The diagrams of figure 3.2 increase in value as a factorial in the number of fermion loops, as in the QED case, and if the contributions of this type of diagram are to be considered to all orders, then a resummation method such as the Borel integral is required.

3.4.2 Leading-b approximation

In QED the diagrams of figure 3.1 would include all diagrams with one chain within the fermion loop. However, in QCD the loops can also contain gluons and ghosts and so a large-N_f approximation will not cover all the loops in the gluon chain. With these new loops comes a dependence upon the gauge parameter, which the Adler D-function, order-by-order in the perturbation series, will not depend upon.

One approach is to replace the series in N_f for each coefficient d_n with a series in the first QCD beta function coefficient b. As the QED case has the first beta function coefficient to the power of n when there are n loops in the photon chain, expressing the QCD case in terms of its first beta function coefficient may describe the case for n loops in the gluon fairly well. Firstly the coefficients written as a series in N_f are re-written as a series in the first beta function coefficient b through the relation

$$N_f = -3b + \frac{11}{2} N \;, \tag{3.29}$$

where N is the number of colours ($N = 3$ for QCD). This allows each coefficient d_n to be expressed as a series in b, and if the leading-N_f series is known then this leading-b series can be calculated as well.

Simply replacing the known leading-N_f term with $-3b + 11N/2$ and taking the leading-b term in the hope that it will describe the single gluon chain diagrams needs some justification. Such a substitution is sometimes called naive nonabelinisation (NNA). It should be noted that the result of this substitution is not equivalent to a set of diagrams.

One advantage of a leading-b series is that it is independent of the choice of renormalisation scale when a one-loop beta function is used. This scale invariance can be seen from the scale invariance of the full perturbation series

$$\mu\frac{d}{d\mu}\left(\sum_{n=0}^{\infty} d_n a^{n+1}\right) = 0 \; . \tag{3.30}$$

In Eq.(3.30) the term $a^{n+1}\mu\frac{d}{d\mu}d_n$ will cancel with all other terms of order a^{n+1}. With just a one-loop beta function this gives

$$\mu\frac{d}{d\mu}d_n = nbd_{n-1} \; . \tag{3.31}$$

This will apply as well to the leading-b coefficients, making the perturbation series scale invariant when only constructed out of them.

Further justification for the leading-b series comes from considering the full gluon propagator within the quark loop of figure 3.2.

Using all the different loops in the gluon propagator instead of just the fermion loop the gluon vacuum polarisation is then used n times. At one loop the gluon vacuum polarisation is [31]

$$\begin{aligned}\Pi_{\text{gluon}}(k^2) = a(\mu^2)\Bigg[&-\frac{b}{2}\left(\ln\left(\frac{k^2}{\mu^2}\right)-\frac{5}{3}\right)\\ &+\frac{N}{3}\left(1-\frac{3}{16}(1-\xi_{BFM})(7+\xi_{BFM})\right)\Bigg] \; ,\end{aligned} \tag{3.32}$$

where the $\overline{MS}$ scheme has been chosen. The background field method (BFM) has been used to make this calculation; this is where the field has been split into a classical background field and a quantum field, and an effective Lagrangian for the quantum field is created. ξ_{BFM} is the BFM gauge parameter. The BFM does not work for nested loops, as the background field does not propagate inside the loops. The gauge parameter dependence can be absorbed into the logarithm for a suitable choice of renormalisation scale. Any scale-invariant quantity calculated in the leading-b approximation, such as $d_2 - d_1^2$ which in the leading-b case is the Effective Charge beta function coefficient ρ_2 (Eq.(2.39)), will then be independent of ξ_{BFM}.

The leading-N_f coefficient $d_n^{[n]}$ is given by references [32–34] in terms of the V-scheme [35]. This is the $\overline{\mathrm{MS}}$-scheme with $\mu = e^{-5/6}Q$, which sets $Q^2 e^C/\mu^2 = 1$ in Eq.(3.19). Here μ is the renormalisation scale, and Q is the physical scale (i.e. $D(Q^2)$). In this scheme

$$\begin{aligned} d_n^{[n]}(V) &= \frac{-2}{3}(n+1)\left(-\frac{1}{6}\right)^n \left[-2n - \frac{n+6}{2^{n+2}}\right. \\ &+ \left.\frac{16}{n+1}\sum_{\frac{n}{2}+1>m>0} m(1-2^{-2m})(1-2^{2m-n-2})\zeta_{2m+1}\right] n! \quad (3.33) \end{aligned}$$

Expressing each coefficient, d_n, as an expansion in the first beta function coefficient (b) one obtains

$$d_n = d_n^{(n)} b^n + d_n^{(n-1)} b^{n-1} + \ldots + d_n^{(0)} \; . \quad (3.34)$$

Using Eq.(3.29) $d_n^{(n)} = (-3)^n d_n^{[n]}$, so the leading large-$b$ coefficient can then be calculated to all orders

$$\begin{aligned} d_n^{(n)}(V) &= \frac{-2}{3}(n+1)\left(\frac{1}{2}\right)^n \left[-2n - \frac{n+6}{2^{n+2}}\right. \\ &+ \left.\frac{16}{n+1}\sum_{\frac{n}{2}+1>m>0} m(1-2^{-2m})(1-2^{2m-n-2})\zeta_{2m+1}\right] n! \, . \quad (3.35) \end{aligned}$$

To arrive at a function to which the perturbation series, $\mathcal{D}_{PT}$, is asymptotic Borel summation is used. The leading-b part of $\mathcal{D}_{PT}$ will be represented by $\mathcal{D}_{PT}^{(L)}$; this has the perturbation series

$$\mathcal{D}_{PT}^{(L)} = a + d_1^{(1)} b a^2 + d_2^{(2)} b^2 a^3 + \cdots = \sum_n d_n^{(L)} a^{n+1} \; , \quad (3.36)$$

Where the leading-b coefficients are (then) $d_n^{(L)} \equiv d_n^{(n)} b^n$ and are used to approximate d_n.

The leading-b result for the Borel transform of the Adler-D function in the

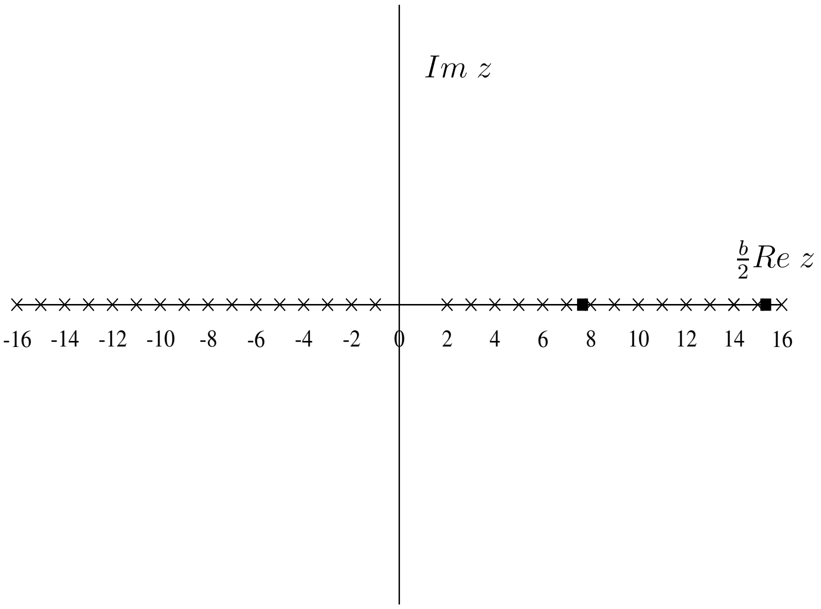

Figure 3.3: Singularities in the Borel plane for the Adler D-function with the number of flavours chosen to be 5 corresponding to $b = 23/6$.

V-scheme can then be obtained from Eq.(3.35) [36].

$$B[\mathcal{D}^{(L)}](z) = \sum_{j=1}^{\infty} \frac{A_0(j) + zA_1(j)}{(1+\frac{z}{z_j})^2} + \frac{B_0(2)}{(1-\frac{z}{z_2})} + \sum_{j=3}^{\infty} \frac{B_0(j) + zB_1(j)}{(1-\frac{z}{z_j})^2}\ , \quad (3.37)$$

where $z_j = 2j/b$.

The residues of the UV_j poles, $A_0(j)$ and $A_1(j)$, are given by [36]

$$A_0(j) = \frac{8}{3}\frac{(-1)^{j+1}(3j^2+6j+2)}{j^2(j+1)^2(j+2)^2} \quad A_1(j) = \frac{4}{3}\frac{b(-1)^{j+1}(2j+3)}{j^2(j+1)^2(j+2)^2}\ . \quad (3.38)$$

The IR_j residues, $B_0(j)$ and $B_1(j)$, are directly related to the UV_j ones, with $B_0(j) = -A_0(-j)$ and $B_1(j) = -A_1(-j)$ for $j > 2$. $B_0(1) = B_1(1) = B_1(2) = 0$, and $B_0(2) = 1$.

In figure 3.3 the singularities in the Borel plane are shown. The crosses represent the renormalon singularities, whereas the squares represent instantons. Instantons are non-perturbative effects that are linked to the factorial growth of the number of diagrams with the order in a perturbation series.

The singularity due to the first instanton contribution in this case has been calculated to have a branch point of the form $(1-z/4)^{11(N-N_f)/6}$ [37]. The location of the IR renormalons on the positive z-axis means that a choice for the prescription for integrating around these poles in the Borel plane must be made. These ambiguities are of the form as in section 3.2 when $\kappa > 0$. The locations of the IR renormalons give a dependence on the energy scale that corresponds exactly with that of the terms in the OPE, as would be expected if the ambiguities are to be cancelled out.

It is easy to check that, taking $\mathcal{D}$ in the Borel integral to be a generic QED or QCD observable with branch-point singularities $(1-z/z_k)^{-\gamma_k}$ in the Borel plane, the resulting ambiguity for the singularity at $z = z_k$ is of the form

$$\Delta\mathcal{D}_{PT} \sim Ke^{-|z_k|/a(Q^2)}a^{1-\gamma_k} \ , \tag{3.39}$$

where K is complex.

Using the one-loop form $a(Q^2) = 2/b\ln(Q^2/\tilde{\Lambda}^2)$, for the coupling after some choice of scale has been chosen to obtain the Borel integral, one finds that in the QCD case,

$$\Delta\mathcal{D}_{PT} \approx K a^{1-\gamma_k}\left(\frac{\tilde{\Lambda}^2}{Q^2}\right)^k . \tag{3.40}$$

This has exactly the same structure as a term in the OPE expansion shown in Eq.(3.26). It should be noted that in both cases the $\left(\frac{\tilde{\Lambda}^2}{Q^2}\right)^k$ terms start at the $k = 2$ term and not $k = 1$. The first IR renormalon is not located as one might expect at $z = 2/b$, but at $z = 4/b$, and in the OPE the first term that contributes to $\mathcal{D}_{NP}$ is the mass-dimension-four gluon condensate. The idea is that the coefficient function, in particular the constant K, is ambiguous in the OPE because of non-logarithmic UV divergences [24, 38]. This ambiguity can be compensated by the IR renormalon ambiguity in the PT Borel integral, and so regulating the Borel integral, using for instance a principal-value (PV) prescription, induces a particular definition of the coefficient functions in the OPE, and the PT and OPE components are then separately well-defined. That this scenario works in detail can be confirmed in toy models such as the non-linear $O(N)$ σ-model [24,25]. For the QED case the ambiguity corresponds to a $Q^2/\tilde{\Lambda}^2$ effect, so all-orders QED perturbation theory is only defined if there are in addition power corrections in Q^2. Such effects are only important if $Q^2 \sim \tilde{\Lambda}^2$. Here $\tilde{\Lambda}$ corresponds to the Landau ghost in QED, $\tilde{\Lambda}^2 \sim 10^{560} m^2$, with m the fermion mass. Thus in QED such power corrections can have no phenomenological consequences and can be completely ignored.

The leading-b Borel integral for the Adler D-function can be solved in terms of the exponential integral function. The solution for the UV renormalons is [36],

$$\mathcal{D}_{PT}^{(L)}(s)|_{UV} = \sum_{j=1}^{\infty} z_j \{ e^{z_j/a_V(s)} Ei(-z_j/a_V(s)) \\ [z_j/a_V(s)(A_0(j) - z_j A_1(j)) - z_j A_1(j)] + (A_0(j) - z_j A_1(j)) \} \;, \quad (3.41)$$

where $a_V(s)$ is the V-scheme coupling.

The exponential integral function is defined in Eq.(3.12)

For the IR renormalons a choice for the prescription for integrating around the poles along the positive z-axis in the Borel plane must be made. This prescription will manifest itself in how $Ei(x)$ is defined for positive x. For now the principal-value prescription is chosen, which corresponds to $Ei(x)$ being real for a real, positive argument. Performing the Borel integral one obtains,

$$\mathcal{D}_{PT}^{(L)}(s)|_{IR} = e^{-z_2/a_V(s)} z_2 B_0(2) Ei(z_2/a_V(s)) \\ + \sum_{j=3}^{\infty} z_j \{ e^{-z_j/a_V(s)} Ei(z_j/a_V(s)) [z_j/a_V(s)(B_0(j) \\ + z_j B_1(j)) - z_j B_1(j)] - (B_0(j) + z_j B_1(j)) \} \;. \quad (3.42)$$

3.5 Summary

The perturbation series for some process calculated from a QFT may be divergent. In fact in QED it was shown by Dyson that the series will diverge for a non-zero coupling.

The Borel integral is used to obtain a mathematical expression containing the coupling to which the series is asymptotic. Series with a factorial divergence have zero radius of convergence in the complex coupling plane. Such a series can be evaluated using the Borel integral.

In QFT one expects on general grounds factorial growth which will have branch points (poles) in the Borel plane; these are known as renormalons. These will be evenly spread in the Borel plane, with the spacing related to b, the first beta function coefficient of the QFT. The renormalons along the positive real axis of the Borel plane will lie along the path of the Borel integral, leaving an ambiguity in its evaluation. Such ambiguities are of the same form as non-perturbative corrections found in the operator product expansion and are expected to cancel with ambiguous terms found there.

In QED a factorial growth of perturbation theory coefficients can be found when a chain of fermion loops linked by photon propagators is integrated with respect to the momentum flowing through the chain. By splitting the integral into high-and-low momentum parts the integral is estimated, giving a series with coefficients that have factorial growth. The low-momentum IR part has renormalons on the negative real axis of the Borel plane, but the high-momentum UV part has renormalons on the positive real axis, leaving the evaluation of the chain ambiguous.

A diagram with such a single chain of fermion loops will give the term with the highest power in the number of fermions at each order in the perturbation series. This means that the contribution from the single chain gives the full result in the large number of fermions (N_f) limit.

In QCD the photons are replaced by gluons, which will have gluon and ghost loops as well as fermion loops inside them. The large-N_f approximation is not guaranteed to give the dominant factorial divergence as it is in QED. One approach to deal with this is to convert the large-N_f approximation into the large-b approximation, where b is the first beta function coefficient.

A simple linear equation relates N_f and b, and the leading-b coefficient is proportional to the leading-N_f coefficient with the constant of proportionality $(-3)^n$, where n is the order of the perturbation series. Using the leading-b approximation the UV and IR renormalon contributions for the Adler D-function are found in terms of the exponential integral function.

Chapter 4

Infrared behaviour of $R_{e^+e^-}$

4.1 Introduction

Consider the QCD beta function

$$\frac{\partial a}{\partial \ln(\mu/\Lambda)} = \beta(a) \ . \tag{4.1}$$

For small enough a the beta function is negative, causing the coupling to rise for lower values of $\ln(\mu/\Lambda)$. If the beta function does not become zero for some positive value of the couping, then the coupling will continue to rise and eventually become infinite for a low enough value of μ/Λ. For a one-loop or a two-loop coupling this "Landau pole" occurs when $\mu = \tilde{\Lambda}$, as can be seen by solving Eq.(2.32).

Having an apparently infinite result from the perturbation series at some energy scale is often dealt with by assuming that the unknown non-perturbative part from the OPE will cancel out such a divergence. There are, however, other approaches that will leave the perturbative part expressed as a series of finite terms.

One method alluded to earlier is having a beta function that becomes zero for some value of the coupling a^*. The value of the coupling will rise and eventually reach the region of a^*; there the beta function will be approximately

$$\beta(a) \approx (a - a^*)\beta'(a^*) \ . \tag{4.2}$$

Solving the beta function equation around this region gives

$$(a^* - a) \propto \left(\frac{\mu}{\Lambda}\right)^{\gamma} , \tag{4.3}$$

$\gamma = \beta'(a^*)$ is a constant which is positive in order to keep $\beta(a) < 0$ for $a < a^*$. The result of Eq.(4.3) is that for $a = a^*$ the scale μ must be zero, and so the coupling never becomes infinite.

In this chapter a method of summing the extra terms that come from the analytical continuation of the Adler D-function when calculating the R-ratio is demonstrated. This leaves behind a series of terms that are finite for any choice of scale, but when expanded in the coupling return the perturbation series for the R-ratio.

4.2 Landau divergence of $\mathcal{R}$

Starting with the definition of the ratio $R_{e^+e^-}$, which was introduced in section 1.10, for some value of the centre of mass energy squared s,

$$R_{e^+e^-}(s) \equiv \frac{\sigma_{tot}(e^+e^- \to \text{hadrons})}{\sigma(e^+e^- \to \mu^+\mu^-)} = 3\sum_f Q_f^2(1 + \mathcal{R}(s)) + (\sum_f Q_f)^2\tilde{\mathcal{R}}(s) . \tag{4.4}$$

The sum is over the different flavours of quarks, which we take to be massless in this case, and Q_f is the electric charge of each quark. The quantity $\mathcal{R}(s)$ is the QCD correction to the parton model result, where the quarks produced by the electromagnetic interaction become part of the final-state hadrons, and in perturbative QCD it has the form,

$$\mathcal{R}(s) = \sum_{n=0}^{\infty} r_n(\mu^2, s)a^{n+1}(\mu^2) , \tag{4.5}$$

where $r_0 = 1$ [8]. The variable μ is the renormalisation scale that appears when the theory is renormalised. The coefficients up to and including r_2 have been computed in the $\overline{MS}$ scheme with $\mu^2 = s$ [39]. $\tilde{\mathcal{R}}(s)$ is the small "light-by-light" part, with a perturbation series that starts at $\mathcal{O}(a^3)$; this contribution will be taken as negligible. A diagram contributing to the light-by-light part is shown in figure 4.1

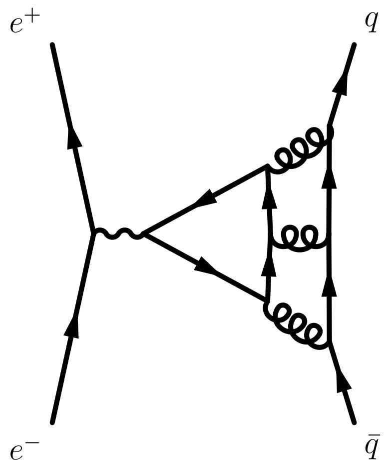

Figure 4.1: Light-by-light diagram contributing to $R_{e^+e^-}$

In section 1.11 the relation between the Adler D-function and the R-ratio was obtained through the optical theorem. This gave the R-ratio in terms of the hadronic vacuum polarisation, from which the Adler D- function is defined.

The Adler D-function is related to its QCD quantity $\mathcal{D}$ in the same way as for the R-ratio in Eq.(4.4) (as was mentioned in section 3.4)

$$D(Q^2) = 3\sum_f Q_f^2(1 + \mathcal{D}(s)) + (\sum_f Q_f)^2\tilde{\mathcal{D}}(s) \ . \tag{4.6}$$

This result was mentioned earlier in Eq.(3.20).

The relation between the Adler D-function and the R-ratio in Eq.(1.97) can be used to give us the perturbation series for $\mathcal{R}(s)$. The QCD quantity $\mathcal{D}(s)$ has a perturbation series associated with it: this series was introduced in Eq.(3.22) and takes the same form as Eq.(4.5).

Using the relation between the R-ratio and the Adler D-function in Eq.(1.97) a relation between the QCD quantities $\mathcal{R}(s)$ and $\mathcal{D}(s)$ can now be found.

$$\mathcal{R}(s) = \frac{1}{2\pi i}\int_{-s-i\epsilon}^{-s+i\epsilon} \mathcal{D}(t)\frac{dt}{t} \ . \tag{4.7}$$

Choosing a circular contour and changing variable we find,

$$\mathcal{R}(s) = \frac{1}{2\pi}\int_{-\pi}^{\pi} d\theta \mathcal{D}(se^{i\theta}) \ . \tag{4.8}$$

We have analytically continued the Adler D-function into the complex plane, with the complex variable $t = |t|e^{i\theta}$. We can expand $a(\mu^2)$ about the point $\mu = \mu'$,

$$\begin{aligned} a(\mu^2) = a(\mu'^2) \ &+ \ \ln(\mu^2/\mu'^2)\mu^2 \frac{da(\mu^2)}{d\mu^2}\bigg|_{\mu=\mu'} \\ &+ \ \frac{(\ln(\mu^2/\mu'^2))^2}{2}\mu^2\frac{d}{d\mu^2}\left(\mu^2\frac{da(\mu^2)}{d\mu^2}\right)\bigg|_{\mu=\mu'} + \cdots \ . \end{aligned} \tag{4.9}$$

Choosing $\mu^2 = xt$, $\mu'^2 = x|t| = xs$, and inserting the beta function converts this into a series in $a(x|t|)$,

$$a(xt) = a(xs) + a^2(xs)(-i\theta b/2) + a^3(xs)(-i\theta bc/2 - \theta^2 b^2/4) + \cdots \ . \tag{4.10}$$

The coefficients $d_n(s,\mu^2)$ are dimensionless and so only depend on the ratio μ'^2/s, our choice of renormalisation scale has removed the θ dependence from the coefficients. The θ dependence of $\mathcal{D}(t)$ is now made clear, and we can now integrate to obtain the perturbation series in Eq.(4.5),

$$\begin{aligned} \mathcal{R}(s) \ &= \ a(\mu'^2) + d_1(x)a^2(\mu'^2) \\ &+ \ (d_2(x) - d_0(x)\pi^2 b^2/12)a^3(\mu'^2) + \cdots \ . \end{aligned} \tag{4.11}$$

This, like the series for $\mathcal{D}(s)$, suffers from the problem of having a Landau pole in the coupling for a low enough value of μ^2. Keeping μ^2 fixed would avoid the Landau pole, but would make the series divergent, due to logarithms of μ'^2/s in the coefficients. Another point worth noting is the size of the extra analytical continuation terms introduced into the series for $\mathcal{R}(s)$: for five flavours of quark with $\mu^2 = s$ we find $d_2 = -0.681369$, $r_2 = -12.767065$ [39]. Clearly the extra terms can have a large effect. We are able to calculate these extra terms occurring in any part of $\mathcal{R}(s)$ provided they only involve coefficients of $\mathcal{D}(s)$ that have been calculated; that is we can calculate all extra terms proportional to d_0, d_1, or d_2.

We would like to be able to include all these extra terms. What follows is a mechanism to achieve this which is equivalent to the approach in [40], and also to the Analytic Perturbation Theory (APT) approach initiated by Shirkov and Solovtsov [41, 42]. In the APT approach each term in the perturbation series for the Adler D-function is transformed using Eq.(1.97). The Adler D-function is then transformed back through the inverse transform

$$D(Q^2) = Q^2 \int_0^\infty \frac{1}{(s+Q^2)^2} R(s) ds \; . \tag{4.12}$$

The inverse transform will return the whole Adler function, non-perturbative part included. However such a transform will not transform back its perturbation series $\mathcal{D}(Q^2)$ due to the pole on the real positive axis of Q^2.

For a physical choice of renormalisation scale $\mu^2 = t$, the coupling to some power is transformed into a new function $[a^n]_{an}$. For example in the case of the coupling to the power of one with a one-loop beta function

$$\begin{aligned} a(Q^2) &= \frac{2}{b \ln(Q^2/\tilde{\Lambda}^2)} \; , \\ [a]_{an}(Q^2) &= Q^2 \int_0^\infty \frac{1}{(s+Q^2)^2} \int_{-s-i\epsilon}^{-s+i\epsilon} \frac{2}{b \ln(t/\tilde{\Lambda}^2)} \frac{dt}{t} \, ds \\ &= \frac{2}{b} \frac{\tilde{\Lambda}^2}{\tilde{\Lambda}^2 - Q^2} + \frac{2}{b \ln(Q^2/\tilde{\Lambda}^2)} \; . \end{aligned} \tag{4.13}$$

The parameter $\tilde{\Lambda}$ is defined by the convention of [15] when $c = 0$. The new coupling has an extra non-perturbative part that cancels out the Landau pole. This cancellation is unsurprising, as Eq.(4.13) keeps the coupling's scale away from the region of the unphysical pole. This can be seen more clearly through the relations

$$\begin{aligned} D(Q^2) &= \frac{1}{\pi} \int_0^\infty \frac{Im[D(-t-i\epsilon)]}{t+Q^2} \, dt \; , \\ R(s) &= \frac{1}{\pi} \int_s^\infty \frac{Im[D(-t-i\epsilon)]}{t} \, dt \; . \end{aligned} \tag{4.14}$$

The unphysical pole in the perturbative part of the Adler function is evaded and a finite series for $D(Q^2)$ and $R(s)$ is obtained.

Another possibility for producing a finite infrared freezing result for the perturbative part of the R-ratio is that there is a fixed point in the Effective Charge beta function in Eq.(2.39). Consider the s-dependence of $\mathcal{R}(s)$ at NNLO,

$$s\frac{d\mathcal{R}(s)}{ds} = -\frac{b}{2}\rho(\mathcal{R}) \equiv -\frac{b}{2}\mathcal{R}^2(1 + c\mathcal{R} + \rho_2\mathcal{R}^2) \ . \tag{4.15}$$

The condition for $\mathcal{R}(s)$ to approach the infrared limit $\mathcal{R}^*$ as $s \to 0$ is for the Effective Charge beta function to have a non-trivial zero, $\rho(\mathcal{R}^*) = 0$. At NNLO the condition for such a zero is $\rho_2 < 0$. Putting $N_f = 2$ active flavours the NNLO RS invariant is found to be $\rho_2 = -9.72$, so that $\mathcal{R}(s)$ apparently freezes in the infrared to $\mathcal{R}^* = 0.43$. The freezing behaviour was first investigated in a pioneering paper by Mattingly and Stevenson [48] in the context of the Principle of Minimal Sensitivity (PMS) approach. However, it is not obvious that we should believe this apparent NNLO freezing result. In fact ρ_2 is dominated by a large $b^2\pi^2$ term arising from analytical continuation (AC) of the Adler function, with $\rho_2 = 9.40 - \pi^2 b^2/12$. Similarly the N^{3}LO invariant ρ_3 will contain the large AC term $-5c\pi^2 b^2/12$. This suggests that in order to check freezing we need to resum the analytical continuation terms to all orders.

Returning to Eq.(4.7) it is clear that the Landau pole in $a(t)$ which lies on the positive real axis is not a problem, allowing us to define $\mathcal{R}(s)$ for all s. First we will perform the θ integral of Eq.(4.8) with a suitably large value of s so that we are not bothered by the Landau pole. We shall begin by considering the "contour-improved" series for the simplified case of a one-loop coupling. The one-loop coupling will be given by

$$a(\mu^2) = \frac{2}{b\ln(\mu^2/\tilde{\Lambda}^2)} \ . \tag{4.16}$$

As described above, one can then obtain the "contour-improved" perturbation series for $\mathcal{R}(s)$,

$$\mathcal{R}(s) = \sum_{n=0}^{\infty} d_n(x) A_{n+1}(s) \ , \tag{4.17}$$

where the functions $A_n(s)$ are defined by,

$$A_n(s) \equiv \frac{1}{2\pi}\int_{-\pi}^{\pi} d\theta a^n(xse^{i\theta}) = \frac{1}{2\pi}\int_{-\pi}^{\pi} d\theta \frac{a^n(xs)}{[1 + ib\theta a(xs)/2]^n} \ . \tag{4.18}$$

Again we have set the renormalisation scale to be proportional to the physical scale $\mu^2 = xse^{i\theta}$. Eq.(4.18) is an elementary integral which can be evaluated in closed-form as [52]

$$\begin{aligned} A_1(s) &= \frac{2}{\pi b}\arctan\left(\frac{\pi b a(xs)}{2}\right) \\ A_n(s) &= \frac{2a^{n-1}(xs)}{b\pi(1-n)} Im\left[\left(1+\frac{ib\pi a(xs)}{2}\right)^{1-n}\right] \ (n>1)\ . \end{aligned} \tag{4.19}$$

We then obtain the one-loop "contour-improved" perturbation series (CIPT) for $\mathcal{R}(s)$,

$$\begin{aligned} \mathcal{R}(s) = d_0(x)\frac{2}{\pi b}\arctan\left(\frac{\pi b a(xs)}{2}\right) + d_1(x)\left[\frac{a^2(xs)}{(1+b^2\pi^2a^2(xs)/4)}\right] \\ +d_2(x)\left[\frac{a^3(xs)}{(1+b^2\pi^2a^2(xs)/4)^2}\right] + d_3(x)\left[\frac{a^4(xs)-\pi^2b^2a^6(xs)/4}{(1+b^2\pi^2a^2(xs)/4)^3}\right]\cdots . \end{aligned} \tag{4.20}$$

Each part of this series corresponds to the resummation to all orders of the infinite subset of terms in Eq.(4.5) proportional to the relevant coefficient, that is proportional to $d_0, d_1, d_2, \ldots$, etc. In each case the resummation is convergent, provided that $|a(xs)| < 2/\pi b$; this holds true for the ultraviolet, $s \to \infty$ limit, where the $A_n(s)$ vanish. For a low enough value of s we have a singularity in the coupling. However, the $A_n(s)$, if analytically continued, are well defined for all real values of s. $A_1(s)$ smoothly approaches the value $2/b$ from below, provided we are careful to remain on the branch of the arctan that keeps $A_1(s)$ continuous. To illustrate it is perhaps more useful to re-express the arctan as,

$$\frac{2}{\pi b}\arctan\left(\frac{\pi b a(xs)}{2}\right) = \frac{2}{\pi b}\left[\frac{\pi}{2} - \arctan\left(\frac{2}{\pi b a(xs)}\right)\right] . \tag{4.21}$$

Here we stay on the same branch of the arctan for all s. For $n > 1$ the $A_n(xs)$ vanish for $s \to 0$.

We should also note that the functions $A_n(s)$ in Eq.(4.19) can also be obtained by simple manipulation of the dispersion relation in Eq.(1.97), which is defined for all real s. This avoids the possible objection that the contour integral in Eq.(4.8) is only defined for s above the "Landau pole".

Beyond the simple one-loop approximation the freezing can be analysed by choosing a renormalisation scheme in which the beta-function equation has its two-loop form,

$$\frac{\partial a(\mu^2)}{\partial \mathrm{ln}\mu^2} = -\frac{b}{2}a^2(\mu^2)(1+ca(\mu^2)) \ . \tag{4.22}$$

This corresponds to a so-called 't Hooft scheme [53] in which the non-universal beta-function coefficients are all zero. Here $c = (153 - 19N_f)/12b$ is the second universal beta-function coefficient. The key feature of these schemes is that the coupling can be expressed analytically in closed form in terms of the Lambert W function, defined implicitly by $W(z)\mathrm{exp}(W(z)) = z$ [54, 55].

The Lambert W function is similar to the logarithm; if the $W(z)$ that multiplies the exponential is removed from this definition then you are left with the logarithm, and like the logarithm there are different branches. For the logarithm, $W = \ln z$, the branches can be chosen so that there is one branch that has *Re* W running from $-\infty \to \infty$, and $Im\ W$ running from $-i\pi \to i\pi$. The other branches cover exactly the same range for *Re* W with the $Im\ W$ taking a range of $2i\pi$ in width : $i\pi \to 3i\pi$, $-i\pi \to -3i\pi$, etc. Each of theses branches in the z-plane has a branch cut along the real negative axis. For the Lambert W function there is a similar structure when it is large and real. Taking the limit *Re* $W \to \infty$ there is a branch denoted by W_0 with the imaginary range $-i\pi \to i\pi$. In this limit the branch $W_{\pm 1}$ has the range for $Im\ W$ to be $\pm i\pi \to \pm 3i\pi$, and so on for $W_{\pm 2}$, etc. Taking the limit *Re* $W \to -\infty$ the $W_{\pm 1}$ branches have an imaginary range running from $0 \to \pm 2i\pi$, $\pm 2i\pi \to \pm 4i\pi$ for $W_{\pm 2}$, etc. The W_0 branch closes up at a point on the real axis where *Re* $W = -1$. In the z-plane all the branches have a branch cut along the real negative z-axis except the W_0 branch, this has a branch cut along the real negative axis starting at $z = -1/e$. One important thing to note is that $W_n(z) = W^*_{-n}(z^*)$.

Solving the beta function equation one has

$$\begin{aligned} a(\mu^2) &= -\frac{1}{c[1+W_{-1}(z(\mu))]} \\ z(\mu) &\equiv -\frac{1}{e}\left(\frac{\mu}{\tilde{\Lambda}}\right)^{-b/c} , \end{aligned} \tag{4.23}$$

The "-1" subscript on W denotes the branch of the Lambert W function required for Asymptotic Freedom, the nomenclature being that of Ref. [55]. This choice is made as we need a real value for the coupling for large enough μ, the only branches of the Lambert W function that can take real values are W_0, $W_{\pm 1}$. Asymptotic freedom would not be given by W_0, which would go to zero in the limit $\mu \to \infty$, giving a non-zero coupling. The choice of W_{-1} is made by demanding that $W(z(\mu))$ be continuous as a function of the phase of μ when looking at the complex plane for μ [54]. For this to be so the W_1 branch would return a non-zero imaginary part for the $\mu = |\mu|$ case where we would expect a real coupling. It should be noted that this only applies for $Im \ln \mu > 0$, i.e. $\mu/|\mu| = e^{i\gamma}$ $\gamma = 0 \to \pi$. For negative γ the W_1 branch is chosen.

Taking the choice of renormalisation scale $\mu^2 = xs$, for the perturbation series of $\mathcal{D}(s)$ in Eq.(3.22), one can then expand the integrand in Eq.(1.97) for $\mathcal{R}(s)$ in powers of $\bar{a} \equiv a(xse^{i\theta})$, which can be expressed in terms of the Lambert W function using Eq.(4.23),

$$\bar{a} = \frac{-1}{c[1 + W(A(xs)e^{iK\theta})]} , \tag{4.24}$$

where

$$A(xs) = \frac{-1}{e}\left(\frac{xs}{\tilde{\Lambda}^2}\right)^{-b/2c} , K = \frac{-b}{2c} . \tag{4.25}$$

The functions $A_n(s)$ in the "contour-improved" series are then given, using Eqs(4.24,4.25), by

$$\begin{aligned} A_n(s) \equiv & \frac{1}{2\pi}\int_{-\pi}^{\pi} d\theta \bar{a}^n = \frac{1}{2\pi}\int_{-\pi}^{0} d\theta \frac{(-1)^n}{c^n}[1 + W_1(A(xs)e^{iK\theta})]^{-n} \\ + & \frac{1}{2\pi}\int_{0}^{\pi} d\theta \frac{(-1)^n}{c^n}[1 + W_{-1}(A(xs)e^{iK\theta})]^{-n} . \end{aligned} \tag{4.26}$$

Here the appropriate branches of the W function are used in the two regions of integration. As discussed in Refs. [46,47], by making the change of variable $w = W(A(xs)e^{iK\theta})$ we can then obtain

$$A_n(s) = \frac{(-1)^n}{2iKc^n\pi}\int_{W_1(A(xs)e^{-iK\pi})}^{W_{-1}(A(xs)e^{iK\pi})} \frac{dw}{w(1+w)^{n-1}} . \tag{4.27}$$

Noting that $W_1(A(xs)e^{-iK\pi}) = [W_{-1}(A(xs)e^{iK\pi})]^*$, we can evaluate the elementary integral to obtain for $n = 1$,

$$A_1(s) = \frac{2}{b} - \frac{1}{\pi K c} Im[\ln(W_{-1}(A(xs)e^{iK\pi}))] \,, \tag{4.28}$$

where the $2/b$ term is the residue of the pole at $w = 0$. For $n > 1$ we obtain

$$A_n(s) = \frac{(-1)^n}{c^n K\pi} Im \left[\ln\left(\frac{W_{-1}(A(xs)e^{iK\pi})}{1 + W_{-1}(A(xs)e^{iK\pi})} \right) + \sum_{k=1}^{n-2} \frac{1}{k(1 + W_{-1}(A(xs)e^{iK\pi}))^k} \right] . \tag{4.29}$$

Crucially the contribution from the poles at $w = 0$ and $w = -1$ cancel exactly. Equivalent expressions have been obtained in the APT approach [47]. Provided that $b/c > 0$, which will be true for $N_f < 9$, we find the same behaviour as in the one-loop case, with the $A_n(s)$ vanishing in the ultraviolet limit consistent with Asymptotic Freedom, and with $A_n(s)$ vanishing in the infrared limit for $n > 1$, and $A_1(s)$ freezing to $2/b$. To the extent that the freezing holds to all orders in perturbation theory it should hold irrespective of the choice of renormalisation scheme (RS), The use of the 't Hooft scheme simply serves to make the freezing manifest. Graphs of the functions $A_n(s)$ for $n = 1 \to 3$ calculated in the 't Hooft scheme are shown in figures 4.2 to 4.4.

4.3 Freezing behaviour of the Borel integral

In the previous section a series for $\mathcal{R}(s)$ was produced where each term in the series was finite for all s. There is still the problem that the series itself is still divergent due to the factorial growth of the series coefficients demonstrated in Chapter 3. This factorial divergence requires a method such as Borel summation to be used if the approach of the previous section is to be applied to all orders.

Now let us turn to the infrared behaviour of the regulated Borel integral. First, using the relation in Eq.(4.7) the Borel integral for $\mathcal{R}(s)$ can be obtained. This may be split into its perturbative component $\mathcal{R}_{PT}(s)$, and its

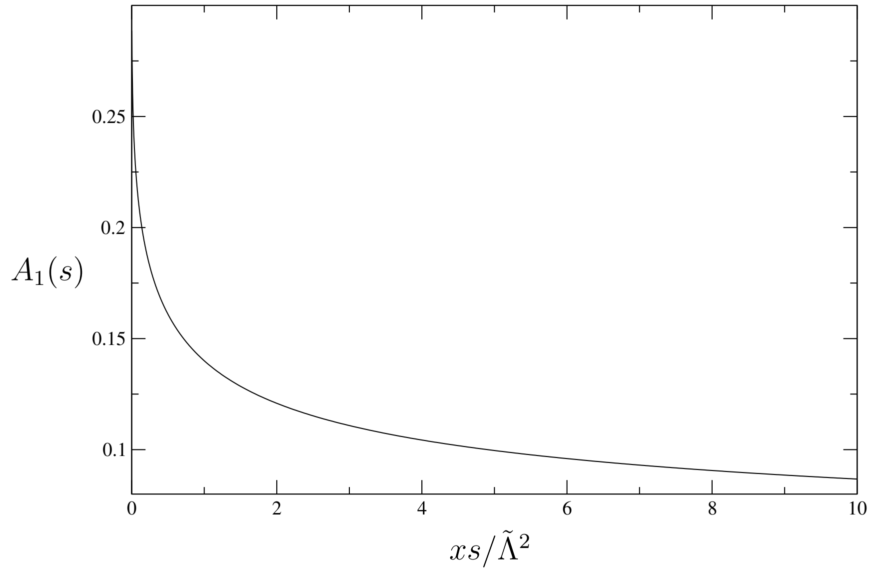

Figure 4.2: $A_1(s)$

non-peturbative OPE component $\mathcal{R}_{NP}(s)$, Inserting the Borel representation for $\mathcal{D}_{PT}$ of Eq.(3.23) into the dispersion relation of Eq.(1.97) one finds the representation

$$\mathcal{R}_{PT}(s) = \frac{1}{2\pi i}\int_{-s-i\epsilon}^{-s+i\epsilon} \frac{dt}{t} \int_0^\infty dz e^{-z/a(t)} B[\mathcal{D}](z) \ . \tag{4.30}$$

For a one-loop beta function the t integration is trivial and one finds,

$$\mathcal{R}_{PT}^{(L)}(s) = \int_0^\infty dz e^{-z/a(s)} \frac{\sin(\pi bz/2)}{\pi bz/2} B[\mathcal{D}^{(L)}](z) \ , \tag{4.31}$$

where $B[\mathcal{D}^{(L)}](z)$ (in the V-scheme) is given by Eq.(3.37). The coupling depends upon the choice of scheme, and is given by $a(s) = a_V(s) = 2/b(\ln(s/\tilde{\Lambda}_V^2))$. It is now possible to explicitly evaluate $\mathcal{R}_{PT}^{(L)}(s)$ in terms of generalised exponential integral functions $Ei(n, w)$, defined for $Re(w) > 0$ by

$$Ei(n, w) = \int_1^\infty dt \frac{e^{-wt}}{t^n} \ . \tag{4.32}$$

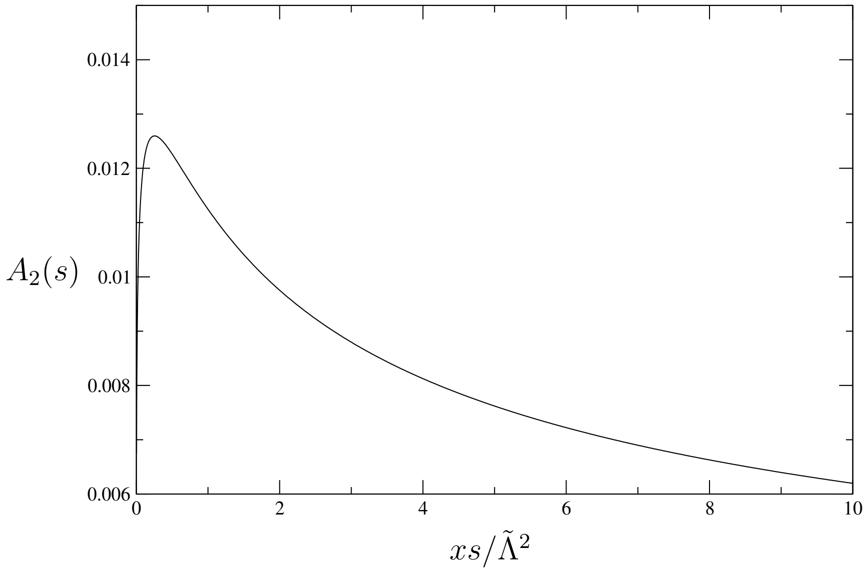

Figure 4.3: $A_2(s)$

One also needs the integral

$$\int_0^\infty dz e^{-z/a} \frac{\sin(\pi b z/2)}{z} = \arctan\left(\frac{\pi b a}{2}\right) . \tag{4.33}$$

Writing the 'sin' in Eq.(4.31) as a sum of complex exponentials and using partial fractions one can then evaluate the contribution to $\mathcal{R}^{(L)}_{PT}(s)$ coming from the UV renormalon singularities, i.e. from the terms involving $A_0(j)$ and $A_1(j)$ in Eq.(3.37) [36]

$$\begin{aligned}\mathcal{R}^{(L)}_{PT}(s)|_{UV} = & \frac{2}{\pi b}\left(\frac{8\zeta_2}{3} - \frac{11}{3}\right)\arctan\left(\frac{\pi b a(s)}{2}\right) \\ & + \frac{2}{\pi b}\sum_{j=1}^{j=\infty}\left(A_0(j)\phi_+(1,j) + (A_0(j) - A_1(j)z_j)\phi_+(2,j)\right) ,\end{aligned} \tag{4.34}$$

where $\zeta_2 = \pi^2/6$ is the Riemann zeta-function, and we have defined

$$\phi_+(p,q) \equiv e^{z_q/a(s)}(-1)^q Im[Ei(p,(1/a(s)) + i\pi b/2z_q)] . \tag{4.35}$$

To evaluate the remaining contribution involving the IR renormalon singularities the integral must be regulated to deal with the singularities on the integration contour. For simplicity we could choose to take a principal value

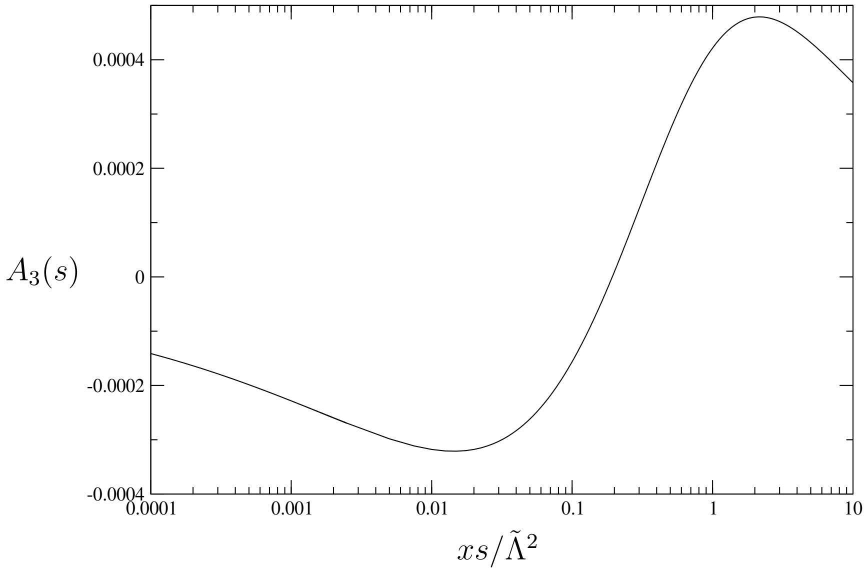

Figure 4.4: $A_3(s)$

prescription. The function $Ei(n,w)$ defined for $Re(w) > 0$ by Eq.(4.32), must be continued to $Re(w) < 0$. With the standard continuation one arrives at a function analytic everywhere in the cut complex w-plane, except at $w = 0$; with a branch cut running along the negative real axis. Explicitly

$$Ei(n,w) = \frac{(-w)^{n-1}}{(n-1)!}\left[-\ln w - \gamma_E + \sum_{m=1}^{n-1}\frac{1}{m}\right] - \sum_{\substack{m=0\\ m\neq n-1}}^{\infty}\frac{(-w)^m}{(m-n+1)m!}\,, \tag{4.36}$$

with $\gamma_E = 0.5722\ldots$, Euler's constant. The $\ln w$ contributes the branch cut along the negative real w-axis. To obtain the principal value of the Borel integral one needs to compensate for the discontinuity across the branch cut, and make the replacement $\ln w \to \ln w + i\pi sign(Im(w))$. This leads one to introduce, analogous to Eq.(4.35),

$$\begin{aligned}\phi_-(p,q) &\equiv e^{-z_q/a(s)}(-1)^q Im[Ei(p,(-1/a(s)) - i\pi b/2z_q)]\\ &- \frac{e^{-z_q/a(s)}(-1)^q z_q^{p-1}}{(p-1)!}\pi Re[(1/a(s)) + i\pi b/2)^{p-1}]\,. \end{aligned}\tag{4.37}$$

The principal value of the IR renormalon contribution is then given by

$$\mathcal{R}^{(L)}_{PT}(s)|_{IR} = \frac{2}{\pi b}\left(\frac{14}{3} - \frac{8\zeta_2}{3}\right)\arctan\left(\frac{\pi b a(s)}{2}\right) + \frac{2B_0(2)}{\pi b}\phi_-(1,2)$$
$$+ \frac{2}{\pi b}\sum_{j=3}^{j=\infty}\left(B_0(j)\phi_-(1,j) + (B_0(j) + B_1(j)z_j)\phi_-(2,j)\right) \; . \quad (4.38)$$

The perturbative component is then the sum of the UV and (regulated) IR contributions,

$$\mathcal{R}^{(L)}_{PT}(s) = \mathcal{R}^{(L)}_{PT}(s)|_{UV} + \mathcal{R}^{(L)}_{PT}(s)|_{IR} = \frac{2}{\pi b}\arctan\left(\frac{\pi b a(s)}{2}\right)$$
$$+ \frac{2}{\pi b}\sum_{j=1}^{\infty}\left(A_0(j)\phi_+(1,j) + (A_0(j) - A_1(j)z_j)\phi_+(2,j)\right) + \frac{2B_0(2)}{\pi b}\phi_-(1,2)$$
$$+ \frac{2}{\pi b}\sum_{j=3}^{\infty}\left(B_0(j)\phi_-(1,j) + (B_0(j) + B_1(j)z_j)\phi_-(2,j)\right) \; . \quad (4.39)$$

Note that the ζ_2 contributions cancel, and one obtains the arctan term, which is the leading contribution, $A_1(xs)$, in the CIPT/APT reformulation of fixed-order perturbation theory with $x = e^{-5/3}$.

In the one-loop (leading-b) case the V-scheme coupling $a(s)$ becomes infinite at $s = s_L \equiv \tilde{\Lambda}^2_V$. The $e^{-z/a(s)}$ term in the Borel integrand approaches unity at $s = s_L$, but the trigonometric factor $\sin(\pi b z/2)/(\pi b z/2)$ ensures that the integral in Eq.(4.31) is defined at $s = s_L$. For $s < s_L$, however, $a(s)$ becomes negative, and the $e^{-z/a(s)}$ factor diverges at $z = \infty$, the Borel transform in the V-scheme does not contain any exponential z-dependence to compensate, so the Borel integral is not defined. We shall refer to this pathology of the Borel integral at $s = s_L$ as the "Landau divergence". It is important to stress that the Landau divergence is to be carefully distinguished from the Landau pole in the coupling. The Landau pole in the coupling depends on the chosen renormalisation scale. At one-loop order choosing an $\overline{MS}$ scale $\mu^2 = xs$, the coupling $a(xs)$ has a Landau pole at $s = \tilde{\Lambda}^2_{\overline{MS}}/x$. The Borel integral of Eq.(4.31) can then be written in terms of this coupling as,

$$\mathcal{R}^{(L)}_{PT}(s) = \int_0^{\infty} dz e^{-z/a(xs)}\frac{\sin(\pi b z/2)}{\pi b z/2}\left[xe^{5/3}\right]^{bz/2} B[\mathcal{D}^{(L)}](z) \; . \quad (4.40)$$

In a general scheme the Borel transform picks up the extra factor $[xe^{5/3}]^{bz/2}$ multiplying the V-scheme result. The Borel integrand is scheme (x) invariant. The extra factor has to be taken into account when identifying where the integral breaks down, and one of course finds the Landau divergence to be at the same x-independent energy, $s = s_L = e^{5/3}\tilde{\Lambda}^2_{\overline{MS}} = \tilde{\Lambda}^2_V$. Thus the Borel representation of Eq.(4.30) for $\mathcal{R}^{(L)}_{PT}(s)$ only applies for $s \geq s_L$. For $s < s_L$ the one-loop (V-scheme) coupling $a(s)$ becomes negative. We can rewrite the perturbative expansion of $\mathcal{R}_{PT}(s)$ as an expansion in $(-a(s))$,

$$\begin{aligned}\mathcal{R}_{PT}(s) &= a(s) + r_1 a^2(s) + {r_2}^3 a(s) + \cdots \\ &= -[(-a(s)) - r_1(-a(s))^2 + r_2(-a(s))^3 + \cdots] \ . \end{aligned} \tag{4.41}$$

The expansion in $(-a(s))$ follows from the modified Borel representation

$$\begin{aligned}\mathcal{R}_{PT}(s) &= -\int_0^{\infty} dz e^{-z/(-a(s))} B[\mathcal{R}](-z) \\ &= \int_0^{-\infty} dz e^{z/(-a(s))} B[\mathcal{R}](z) \ . \end{aligned} \tag{4.42}$$

This modified form of Borel representation will be valid when $Re(a(s)) < 0$, and involves an integration contour along the negative real axis. Thus, it is now the *ultraviolet* renormalons UV_k which render the Borel integral ambiguous.

The ambiguity in taking the contour around these UV_k singularities (analogous to Eq.(3.40)) now involves $(s/\tilde{\Lambda}^2)^k$. Of course it is now unclear how these ambiguities can cancel against the corresponding OPE ambiguities. The key point is that since only the sum of the PT and OPE components is well-defined, the Landau divergence of the Borel integral at $s = s_L$, must be accompanied by a corresponding breakdown in the validity of the OPE as an expansion in powers of $(\tilde{\Lambda}^2/s)$, at the same energy. The idea is illustrated by the following toy example, where the OPE is an alternating geometric progression,

$$\begin{aligned}
\mathcal{R}_{NP}(s) &= \left(\frac{\tilde{\Lambda}^2}{s}\right) - \left(\frac{\tilde{\Lambda}^2}{s}\right)^2 + \left(\frac{\tilde{\Lambda}^2}{s}\right)^3 - \cdots \\
&= \frac{\frac{\tilde{\Lambda}^2}{s}}{1+\frac{\tilde{\Lambda}^2}{s}} = \frac{1}{1+\frac{s}{\tilde{\Lambda}^2}} \\
&= 1 - \left(\frac{s}{\tilde{\Lambda}^2}\right) + \left(\frac{s}{\tilde{\Lambda}^2}\right)^2 - \left(\frac{s}{\tilde{\Lambda}^2}\right)^3 + \cdots \, . \qquad (4.43)
\end{aligned}$$

At any value of s, $\mathcal{R}_{NP}(s)$ is given by the equivalent functions in the middle line. For $s > \tilde{\Lambda}^2$ these have a valid expansion in powers of $\tilde{\Lambda}^2/s$, the standard OPE, given in the top line. For $s < \tilde{\Lambda}^2$ the standard OPE breaks down, but there is a valid expansion in powers of $s/\tilde{\Lambda}^2$ given in the bottom line. Thus for $s < s_L$, the OPE should be resummed and recast in the form,

$$\mathcal{R}_{NP}(s) = \sum_n \tilde{\mathcal{C}}_n \left(\frac{s}{\tilde{\Lambda}^2}\right)^n . \qquad (4.44)$$

The modified OPE can contain a $\tilde{\mathcal{C}}_0$ term independent of s, as in the toy example of Eq.(4.43). In contrast any term independent of s in the large s standard OPE expansion would lead to a violation of asymptotic freedom. As a result $\mathcal{R}_{NP}$ can have a non-vanishing infrared limit. Perturbation theory by itself cannot determine the infrared behaviour of observables, but a well-defined perturbative component that can be computed at all energy values is a noteworthy feature.

The terms present in this modified OPE should then be in one-to-one correspondence with the UV_n renormalon singularities in the Borel transform of the PT component, and the PT renormalon ambiguities can cancel against corresponding OPE ones, and again each component separately be well-defined. The modified coefficient functions $\tilde{\mathcal{C}}_n$ will have a form analogous to Eq.(3.27),

$$\tilde{\mathcal{C}}_n = K a^{\tilde{\delta}_n}(\mu^2)[1 + \mathcal{O}(a)] \, . \qquad (4.45)$$

The ambiguity (analogous to Eq.(3.40)) for the modified Borel representation of Eq.(4.42), obtained by taking UV_k to be a branch point singularity

$(1-z/z_k)^{\tilde{\gamma}_k}$, is

$$\Delta R_{PT}{\approx}Ka^{1-\tilde{\gamma}_k}\left(\frac{s}{\tilde{\Lambda}^2}\right)^k \ . \tag{4.46}$$

Comparing with Eq.(4.45) one finds $\tilde{\delta}_k = 1-\tilde{\gamma}_k$. The modified Borel representation for $\mathcal{R}^{(L)}_{PT}$ valid for $s<s_L$ will be,

$$\mathcal{R}^{(L)}_{PT}(s) = -\int_0^\infty dz e^{-z/(-a(s))}B[\mathcal{R}^{(L)}](-z) \ . \tag{4.47}$$

This may again be written explicitly in terms of $Ei(n,w)$ functions. One simply needs to change $a(s)\rightarrow -a(s)$, $z_j\rightarrow -z_j$, and $A_1(j)\rightarrow -A_1(j)$, $B_1(j)\rightarrow -B_1(j)$ in Eq.(4.39). One finds that the result of Eq.(4.39) is invariant under these changes, apart from the additional terms which we added to the $Ei(n,w)$ in continuing from $Re\ w>0$ to $Re\ w<0$, in order to obtain the Principal Value. In fact the PV Borel integral is not continuous at $s=s_L$. Continuity is obtained if rather than the Principal Value we use the standard continuation of the $Ei(n,w)$ defined by Eq.(4.36). That is, we redefine

$$\phi_-(p,q){\equiv}e^{-z_q/a(s)}(-1)^q Im[Ei(p,(-1/a(s))-i\pi b/2)z_q] \ . \tag{4.48}$$

This simply corresponds to a different regulation of singularities. We then see that Eq.(4.39) for $\mathcal{R}^{(L)}_{PT}(s)$ is a function of $a(s)$ which is well-defined at all energies, and freezes to $2/b$ in the infra-red. We note that the branch of the arctan changes at $s=s_L$, so that the arctan smoothly changes from zero at $s=\infty$ to π at $s=0$. Alternatively one can use the relation $\arctan(x)=\pi/2-\arctan(1/x)$, used in Eq.(4.21). The connection with the CIPT/APT rearrangement of fixed-order perturbation theory is now clear. It is obtained by keeping the $\sin(\pi bz/2)/(\pi bz/2)$ term in the Borel transform, and expanding the remainder in powers of z. Ordinary fixed-order perturbation theory, of course, corresponds to expanding the whole Borel transform in powers of z. The retention of the oscillatory sin factor in the Borel transform ensures that the reformulated perturbation theory remains defined at all energies. One finds the $A_n(s)$ given by Eqs.(4.19) for $s{\geq}s_L$,

$$A_n(s) = \int_0^\infty dz e^{-z/a(s)}\frac{\sin(\pi bz/2)}{\pi bz/2}\frac{z^{n-1}}{(n-1)!} \ , \tag{4.49}$$

Similarly for $s \leq s_L$ one finds

$$A_n(s) = \int_0^{-\infty} dz e^{z/(-a(s))} \frac{\sin(\pi bz/2)}{\pi bz/2} \frac{z^{n-1}}{(n-1)!} \,. \tag{4.50}$$

Thus the CIPT/APT fixed-order result should be an asymptotic approximation to the Borel integral at both large and small values of s. In figure 4.5 we compare the all-orders leading-b result for $\mathcal{R}^{(L)}_{PT}(s)$ given by Eq.(4.39), with the NNLO CIPT/APT prediction,

$$\mathcal{R}^{(L)}_{APT}(s) = A_1(s) + d_1^{(L)} A_2(s) + d_2^{(L)} A_3(s) \,. \tag{4.51}$$

The one-loop $A_n(s)$ are given by Eqs.(4.19) and, as in Eq.(4.39), the V-scheme is assumed. We assume $N_f = 2$ quark flavours. One sees that there is good agreement at all values of $s/\tilde{\Lambda}_V^2$.

We now turn to the full QCD result beyond the one-loop approximation and, as in Section 4.2, it will be sufficient to consider the two-loop result since one can always use an 't Hooft scheme. Consider the Borel representation for $\mathcal{R}_{PT}(s)$ of Eq.(4.30). We shall assume that, as in the leading-b approximation, the Borel transform $B[\mathcal{D}](z)$ in the V-scheme does not contain any exponential dependence on z, but is simply a combination of branch point singularities. It is then clear that the Landau divergence occurs when the factor $e^{-z/a(-s)}$ becomes a diverging exponential, that is when $Re(1/a(-s)) < 0$. This shall be shown explicitly in Eq.(4.55). Thus the critical energy s_L is given by the condition $Re(1/a(-s)) = 0$. At one-loop level one has

$$\frac{1}{a(-s)} = \frac{b}{2} \ln\left(\frac{s}{\tilde{\Lambda}_V^2}\right) + \frac{i\pi b}{2} \,, \tag{4.52}$$

and so the condition yields $s = s_L = \tilde{\Lambda}_V^2$, as we found before. At the two-loop level the situation is slightly different. Integrating the two-loop beta-function in Eq.(4.22) now gives,

$$\frac{1}{a(-s)} + c \ln\left[\frac{ca(-s)}{1 + ca(-s)}\right] = \frac{b}{2} \ln\left(\frac{s}{\tilde{\Lambda}_V^2}\right) + \frac{i\pi b}{2} \,. \tag{4.53}$$

The vanishing of $Re(1/a(-s))$ then corresponds to the solution of the transcendental equation

$$Re\left\{c\ln\left[\frac{ca(-s)}{1+ca(-s)}\right]\right\}=\frac{b}{2}\ln\left(\frac{s}{\tilde{\Lambda}_V^2}\right)\ . \qquad (4.54)$$

Assuming $N_f = 2$ flavours, which gives $b = 29/6$ and $c = 115/58$, one finds $s = s_L = 0.4574\tilde{\Lambda}_V^2$. Since the Borel integral is scheme-invariant so must the value of s_L be. In particular the breakdown of the Borel representation would occur in any scheme, not just an 't Hooft one. We can perform the t-integration in Eq.(4.30) in closed form, and arrive at the two-loop Borel representation

$$\mathcal{R}_{PT}(s)=\frac{-2}{\pi b}\int_0^{\infty}dzIm\left[\frac{e^{-z/a(-s+i\epsilon)}}{z}\right.$$
$$\left.-ce^{zc}Ei\left(1,zc+\frac{z}{a(-s+i\epsilon)}\right)\right]B[\mathcal{D}](z)\ . \qquad (4.55)$$

The factor in the square bracket plays the role of the $e^{-z/a(s)}\frac{\sin(\pi bz/2)}{(\pi bz/2)}$ factor in the one-loop case in Eq.(4.31). It provides an oscillatory factor so that at $s = s_L$ the Borel representation remains defined. For $s < s_L$ one must switch to a modified Borel representation as in Eq.(4.42), writing

$$\mathcal{R}_{PT}(s)=-\frac{1}{2\pi i}\int_{-s-i\epsilon}^{-s+i\epsilon}\frac{dt}{t}\int_0^{\infty}dze^{-z/(-a(t))}B[\mathcal{D}](-z)\ . \qquad (4.56)$$

Performing the t-integration this gives

$$\mathcal{R}_{PT}(s)\ =\ \frac{2}{\pi b}\int_0^{\infty}dzIm\left[-\frac{e^{-z/(-a(-s+i\epsilon))}}{z}\right.$$
$$\left.-\ ce^{-zc}Ei\left(1,-zc+\frac{z}{(-a(-s+i\epsilon))}\right)\right]B[\mathcal{D}](-z)\ . \qquad (4.57)$$

Unfortunately we cannot write down a function analogous to Eq.(4.39) which gives $\mathcal{R}_{PT}(s)$ at all energies, because we do not know $B[\mathcal{D}](z)$ exactly. The two-loop situation, however, is the same as that at one-loop. The regulated representation of Eq.(4.55) applies for $s{\geq}s_L$. Below $s = s_L$ one needs the modified representation of Eq.(4.57) . The perturbative component $\mathcal{R}_{PT}(s)$ then freezes to $2/b$ in the infra-red; we can see this if we split $B[\mathcal{D}](-z)$ into $(1+(B[\mathcal{D}](-z)-1))$. The part of the integrand proportional to $B[\mathcal{D}](-z)-$

1 vanishes for all z from $0 \to \infty$ in the infra-red limit. The remaining term integrates to give us $A_1(xs)$, which freezes to $2/b$ as $s \to 0$. There is again a direct connection with the CIPT/APT reformulation of fixed-order perturbation theory.

Using integration by parts it is possible to show that for $s \geq s_L$

$$A_n(s) = \frac{-2}{\pi b} \int_0^\infty dz Im \left[\frac{e^{-z/a(-s+i\epsilon)}}{z} - c e^{zc} Ei \left(1, zc + \frac{z}{a(-s+i\epsilon)} \right) \right] \frac{z^{n-1}}{(n-1)!} , \quad (4.58)$$

where the $A_n(s)$ correspond to the two-loop results in Eqs.(4.28,4.29). Once again CIPT/APT corresponds to keeping the oscillatory function in the Borel transform, and expanding the remainder in powers of z. Similarly for $s \leq s_L$ one has,

$$A_n(s) = \frac{2}{\pi b} \int_0^\infty dz Im \left[- \frac{e^{-z/(-a(-s+i\epsilon))}}{z} - c e^{-zc} Ei \left(1, -zc + \frac{z}{(-a(-s+i\epsilon))} \right) \right] \frac{(-z)^{n-1}}{(n-1)!} . \quad (4.59)$$

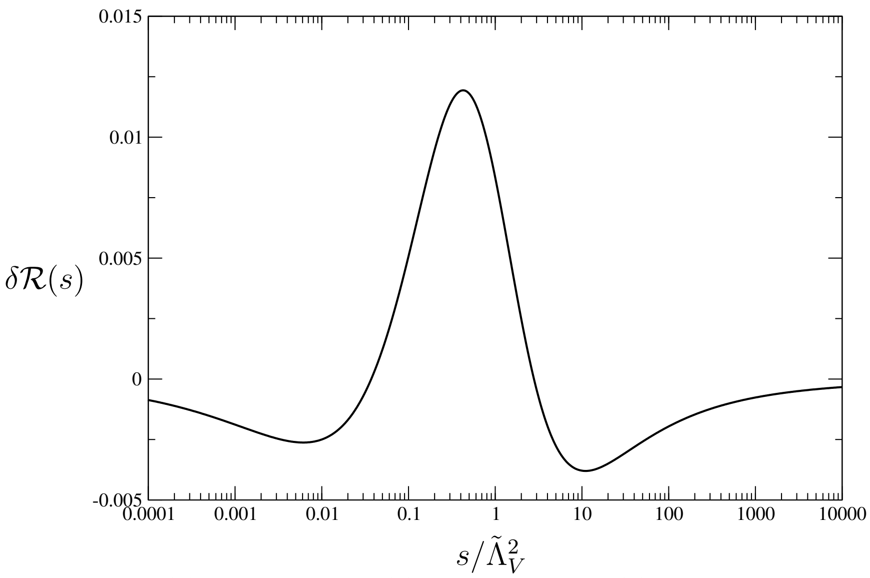

Figure 4.5: $\delta\mathcal{R}(s) =$ all orders$\mathcal{R}(s)$ $-$ fixed order$\mathcal{R}(s)$ at the one-loop level for 2 flavours of quark.

Thus, as in the one-loop case, the CIPT/APT reformulation of fixed-order perturbation theory will be asymptotic to the Borel representations at small and large energies. We would like, as in figure 4.5 for the one-loop case, to compare how well the fixed-order CIPT/APT perturbation theory corresponds with the all-orders Borel representation. We are necessarily restricted to using the leading-b approximation since this is the extent of the exact all-orders information at our disposal. One possibility is to simply use the leading-b result for the Borel transform, $B[\mathcal{D}^{(L)}](z)$, in the two-loop Borel representation of Eq.(4.55). The difficulty though is that with $a(-s)$ the two-loop coupling, the Borel integral is now scheme-dependent, since $B[\mathcal{D}^{(L)}](z)$ has a scale dependence which exactly compensates that of the *one*-loop coupling. Using a renormalisation scale $\mu^2 = xs$ our result for $\mathcal{R}_{PT}(s)$ has an unphysical x-dependence.

This difficulty is exacerbated if we attempt to match the result to the exactly known perturbative coefficients d_1 and d_2, which we could do by adding an additional contribution $(d_1 - d_1^{(L)})z + (d_2 - d_2^{(L)})(z^2/2)$ to the Borel transform. Thus, as has been argued elsewhere, such matching of leading-b results to exact NNLO results yields completely *ad hoc* predictions, which may be varied at will by changing the renormalisation scale [64, 65]. The resolution of this difficulty follows if one accepts that the standard RG-improvement of fixed-order perturbation theory is incomplete, in that only a subset of RG-predictable UV logarithms involving the energy scale s are resummed. Performing a complete resummation of these logs together with the accompanying logs involving the renormalisation scale, yields a scale-independent result. This is the Complete Renormalisation Group Improvement (CORGI) approach [18, 21] introduced previously in section 2.5. We can attempt to perform the leading-b μ-independent CORGI resummation,

$$\mathcal{D}^{(L)}_{CORGI}(t) = a_0(t) + X_2 a_0^3(t) + \sum_{n>2} X_n^{(L)} a_0^{n+1}(t) + \dots \ , \tag{4.60}$$

so that the exactly known NNLO X_2 coefficient is included, with the remaining unknown coefficients approximated by $X_3^{(L)}$, $X_4^{(L)}$, . . ., the leading-b approximations. We stress that $a_0(t)$ denotes the full CORGI coupling defined in Eq.(2.52), with its t dependence given in terms of the Lambert W function in Eq.(4.23) with $z = -1/e(t/\Lambda^2_{\mathcal{D}})^{-b/2c}$. One can define this formal sum using the Borel representation of $\mathcal{D}_{PT}$,

$$\mathcal{D}_{PT}(t) = \int_0^\infty e^{-z/a(t)} B[\mathcal{D}](z)\, dz \; . \tag{4.61}$$

Combining this with the result for $B[\mathcal{D}^{(L)}]$ in Eq.(3.37) the integral can be expressed in closed form in terms of the Exponential Integral functions $Ei(n, w)$ of Eq.(4.32), with the result [46]

$$\begin{aligned}
&\mathcal{D}^{(L)}_{PT}(1/a(t)) \\
&= \sum_{j=1}^{\infty} z_j \{ - e^{z_j/a(t)} Ei(1, z_j/a(t))[(z_j/a(t))(A_0(j) - z_j A_1(j)) - z_j A_1(j)] \\
&+ (A_0(j) - z_j A_1(j))\} - e^{-z_j/a(t)} + B_0(2) Ei(1, -z_j/a(t)) \\
&+ \sum_{j=3}^{\infty} \{ - e^{-z_j/a(t)} Ei(1, -z_j/a(t))[(z_j/a(t))(B_0(j) + z_j B_1(j))] \\
&- (B_0(j) + z_j B_1(j))\} \; .
\end{aligned} \tag{4.62}$$

To define the infra-red renormalon contribution we have assumed the standard continuation of $Ei(n, w)$ from $Rew > 0$ to $Rew < 0$, defined by Eq.(4.39). In [48] a principal value was assumed, which corresponds to adding $-i\pi sign(Im(z_j/a(t))$ to the $Ei(1, -z_j/a(t))$ term. As we found for $\mathcal{R}^{(L)}_{PT}(s)$, the principal value is not continuous at $s = s_L$, whereas the standard continuation is.

The leading-b parts of a_V and a_0 are related via the scheme-invariant quantity ρ_0 defined in Eq.(2.48), giving [46]

$$\frac{1}{a^{(L)}_V} = \frac{1}{a^{(L)}_0} + d^{(L)}_1(V) \; . \tag{4.63}$$

By equating the leading-b part of the CORGI and V-scheme series, the formal resummation in Eq.(4.60) can be related to the result of Eq.(4.62) [46],

$$\mathcal{D}^{(L)}_{CORGI}(t) = \mathcal{D}^{(L)}_{PT}\left(\frac{1}{a_0(t)} + d^{(L)}_1(V)\right) + (X_2 - X^{(L)}_2) a^3_0(t) \; . \tag{4.64}$$

Once again $a_0(t)$ is the full CORGI coupling, and $d^{(L)}_1(V)$ denotes the NLO

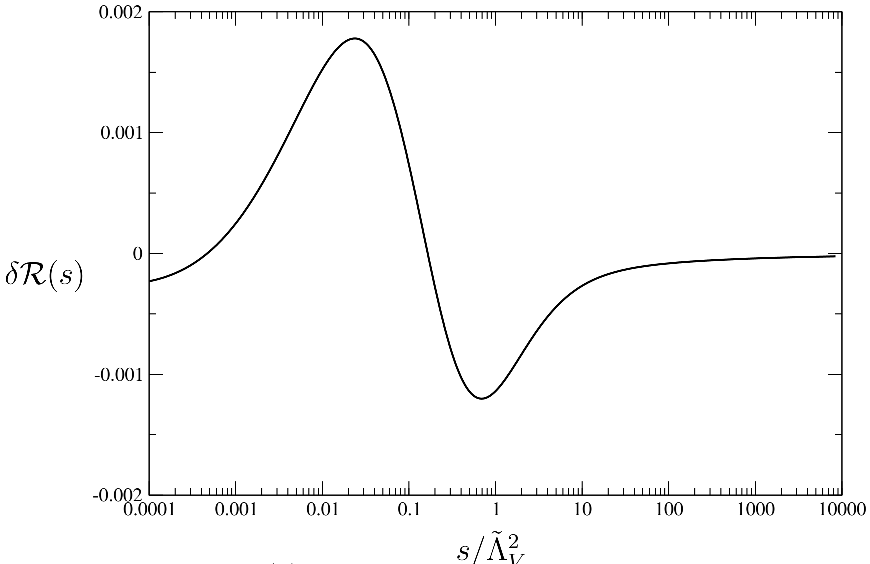

Figure 4.6: $\delta\mathcal{R}(s) = \mathcal{R}^{(L)}_{CORGI}(s) - \mathcal{R}_{APT}(s)$ at the two-loop level for 2 flavours of quark.

leading-b correction in the V-scheme. The $X_n^{(L)}$ can now also be obtained

$$\begin{aligned} X_n^{(L)} &= \mathfrak{C}_{n+1}\left[\sum_{k=0}^{\infty} d_k^{(L)}(V)\left(\frac{a}{1+ad_1^{(L)}(V)}\right)^{k+1}\right] \\ &= \sum_{k=0}^{n} d_k^{(L)}(V)\frac{n!}{k!(n-k)!}(-d_1^{(L)}(V))^{n-k}\ , \end{aligned} \tag{4.65}$$

where $\mathfrak{C}_{n+1}$ denotes taking the coefficient of the a^{n+1} term.

Inserting $\mathcal{D}_{CORGI}(t)$ inside the dispersion relation of Eq.(1.97) one can then define,

$$\mathcal{R}^{(L)}_{CORGI}(s) = \frac{1}{2\pi i}\int_{-s-i\epsilon}^{-s+i\epsilon} dt\frac{\mathcal{D}^{(L)}_{CORGI}(t)}{t}\ . \tag{4.66}$$

This can be evaluated numerically. If we have $\mathcal{R}^{(L)}_{CORGI}(s_1)$ then we can obtain

$$\begin{aligned} &\mathcal{R}^{(L)}_{CORGI}(s_2) = \mathcal{R}^{(L)}_{CORGI}(s_1) \\ &+\frac{1}{2\pi i}\left(\int_{-s_2-i\epsilon}^{-s_1-i\epsilon} dt\frac{\mathcal{D}^{(L)}_{CORGI}(t)}{t} + \int_{-s_1+i\epsilon}^{-s_2+i\epsilon} dt\frac{\mathcal{D}^{(L)}_{CORGI}(t)}{t}\right)\ . \end{aligned} \tag{4.67}$$

If we set s_1 to be large enough we can evaluate the s_1 integral using the circular contour in the s plane, as in Eq.(4.8). Combining this circular integral with the integrals above and below the real negative axis we arrive at $\mathcal{R}^{(L)}_{CORGI}(s_2)$, where s_2 can be as far into the infra-red as we want. The all-orders CORGI result can be compared with the NNLO CIPT/APT CORGI result:

$$\mathcal{R}_{APT}(s) = A_1(s) + X_2 A_3(s)\ . \tag{4.68}$$

Here the $A_n(s)$ are the two-loop results of Eqs.(4.28,4.29), with $A(s) = (-1/e)(\sqrt{s}/\Lambda_{\mathcal{D}})^{-b/c}$ in the CORGI scheme. Analogously to figure 4.5 we plot in figure 4.6 the comparison of the all-orders and NNLO APT CORGI results, where $N_f = 2$ quark flavours are assumed. As in the one-loop case, there is extremely close agreement at all values of s. For the fits to low-energy $R_{e^+e^-}(s)$ data to be presented in the next chapter, therefore, we shall use the NNLO CORGI APT result.

4.4 Euclidean freezing

We can define the Adler D-function through the inverse transform shown in Eq.(4.12). That is, we can write,

$$\mathcal{D}(Q^2) = Q^2 \int_0^\infty \frac{ds}{(s+Q^2)^2}\mathcal{R}(s)\ . \tag{4.69}$$

This was then used to obtain the APT coupling of Eq.(4.13). This Euclidean APT coupling freezes in the infra-red to $2/b$, but this behaviour is induced by the second non-perturbative contribution, which cancels the Landau pole in the first perturbative term. Due to the lack of the oscillatory factor the Borel integral is potentially divergent at $s = s_L$, leading now to a direct connection between the APT coupling and the Borel representation of $\mathcal{D}_{PT}$. One can explicitly exhibit this divergent behaviour working in the leading-b approximation. The Borel integral can then be explicitly evaluated in terms of exponential integral functions as in, Eq.(4.62). Using Eq.(4.36) one can find the divergent behaviour as $s \to s_L$ to be proportional to $\ln a$:

$$\mathcal{D}_{PT} \to \left[\sum_{j=1}^{\infty}(z_j^2 A_1(j) + z_j^2 B_1(j)) - z_2 B_0(2)\right] \ln a + \cdots\ , \quad B_1(1) = B_2(1) = 0\ .$$

However, remarkably the factor in the square brackets vanishes and the result is finite at $s = s_L$, provided that all the renormalon singularities are included. The individual renormalon contributions are divergent, but there is a cancellation between the UV and IR renormalons due to the relation

$$z_j^2 A_1(j) = -z_{j+3}^2 B_1(j+3) \; , \tag{4.70}$$

and the cancellation between the term $z_3^2 B_1(3)$ and $-z_2 B_0(2)$. The above finiteness at $s = s_L$ means that one can obtain a $\mathcal{D}_{PT}(Q^2)$ component well-defined in the infrared by changing to the modified form of Borel integral for $s < s_L$. One finds that $\mathcal{D}_{PT}$ becomes negative before approaching the freezing limit $\mathcal{D}_{PT}(0) = 0$. Phenomenological investigations are planned [67]. Comparable investigations in the standard APT approach have been reported [68]. Unfortunately nothing is known about the full renormalon structure beyond leading-b approximation [36]. Correspondingly no analogue of the APT reorganisation of fixed-order perturbation theory asymptotic to $\mathcal{D}_{PT}$ is possible for the Euclidean case.

It should be noted that in the case of $R_{e^+e^-}$ and D it is possible to say something about the separate infrared freezing behaviours of the perturbative and non-perturbative components. Arguments in the limit of a large number of colours [61] imply that $D(0) = 0$, or equivalently $\mathcal{D}(0) = -1$. Furthermore according to [69] $\mathcal{R}$ and $\mathcal{D}$ should have the same freezing limit; this result comes from shrinking the radius of the circular contour in Eq.(4.8) to zero. One would infer then that $\mathcal{R}_{NP} = -1 - 2/b$ in that limit in order to be consistent with $\mathcal{R}_{PT} = 2/b$.

4.5 Summary

A perturbation series for the QCD part of the R-ratio can be obtained from its relation to the Adler D-function. To obtain the series the coupling is expanded about its value on the real axis as a Taylor series. The perturbation series that results has the usual problem that the coupling has a pole for a sufficiently low energy scale.

The solution presented here is to transform each part of the perturbation series for the Adler D-function individually; the transform involves integrating the coupling in the complex plane of its scale. An important point is that the transform involves evaluating the coupling at scales that are not near the Landau pole, and so the result can be finite. What results is a series of terms that are finite summations of a sub-series in the coupling. Each part of the series will be a perturbative coefficient d_n that comes from $\mathcal{D}_{PT}$, multiplied by a function $A_{n+1}(s)$.

As all the beta function coefficients bar the first two are scheme dependent an 't Hooft renormalisation scheme can be used, where only the first two beta function coefficients are non-zero.

There is the added problem that the series coefficients will have a factorial divergence, and so for the all-orders result the Borel transform will need to be considered.

For a one-loop beta function there is a simple relation between the Borel transforms of $\mathcal{R}_{PT}$ and $\mathcal{D}_{PT}$, and the Borel integral for $\mathcal{R}_{PT}^{(L)}$ can be solved, leaving a result much like the result for $\mathcal{D}_{PT}^{(L)}$. Both results have ambiguities arising from the choice of integrating around the IR renormalon poles. These ambiguities are related to the OPE.

The coupling for a perturbation series will have a negative real value when a sufficiently low energy scale is considered. This leads to the Borel integral being re-written to obtain a series in $-a$ as opposed to a. This then requires the Borel integral to go from $z = 0$ to $z = -\infty$. This changes the source of the renormalon ambiguities to be the UV renormalons instead of the IR renormalons. This will lead to the ambiguities being of the form $(s/\tilde{\Lambda}^2)^k$ as opposed to $(\tilde{\Lambda}^2/s)^k$. The OPE is modified as well, and a toy example shows that when moving to a low value of s, the OPE power expansion can be expressed as a series in $(s/\tilde{\Lambda}^2)$ with modified series coefficient functions. The ambiguities from the new coefficient functions will then cancel with the ambiguities from the UV renormalons.

The Borel integral will return the $A_n(s)$ when acting on a Borel transform of $z^{n-1}/(n-1)!$, if the normal or modified Borel integrals are used. When expanding the Borel transform in powers of z one will return the same series that freezes whether the normal or modified Borel integral is used.

The prescription for integrating around the renormalons can be chosen so that the Borel integral for $\mathcal{R}_{PT}^{(L)}$ will be continuous from moving below the Landau divergence.

Moving to the 't Hooft scheme the relation between the Borel transforms for $\mathcal{R}_{PT}$ and $\mathcal{D}_{PT}$ is more complex. However, the same approach as for the one-loop case can still be applied, yielding an infrared-safe Borel integral.

Due to relations between the residues of the renormalon poles a finite result can be found for the Borel integral of the Adler D-function in the leading-b approximation. In general, however, such behaviour is not guaranteed.

Chapter 5

Low energy behaviour of $R_{e^+e^-}$ data

5.1 Mass thresholds of $R_{e^+e^-}$

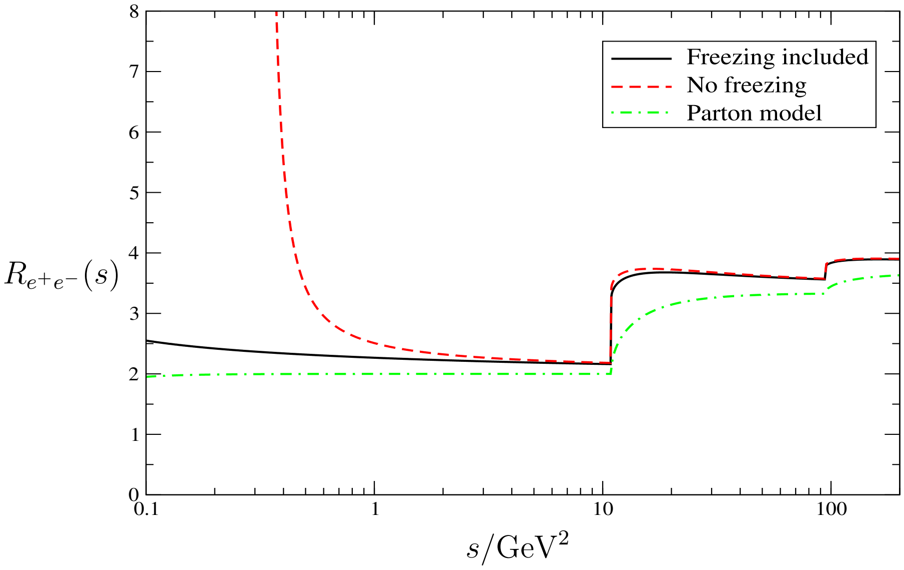

Figure 5.1: Comparison of CORGI APT and standard NNLO CORGI calculations of $R_{e^+e^-}(s)$ at low energies.

In this section the NNLO CORGI APT perturbative predictions are compared with low-energy experimental data for $R_{e^+e^-}$. The discussion so far has assumed massless quarks. To include quark masses we use the approximate result [44]

$$R_{e^+e^-}(s) = 3\sum_f Q_f^2 T(v_f)[1 + g(v_f)\mathcal{R}(s)] \; , \tag{5.1}$$

with the sum over all active quark flavours, i.e. those with masses $m_f < \sqrt{s}/2$, and where

$$\begin{aligned} v_f &= (1 - 4m_f^2/s)^{\frac{1}{2}} \; , \\ T(v) &= v(3 - v^2)/2 \; , \\ g(v) &= \frac{4\pi}{3}\left[\frac{\pi}{2v} - \frac{3+v}{4}\left(\frac{\pi}{2} - \frac{3}{4\pi}\right)\right] \; . \end{aligned} \tag{5.2}$$

For the theoretical predictions $\mathcal{R}(s)$ is taken to be the NNLO CIPT/APT CORGI result of Eq.(4.68). Starting with $\tilde{\Lambda}^{(5)}_{\overline{MS}} = 216\text{MeV}$ for $N_f = 5$, corresponding to the world average value $\alpha_s(M_Z) = 0.1172$ [71], $\mathcal{R}(s)$ is kept continuous as the quark mass thresholds are crossed. This then determines $\tilde{\Lambda}^{(N_f)}_{\overline{MS}}$ for $N_f = 4, 3, 2, 1$. Standard values for current quark masses for the light quarks are taken [71] : $m_u = 3.0\text{MeV}$, $m_d = 6.75\text{MeV}$, $m_s = 117.5\text{MeV}$, and also from [71] the values for pole masses of the heavy quarks $m_c = 1.65\text{GeV}$, and $m_b = 4.85\text{GeV}$ are used. The approximate result [44] uses pole masses in Eq.(5.2), so we use pole masses where we can. Using these values for the quark masses and $\alpha_s(M_Z)$, we plot the resulting $R_{e^+e^-}(s)$ in figure 5.1. The solid line corresponds to the CORGI APT result for $\mathcal{R}(s)$ in Eq.(4.68). The dashed curve corresponds to the standard NLO fixed-order CORGI result,

$$\mathcal{R}_{CORGI}(s) = a_0(s) + \left(X_2 - \frac{\pi^2 b^2}{12}\right) a_0^3(s) \; . \tag{5.3}$$

The standard fixed-order result breaks down at $s = \Lambda_D^2 = 0.4114\text{GeV}^2$, where there is a Landau pole. The APT result smoothly freezes in the infrared. The dashed-dot curve shows the parton model result (i.e. assuming $\mathcal{R}(s) = 0$).

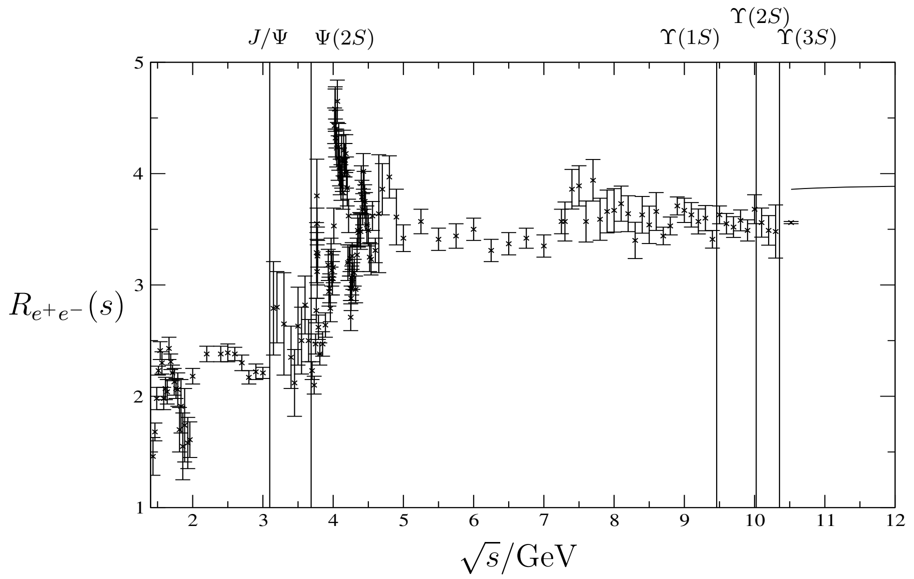

Figure 5.2: Data used to compare with model, statistical errors shown only.

5.2 Experimental data

For a recent comprehensive review see [70]. The experimental data used here come from a variety of sources. From the two-pion threshold up to $\sqrt{s} = 1.43$GeV references [80] are used; the data from these references are given as individual exclusive channels which must be combined to obtain the full hadronic cross section. For 1.43GeV $\rightarrow$ 2.0GeV data from [73], [74] are used, references [75], [76] are used in the region 2.0GeV $\rightarrow$ 5.0GeV. For 5.0GeV $\rightarrow$ 7.25GeV data from [77] are used, and for 7.25GeV $\rightarrow$ 10.52GeV [78], [79] are used. These sets of data all give the inclusive total hadronic cross section. Above 10.52GeV the NNLO CORGI APT prediction is inserted in for $R_{e^+e^-}$; this is represented by the continuous line in figure 5.2.

In order to simplify the analysis of the data we do not use overlapping datasets, instead where one dataset overlapped another we simply took the better, smaller-error, dataset in the region of the overlap in $\sqrt{s}$. Errors were dealt with by taking each data point and calculating the effect of its statistical and systematic error. Each statistical error was added in quadrature with all other statistical errors. The contribution from the systematic error was added to the other systematic errors from the same dataset, then the contribution from the systematic errors of each dataset were added in quadrature with each other and the contribution from the statistical errors.

Also narrow resonances that are not included in the data must be considered; the same approach as used in [48] is employed here. We assume that the narrow resonances have a relativistic Breit-Wigner form

$$R_{res}(s) = \frac{9}{\alpha^2} B_{ll} B_h \frac{M^2\Gamma^2}{(s-M^2)^2 + M^2\Gamma^2} \; , \tag{5.4}$$

where α is the QED coupling, and M, Γ, B_{ll}, B_h are the mass, width, lepton branching ratio, and hadron branching ratio respectively. Since a narrow resonance is assumed, Γ is taken to be small, so the resonance can be approximated with a delta function

$$\begin{aligned} R_{res}(s) = \frac{9}{\alpha^2} B_{ll} B_h M\Gamma\pi \frac{M\Gamma/\pi}{(s-M^2)^2 + M^2\Gamma^2} \\ \approx \frac{9}{\alpha^2} B_{ll} B_h M\Gamma\pi\delta(s-M^2) \; . \end{aligned} \tag{5.5}$$

The compilation of data for $R_{e^+e^-}$ is shown in figure 5.2. Narrow resonances are indicated by the vertical lines. Unfortunately it is not possible to directly compare the experimental data with the theoretical predictions. This is because there is not a direct correspondence between the quark mass thresholds in perturbation theory and the hadronic resonances. This difficulty can be overcome if one employs a "smearing procedure" demonstrated in the next section.

5.3 Phenomenology

In this section the smearing procedure proposed by Poggio, Quinn and Weinberg [44] is employed. The smeared quantity is defined to be

$$\bar{R}_{e^+e^-}(s;\Delta) = \frac{\Delta}{\pi} \int_0^\infty dt \frac{R_{e^+e^-}(t)}{(t-s)^2 + \Delta^2} \; . \tag{5.6}$$

$R_{e^+e^-}(s)$ itself is related to the vacuum-polarisation function $\Pi(s)$, as was shown in section 1.11:

$$R_{e^+e^-}(s) = -6\pi i (\Pi(s+i\epsilon) - \Pi(s-i\epsilon)) \; , \tag{5.7}$$

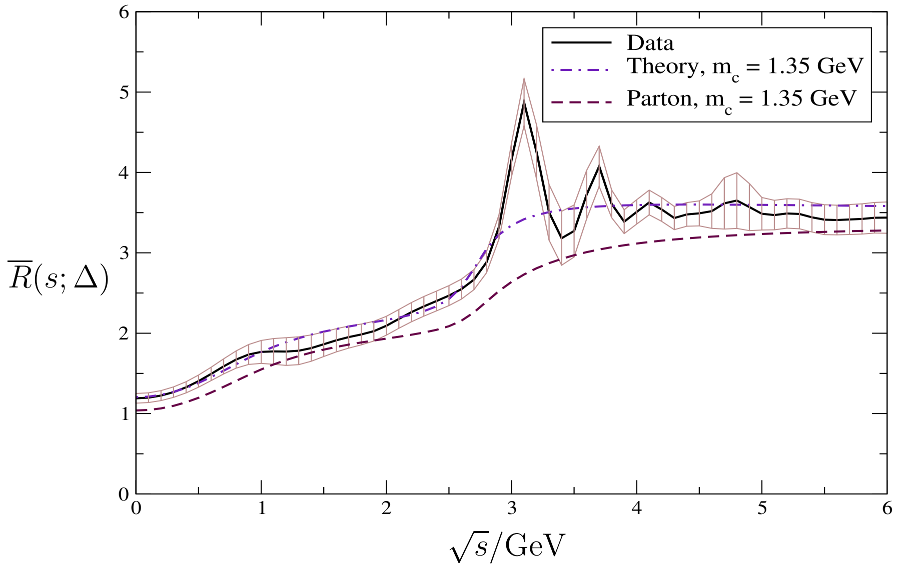

Figure 5.3: $\overline{R}(s;\Delta)$ in the charm region, with $\Delta = 1\text{GeV}^2$.

that is, it is the discontinuity across the cut. Using the dispersion relation the smeared $\bar{R}_{e^+e^-}(s;\Delta)$ can be written as

$$\bar{R}_{e^+e^-}(s;\Delta) = -6\pi i \left(\Pi(s+i\Delta) - \Pi(s-i\Delta)\right) \ . \tag{5.8}$$

If Δ is sufficiently large, one is kept away from the cut, and is insensitive to the infrared singularities which occur there. If both data and theory are smeared they can then be compared. One needs to choose Δ sufficiently large that resonances are averaged out. For the charm region it turns out that $\Delta = 3\text{GeV}^2$ is a good choice, whilst for lower energies $\Delta = 1\text{GeV}^2$ is adequate. In figure 5.3 $\Delta = 1\text{GeV}^2$ is chosen. $\bar{R}_{e^+e^-}(s;\Delta)$ obtained from the data is represented by the solid line. The dashed-dot line is the smeared NNLO CORGI APT prediction, assuming the quark mass thresholds as above with the exception of the charm quark, for reasons that will be shortly discussed. The dashed line is the parton model prediction. The shaded region denotes the error in the data. It is clear that in the charm region the averaging is insufficient, although for lower energies the agreement is extremely good. Figure 5.4 shows the corresponding plot with $\Delta = 3\text{GeV}^2$. There is now good agreement between smeared theory and experiment over the whole s range, for $m_c = 1.35\text{GeV}$. An error band associated with the

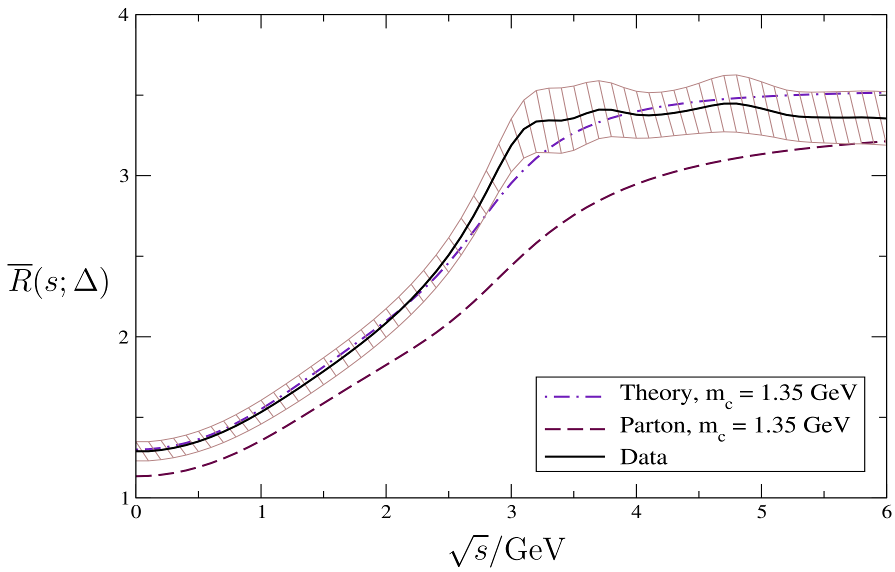

Figure 5.4: $\overline{R}(s;\Delta)$ in the charm region, with $\Delta = 3\text{GeV}^2$.

data has been included, but an error band for the theory prediction has not. There are several potential sources of error to consider. The first is the choice of renormalisation scale. The viewpoint taken here would be that the use of the CORGI scale corresponds to a complete resummation of ultraviolet logarithms. As has been argued in [18], attempts to estimate a theoretical error on the perturbative predictions by making *ad hoc* changes in the renormalisation scale, are simply misleading and give no information on the importance of uncalculated higher-order corrections.

A common approach, for instance, is to use scales $\mu^2 = xs$, where x is varied between $x = \frac{1}{2}$ and $x = 2$, with $x = 1$ providing a central value. It should be noted, however, that were we to have used such a procedure it would not have led to a noticeable difference in the theory curves, since the APT has greatly reduced scale-dependence, as has been noted elsewhere [45]. A more important uncertainty is the precise value of the quark masses assumed, and in particular the choice of the charm quark mass m_c. To illustrate how this affects the results figure 5.5 shows the curves obtained if we assume $m_c = 1.65\text{GeV}$. As can be seen, the theory curve is now inconsistent with the data in the charm region, although for lower energies where the charm quark has decoupled, the agreement is again good.

The uncertainty in the value of the mass of the charm quark is exceptionally

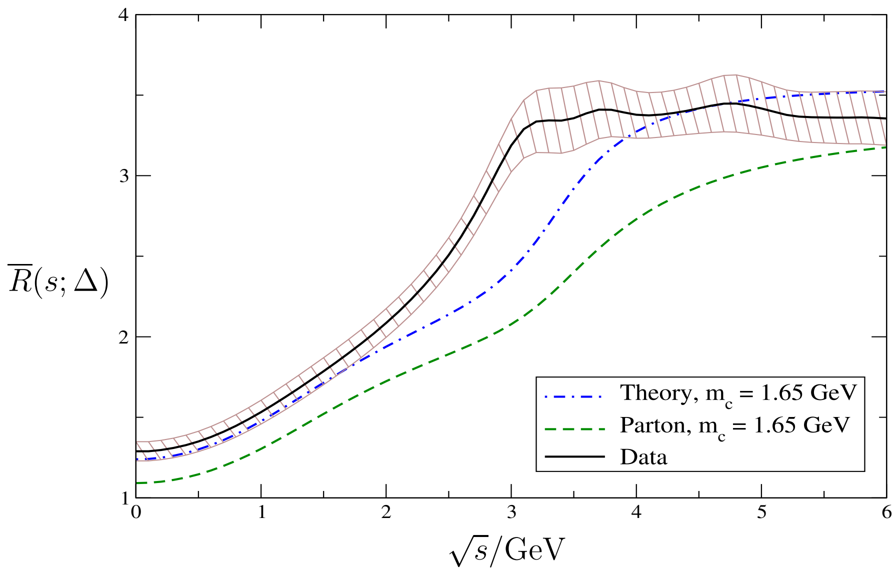

Figure 5.5: $\overline{R}(s;\Delta)$ in the charm region, with $\Delta = 3\text{GeV}^2$ here $m_c = 1.65\text{GeV}$.

large. Looking at the different references used in [71] a value $m_c = 1.35\text{GeV}$ for the pole mass is reasonable, and agrees well with [72], which is referenced in [71]. Part of the problem is the relationship between the pole mass and the $\overline{MS}$ mass for the charm quark, where the α_s^3 contribution is larger than the α_s^2 contribution. Obtaining the pole mass through $\overline{MS}$ mass calculations, which is done in [71], is not very satisfactory. Reference [72] gives a pole mass of $m_c = 1.33 - 1.4\text{GeV}$, and so the choice of 1.35GeV is reasonable.

It is possible to extend the smearing to spacelike values of s. The corresponding curves for $\bar{R}_{e^+e^-}(s;\Delta)$, with $m_c = 1.35\text{GeV}$, over the range $-3 < s < 1$ GeV^2 are displayed in figures 5.6, 5.7, for $\Delta = 1\text{GeV}^2$, and $\Delta = 3\text{GeV}^2$, respectively. The agreement between theory and experiment is extremely good in both cases.

In figure 5.8 $\bar{R}_{e^+e^-}(s;\Delta)$ is shown in the upsilon region. The choice $\Delta = 10\text{GeV}^2$ works quite well: the theory predictions for different m_b values are displayed. A direct comparison between theory and data which does not involve smearing is possible if one evaluates the area under the $R_{e^+e^-}(s)$ data, that is evaluates the integral,

$$I(s) \equiv \int_{4m_\pi^2}^{s} R_{e^+e^-}(t)dt; , \tag{5.9}$$

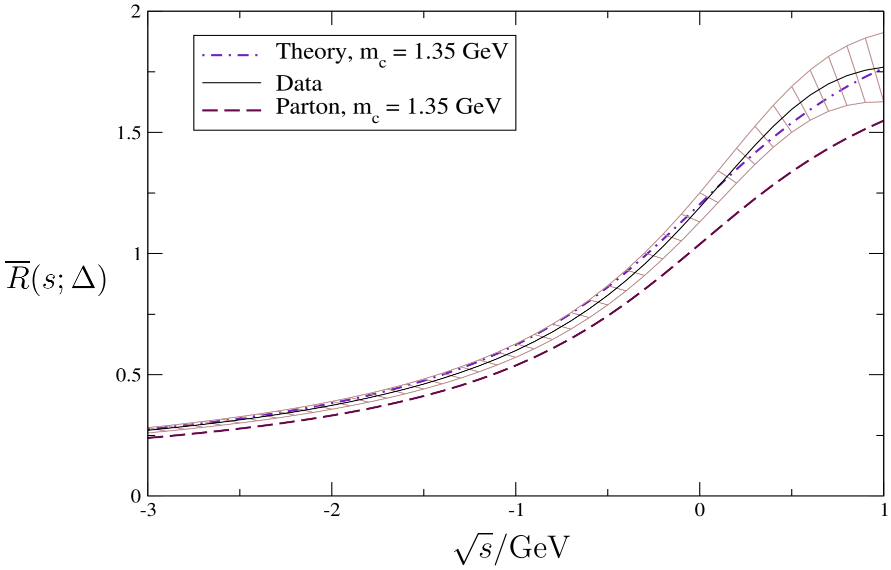

Figure 5.6: $\overline{R}(s;\Delta)$ in the spacelike region, with $\Delta = 1\text{GeV}^2$.

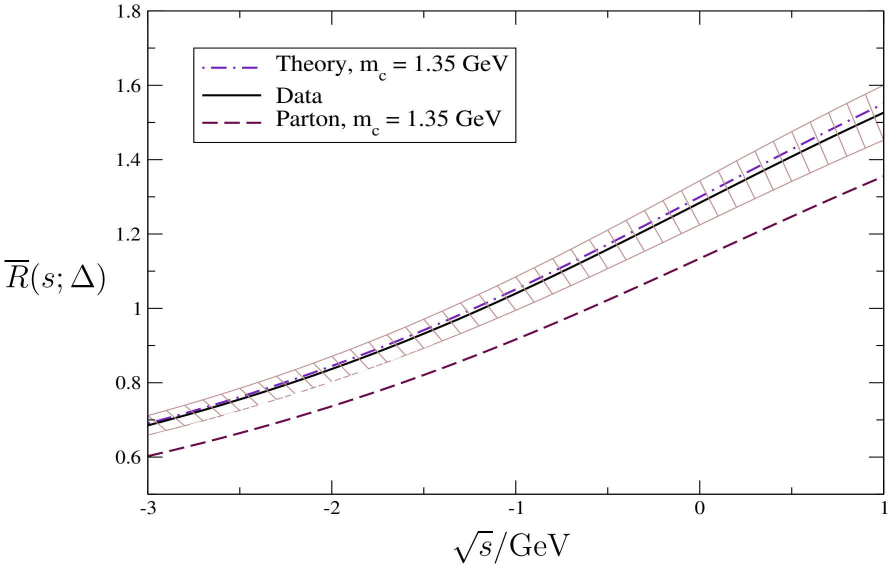

Figure 5.7: $\overline{R}(s;\Delta)$ in the spacelike region, with $\Delta = 3\text{GeV}^2$.

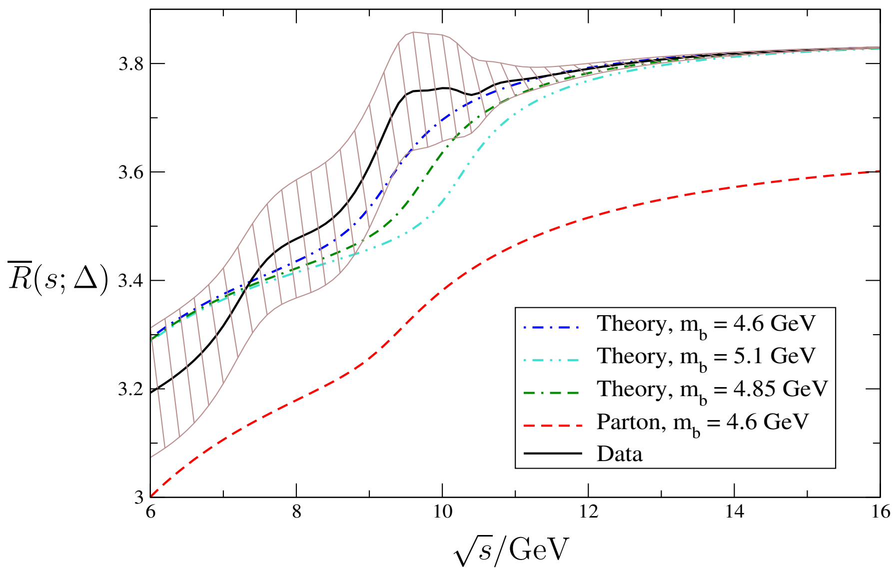

Figure 5.8: $\overline{R}(s;\Delta)$ in the upsilon region, with $\Delta = 10\mathrm{GeV}^2$.

where s lies well above the low-energy resonances in the continuum. The theoretical and experimental $I(s)$ over the range $5 < \sqrt{s} < 9\mathrm{GeV}$ are shown in figure 5.9. There is extremely good agreement. Finally, smearing can be avoided by transforming $R_{e^+e^-}(s)$ to obtain $D(Q^2)$ in the Euclidean region, using the dispersion relation

$$D(Q^2) = Q^2 \int_{4m_\pi^2}^{\infty} \frac{ds}{(s+Q^2)^2} R_{e^+e^-}(s) \ . \tag{5.10}$$

In practice a sufficiently large upper limit of $10^6\mathrm{GeV}^2$ is taken. The theory and data results are shown in figures 5.10, 5.11 . There is good agreement. These results are comparable to the fit obtained in [81], and to the results in [42]. Similar plots to those presented have been made in reference [82] using the variational perturbation theory (VPT) method [83],

5.4 Summary

In this chapter the QCD calculation for $\mathcal{R}$ is related to $R_{e^+e^-}$ including mass thresholds. The resulting theoretical calculation cannot be directly compared with experimental data due to the non-perturbative nature of hadronisation.

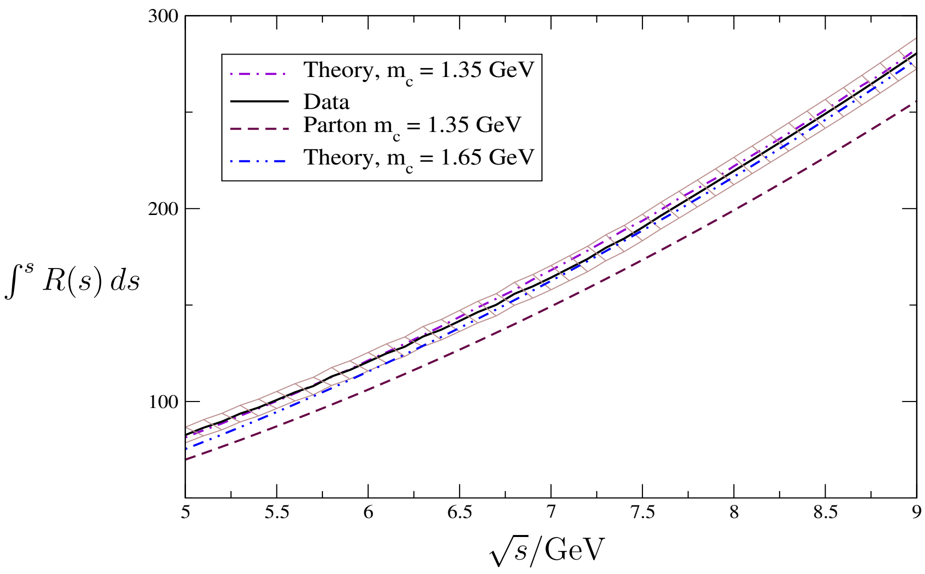

Figure 5.9: Area under $R_{e^+e^-}(s)$

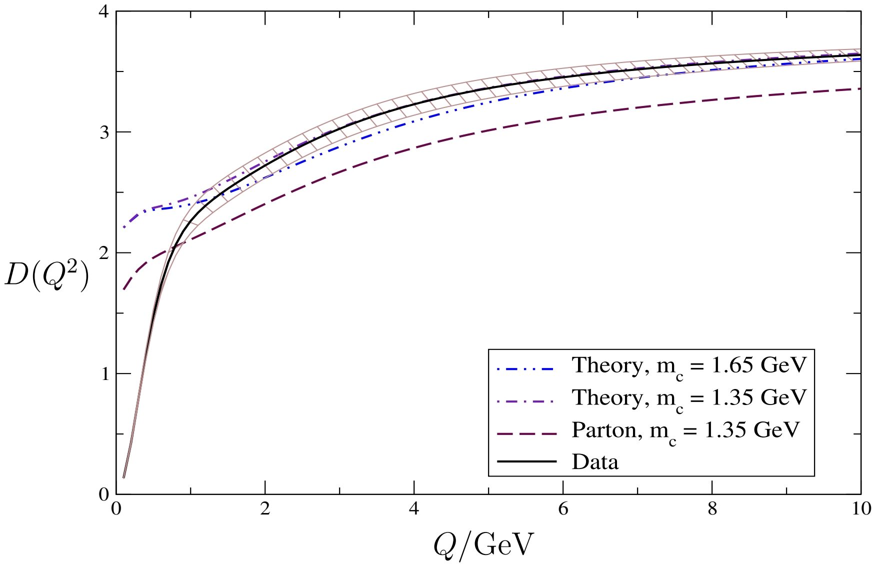

Figure 5.10: $D(Q^2)$ calculated using APT.

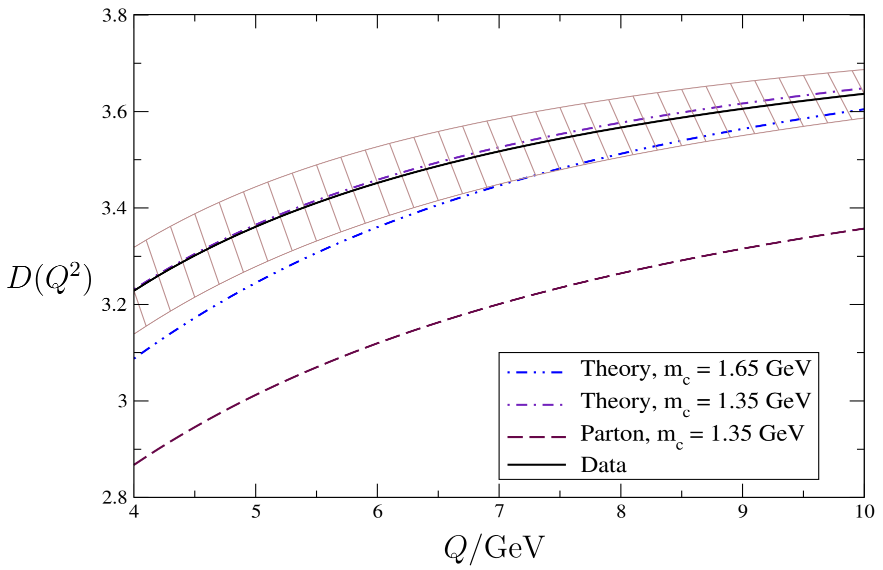

Figure 5.11: Figure 5.10 viewed over a smaller range.

The data and theoretical prediction can, however, be compared if a smearing procedure is used.

As well as smearing, integrating $R_{e^+e^-}(s)$ with respect to s, and transforming back to the Adler D-function are used to compare data and theory. Good agreement with the smeared NNLO CORGI APT results is found.

Chapter 6

IR freezing of $R_\mathcal{T}$

6.1 Hadronic decay of τ lepton

$R_{e^+e^-}$ is not the only quantity that can be related to the Adler D-function. The ratio R_τ, defined to be

$$R_\tau = \frac{\Gamma(\tau^- \to \nu_\tau + \text{hadrons})}{\Gamma(\tau \to \nu_\tau e^- \bar{\nu}_e)} \,, \tag{6.1}$$

can be related to a QCD perturbation series [84]

$$R_\tau = N(|V_{ud}|^2 + |V_{us}|^2) S_{EW} \left[1 + \delta_{EW} + \mathcal{R}_\tau + \delta_{PC}\right] \,. \tag{6.2}$$

$\mathcal{R}_\tau$ is the perturbative QCD correction. The quantities V_{ud}, V_{us}, δ_{EW}, and S_{EW} come from the electroweak theory that describes non-QCD behaviour in particle physics. The electroweak quantities V_{ud} and V_{us} are CKM mixing matrix elements, with values $|V_{ud}| = 0.9738 \pm 0.0005$, $|V_{us}| = 0.2200 \pm 0.0026$ [70]. The electroweak correction S_{EW} takes the value $S_{EW} \approx 1.0194$ [85]. the first term in the higher order electroweak correction is $\delta_{EW} = 5/(12\pi)\alpha(m_\tau^2)$ [84], where α is the QED coupling. There are power corrections including non-perturbative OPE terms represented by δ_{pc} that have been estimated to be $\delta_{PC} = -0.003 \pm 0.004$ [86].

There is a relation between $\mathcal{R}_\tau$ and $\mathcal{D}(s)$ similar to that in Eq.(1.97) [87]

$$\mathcal{R}_\tau = \frac{1}{2\pi i}\int_{-m_\tau^2-i\epsilon}^{-m_\tau^2+i\epsilon} \frac{dt}{t}\mathcal{D}(t)\left(1+2\frac{t}{m_\tau^2}-2\frac{t^3}{m_\tau^6}-\frac{t^4}{m_\tau^8}\right) . \tag{6.3}$$

As with the R-ratio, the one-loop beta function provides a simple example. Solving the beta function equation and assuming the choice of $\mu^2 = xt$ for the renormalisation scale gives the familiar form of the one-loop coupling $a(t) = \frac{2}{b\ln(xt/\tilde{\Lambda}^2)}$.

In Eq.(6.3) the first part of the integral is equivalent to $\mathcal{R}$ evaluated at $s = m_\tau^2$, and so can be approached in the same manner as one would for $\mathcal{R}(m_\tau^2)$. The remaining terms for $\mathcal{R}_\tau$ are included in the following

$$\begin{aligned}\mathcal{R}_\tau = {} & A_1(m_\tau^2) + \sum_{n=1}^{\infty} d_n A_n(m_\tau^2) + 2A_{1,1}(m_\tau^2) + 2\sum_{n=1}^{\infty} d_n A_{1,n}(m_\tau^2) \\ & - 2A_{3,1}(m_\tau^2) - 2\sum_{n=1}^{\infty} d_n A_{3,n}(m_\tau^2) - A_{4,1}(m_\tau^2) - \sum_{n=1}^{\infty} d_n A_{4,n}(m_\tau^2) .\end{aligned} \tag{6.4}$$

The A_n are given in Eq.(4.19). The new $A_{m,n}(s)$ terms can be obtained by taking the perturbation series for the Adler D-function and inserting it into the integral in Eq.(6.3). Making the change of variable to θ such that $t/m_\tau^2 = e^{i\theta}$ gives integrals of the form

$$A_{m,n}(m_\tau^2) = \frac{1}{2\pi}\int_{-\pi}^{\pi} \frac{\exp(im\theta)a^n(m_\tau^2)}{(1+ba(m_\tau^2)i\theta/2)^n}\, d\theta . \tag{6.5}$$

This gives the part of the integral in Eq.(6.3) with an $a^n(t)(t/m_\tau^2)^m$ term. The change of variable used is the same as the one used in Eq.(4.8). Evaluating this integral one obtains for $m > 0$

$$\begin{aligned}A_{m,n}(m_\tau^2) = {} & \left(\frac{-2m}{b}\right)^n \frac{\exp(-2m/ba)}{2\pi i m}\left[\Gamma(-n+1, -im\pi - \frac{2m}{ba})\right. \\ & \left.-\Gamma(-n+1, im\pi - \frac{2m}{ba})\right] + \frac{2}{b}\left(\frac{2m}{b}\right)^{n-1}\frac{1}{(n-1)!}\exp(-2m/ba) ,\end{aligned} \tag{6.6}$$

where $a = a(m_\tau^2)$. For $m = 0$ the result is the same as for the A_n in Eq.(4.19). The integral of Eq.(6.5) has been solved in terms of incomplete gamma functions, defined to be

$$\Gamma(a,b) = \int_b^\infty t^{a-1} e^{-t}\, dt \ . \tag{6.7}$$

Eq.(6.6) has asymptotic freedom as $m_\tau^2 \to \infty$, but in the limit $m_\tau^2 \to 0$ $\mathcal{R}_\tau$ becomes infinite. The integrand in Eq.(6.5) has a pole in the complex θ-plane. In the case of $\mathcal{R}$ the prescription for dealing with such poles is clear, as there is only one choice that gives asymptotic freedom. However, here the residue of the pole is asymptotically free itself and the prescription for the path of integration becomes unclear. The choice of integrating θ from $-\pi$ to π along the real axis leads to the exponential term in Eq.(6.6) which gives the unfortunate divergence in the limit $m_\tau^2 \to 0$.

The residue of the pole in Eq.(6.5) gives the infrared divergent part of $A_{m,n}$, and so one can choose the path of integration in the θ-plane to keep the $A_{m,n}$ finite. For this choice of integration contour the $A_{m,n}$ are now

$$A_{m,n}(m_\tau^2) = \left(\frac{-2m}{b}\right)^n \frac{\exp(-2m/ba(m_\tau^2))}{2\pi i m}$$
$$\left[\Gamma(-n+1, -im\pi - \frac{2m}{ba(m_\tau^2)}) - \Gamma(-n+1, im\pi - \frac{2m}{ba(m_\tau^2)})\right] \ . \tag{6.8}$$

CIPT has been used extensively in phenomenological investigations of $\mathcal{R}_\tau$ [46, 65], and in these investigations the integral in Eq.(6.5) is performed around a circular contour. This path yields the result of Eq.(6.6).

Graphs of the functions $A_{m,n}(m_\tau^2)$ from Eq.(6.6), for m = 1,3,4 with n = 1-3, are displayed in figures 6.1 to 6.3.

Of course $m_\tau^2 \to 0$ for $\mathcal{R}_\tau$ is not physically relevant, but there exists the spectral function

$$\mathcal{R}_\tau(s_0) \equiv \frac{\Gamma(\tau^- \to \nu_\tau + \text{hadrons}; s_{had} < s_0)}{\Gamma(\tau^- \to \nu_\tau e^- \bar{\nu}_e)} \ , \tag{6.9}$$

where s_{had} is the centre of momentum energy squared of the hadrons. The variable s_0 can take values below m_τ^2, and the spectral function can be related to the integrals required for $\mathcal{R}_\tau$ [36, 46, 86]. So the $s_0 \to 0$ behaviour of the spectral function is the actual problem we have in mind.

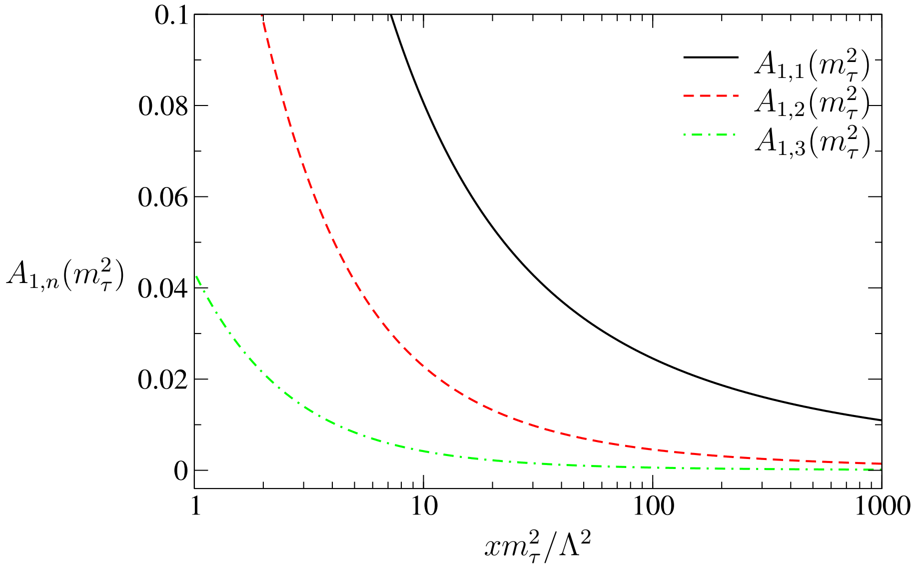

Figure 6.1: CIPT $A_{1,n}$ for n = 1-3

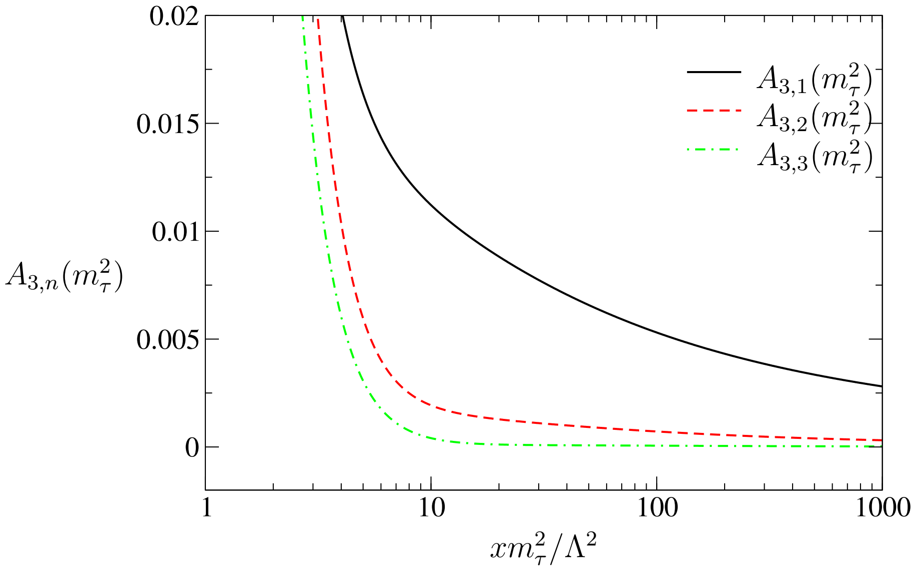

Figure 6.2: CIPT $A_{3,n}$ for n = 1-3

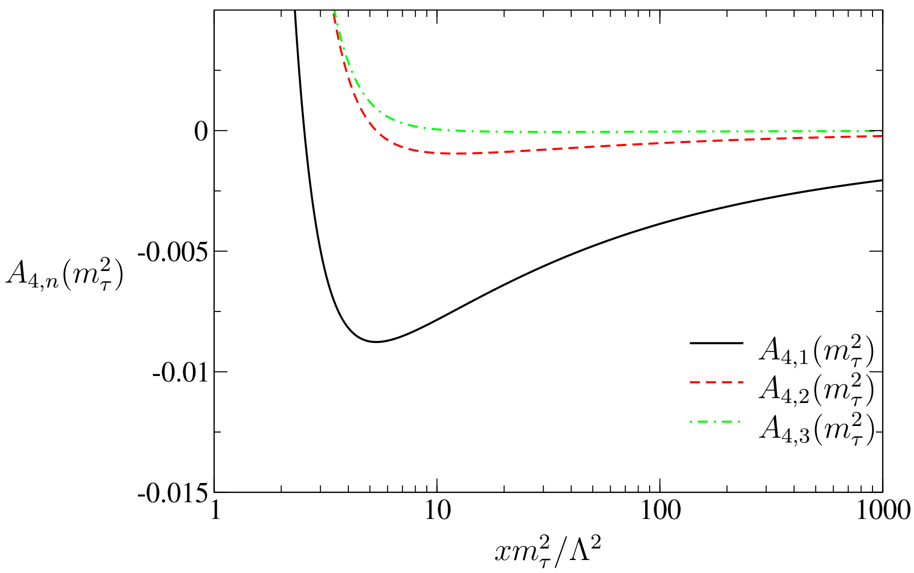

Figure 6.3: CIPT $A_{4,n}$ for n = 1-3

6.2 Borel representation for $\mathcal{R}_\tau$

It appears that the functions $A_{m,n}$ are ambiguous, and depend on the integration path in Eq.(6.5). However, as we shall now show, these functions correspond to a convergent resummation of an infinite subset of terms in the perturbation series for $\mathcal{R}_\tau$. The ambiguity is in fact a pathology of the representation in Eq.(6.5) used to define $A_{m,n}$. One should rather use a Borel sum to define $A_{m,n}$. Since the Borel method is regular, as discussed in chapter 3, it is guaranteed to return the unique result corresponding to the sum of the series within its radius of convergence.

Replacing the Adler D-function with its Borel integral converts Eq.(6.3) to the integral

$$\mathcal{R}_\tau = \int_0^\infty (I_0 + 2I_1 - 2I_3 - I_4)B[\mathcal{D}](z)\, dz\ . \tag{6.10}$$

The I_m are integrals of the form

$$I_m = \frac{1}{2\pi i}\int_{-m_\tau^2-i\epsilon}^{-m_\tau^2+i\epsilon} \frac{dt}{t}\left(\frac{t}{m_\tau^2}\right)^m e^{-z/a(t)}\ . \tag{6.11}$$

Solving the integrals I_m one obtains mathematical expressions analogous to the $\frac{\sin(\pi bz/2)}{\pi bz/2}$ term in the Borel integral for $\mathcal{R}(s)$.

Solving Eq.(6.11) for the one-loop beta-function is straightforward; choosing a circular contour in the t-plane and making the substitution $t = m_\tau^2 e^{i\theta}$ converts the integral to

$$I_m = \frac{1}{2\pi}\int_{-\pi}^{\pi} e^{im\theta} e^{-izb\theta/2} e^{-z/a(m_\tau^2)}\, d\theta\ . \tag{6.12}$$

The θ-integral gives the result

$$I_m = e^{-z/a(m_\tau^2)} \frac{\sin(\pi bz/2 - m\pi)}{\pi bz/2 - m\pi}\ , \tag{6.13}$$

and setting $m = 0$ returns the familiar result for $\mathcal{R}(s)$ with $s = m_\tau^2$.

Inserting Eq.(6.13) into the integral in Eq.(6.10) gives the Borel integral for $\mathcal{R}_\tau$ to be

$$\mathcal{R}_\tau = \int_0^\infty e^{-z/a(m_\tau^2)} \left(\frac{1}{\pi bz/2} - \frac{2}{\pi bz/2 - \pi} + \frac{2}{\pi bz/2 - 3\pi} - \frac{1}{\pi bz/2 - 4\pi}\right) \sin\left(\frac{\pi bz}{2}\right) B[\mathcal{D}](z)\, dz\ . \tag{6.14}$$

Use of partial fractions relates this to the form of the leading-b Borel integral given in [36]:

$$\mathcal{R}_\tau = \int_0^\infty e^{-z/a(m_\tau^2)} \left(\frac{2}{1 - bz/2} - \frac{2}{1 - bz/6} + \frac{1}{1 - bz/8}\right) \frac{\sin(\pi bz/2)}{\pi bz/2} B[\mathcal{D}](z)\, dz\ . \tag{6.15}$$

This is the same as the leading-b integral for $\mathcal{R}$ with some extra IR renormalon-like terms inserted.

It is straightforward for the analytic functions, $A_{m,n}(m_\tau^2)$ that make up the series for $\mathcal{R}_\tau$ to be related to the standard APT functions used for $R_{e^+e^-}$ by looking at the Borel integral. Consider the Borel integral for the function $A_{m,n}$, at one-loop order:

$$A_{m,n}(m_\tau^2) = \int_0^\infty e^{-z/a(m_\tau^2)} \frac{\sin(\pi bz/2 - m\pi)}{\pi bz/2 - m\pi} \frac{z^{n-1}}{(n-1)!}\, dz\ . \tag{6.16}$$

If the denominator in the integral is expanded a series can be obtained that consists of terms of the form you would find for $R_{e^+e^-}$, i.e. the case with $m = 0$:

$$A_{m,n}(m_\tau^2) = \int_0^\infty e^{-z/a(m_\tau^2)} \frac{\sin(\pi bz/2)}{\pi bz/2} (-1)^{m+1} \left[\left(\frac{bz}{2m}\right) + \left(\frac{bz}{2m}\right)^2 + \cdots \right] \frac{z^{n-1}}{(n-1)!} \, dz$$
$$= (-1)^{m+1} \left[\left(\frac{b}{2m}\right) n A_{n+1}(m_\tau^2) + \left(\frac{b}{2m}\right)^2 n(n+1) A_{n+2}(m_\tau^2) + \cdots \right] . \qquad (6.17)$$

The $A_{m,n}$ are then a series in A_n with factorially growing coefficients. This $n!$ growth will be a problem if it also afflicts the series expansion in the coupling, then the $A_{m,n}$ would not correspond to resumming a convergent perturbative sub-series in the coupling.

The $A_{m,n}(m_\tau^2)$ can be given as a series in the coupling: expanding all but the exponential into a series in z gives

$$A_{m,n}(m_\tau^2) = \int_0^\infty e^{-z/a} \frac{(-1)^{m+1}}{m\pi} \sum_{k=0}^{\infty} \left[\sum_{l=0}^{2l \le k-1} (-1)^l \left(\frac{(\pi bz/2)^{2l+1}}{(2l+1)!} \right) \left(\frac{bz}{2m}\right)^{k-2l-1} \right] \frac{z^{n-1}}{(n-1)!} \, dz$$
$$= \int_0^\infty e^{-z/a} \frac{(-1)^{m+1}}{m\pi} \sum_{k=0}^{\infty} \left(\frac{bz}{2m}\right)^k \left[\sum_{l=0}^{2l \le k-1} (-1)^l \frac{(m\pi)^{2l+1}}{(2l+1)!} \right] \frac{z^{n-1}}{(n-1)!} \, dz . \qquad (6.18)$$

The term in the square brackets on the second line is part of the expansion for $\sin(x)$ where $x = m\pi$, $\sin(m\pi) = 0$ and so this equation can be expressed differently

$$A_{m,n}(m_\tau^2) = \int_0^\infty e^{-z/a} \frac{(-1)^{m+1}}{m\pi} \sum_{k=0}^{\infty} \left(\frac{bz}{2m}\right)^k \left[\sum_{2l > k-1}^{\infty} (-1)^l \frac{(m\pi)^{2l+1}}{(2l+1)!} \right] \frac{z^{n-1}}{(n-1)!} \, dz . \qquad (6.19)$$

Eq.(6.19) can be integrated into a series in a which is convergent with a radius of convergence of $|a| < 2/(\pi b)$. This is due to the factorial in the denominator in the l-summation in the square brackets. This convergence is not apparent when observing Eq.(6.17).

The Borel integral does give us a series for $A_{m,n}$ that is convergent for a small enough coupling, and so it is possible to equate the series with the different $A_{m,n}$ resulting from the different prescriptions for integrating around the pole in the θ-plane. This means that a choice of a particular prescription can be shown to match the sub-series in the coupling for A_{mn}.

Performing the integral in Eq.(6.16) one obtains the expression given earlier in Eq(6.6) which corresponds to the standard CIPT used in $\mathcal{R}_\tau$ investigations [46, 65]. To see this, first consider Eq.(6.16) with $n = 1$. Splitting the sine function into exponentials and making a change of variable returns

$$\int_0^\infty e^{-z/a(m_\tau^2)} \frac{\sin(\pi bz/2 - m\pi)}{\pi bz/2 - m\pi}\, dz = \frac{2e^{-2m/ba(m_\tau^2)}}{\pi b} Im\left[PV \int_{-2m/b}^{\infty} e^{-z/a(m_\tau^2)+i\pi bz/2}\, \frac{dz}{z}\right] . \quad (6.20)$$

The PV indicates that the principal value is taken. In Eq.(6.16) there is no pole in the integration. Taking the principal value in Eq.(6.20) ensures that it agrees with Eq.(6.16). Eq.(6.20) can be related to incomplete Γ-functions:

$$\int_0^\infty e^{-z/a(m_\tau^2)} \frac{\sin(\pi bz/2 - m\pi)}{\pi bz/2 - m\pi}\, dz = \frac{2e^{-2m/ba(m_\tau^2)}}{\pi b} Im\left[\Gamma(0, -2m/ba(m_\tau^2) + i\pi m) + i\pi\right] , \quad (6.21)$$

where the $i\pi$ term is due to taking the principal value. This agrees with Eq.(6.6) for $n = 1$. Using induction the general case with $n > 1$ can now be solved.

Assuming that the $n = k$ case agrees with Eq.(6.6), the $n = k + 1$ case will be

$$\begin{aligned}
&\int_0^\infty e^{-z/a(m_\tau^2)} \frac{\sin(\pi bz/2 - m\pi)}{\pi bz/2 - m\pi} \frac{z^k}{k!}\, dz \\
= \frac{2m}{bk} &\int_0^\infty e^{-z/a(m_\tau^2)} \frac{\sin(\pi bz/2 - m\pi)}{\pi bz/2 - m\pi} \frac{z^{k-1}}{(k-1)!}\, dz \\
+\frac{2}{\pi bk} &\int_0^\infty e^{-z/a(m_\tau^2)} \sin(\pi bz/2 - m\pi) \frac{z^{k-1}}{(k-1)!}\, dz\ .
\end{aligned} \tag{6.22}$$

Denoting the integral in Eq.(6.16) as I_n, the recurrence relation is

$$I_{k+1} = \frac{2m}{bk} I_k + \frac{2}{\pi bk}(-1)^m Im\left[\left(\frac{1}{a(m_\tau^2)} - \frac{i\pi b}{2}\right)^{-k}\right]\ . \tag{6.23}$$

This result shows that Eq.(6.16) can be represented as a sum of terms involving the coupling, and an incomplete Γ-function.

An equivalent recurrence relation can be obtained for the Γ-functions of Eq.(6.6). Assuming that the integral I_k agrees with Eq.(6.6) for $n = k$ it can be shown that I_{k+1} agrees with the $n = k+1$ case as well

$$\begin{aligned}
&\left(\frac{-2m}{b}\right)^{k+1} \frac{e^{-2m/ba(m_\tau^2)}}{\pi m} Im\left[-\Gamma(-k, i\pi m - 2m/ba(m_\tau^2))\right] \\
&\qquad\qquad + \frac{2}{b}\frac{e^{-2m/ba(m_\tau^2)}}{k!}\left(\frac{2m}{b}\right)^k \\
&= \left(\frac{-2m}{b}\right)^{k+1} \frac{e^{-2m/ba(m_\tau^2)}}{\pi m} Im\left[\frac{1}{k}\Gamma(-k+1, i\pi m - 2m/ba(m_\tau^2))\right. \\
&\left. - \frac{1}{k} e^{2m/ba(m_\tau^2)}(-1)^m \left(\frac{-2m}{ba(m_\tau^2)} + i\pi m\right)^{-k}\right] + \frac{2}{b}\frac{e^{-2m/ba(m_\tau^2)}}{k!}\left(\frac{2m}{b}\right)^k \\
&= \frac{2m}{bk} I_k + \frac{2}{\pi bk}(-1)^m Im\left[\left(\frac{1}{a(m_\tau^2)} - \frac{i\pi b}{2}\right)^{-k}\right]\ .
\end{aligned} \tag{6.24}$$

The fact that Eq.(6.6) agrees with the result from the Borel resummation implies that one obtains the same result as a resummation of the perturbation series for $\mathcal{R}_\tau$, since the Borel transform is regular. This is despite the seemingly non-perturbative term proportional to $\exp(-2m/ba(m_\tau^2))$ that was left out in Eq.(6.8).

In the low energy $m_\tau^2 < s_L$ region the modified form of the Borel integral is required. The Borel integral for $A_{m,n}(m_\tau^2)$ is now, using the same approach as was used to obtain Eq.(4.50),

$$A_{m,n}(m_\tau^2) = -\int_0^\infty e^{-z/(-a(m_\tau^2))} \frac{\sin(\pi bz/2 + m\pi)}{\pi bz/2 + m\pi} \frac{(-z)^{n-1}}{(n-1)!} \,. \tag{6.25}$$

Repeating as before, the $n = 1$ case can be evaluated, as can a recurrence relation. The $n = 1$ case will now be

$$\begin{aligned} &\frac{2}{\pi b} e^{-2m/ba(m_\tau^2)} Im \left[\int_{2m/b}^\infty e^{-z/(-a(m_\tau^2)) - i\pi bz/2} \frac{dz}{z} \right] \\ &\qquad = \frac{2}{\pi b} e^{-2m/ba(m_\tau^2)} Im \left[\Gamma(0, -2m/ba(m_\tau^2) + i\pi m) \right] \,, \end{aligned} \tag{6.26}$$

which agrees with Eq.(6.8) for the form of $A_{m,1}(m_\tau^2)$.

Denoting the integral in Eq.(6.25) by I_n, the recurrence relation is

$$I_{k+1} = \frac{2m}{bk} I_k + \frac{2}{\pi bk} (-1)^m Im \left[\left(\frac{1}{a(m_\tau^2)} - \frac{i\pi b}{2} \right)^{-k} \right] \,. \tag{6.27}$$

This recurrence relation plus the result for the $n = 1$ case shows that for $m_\tau^2 < s_L$ the equation for the $A_{m,n}$ in Eq.(6.8) agrees with the Borel integral.

Thus the functions $A_{m,n}(m_\tau^2)$ have an apparent discontinuity at $s = s_L$ of $\frac{2}{b}\left(\frac{2m}{b}\right)^{n-1} \frac{1}{(n-1)!}$. Continuity can be restored by adding to Eq.(6.8) the term $\frac{2}{b}\left(\frac{2m}{b}\right)^{n-1} \frac{1}{(n-1)!} e^{2m/ba}$, which is an $\left(\frac{m_\tau^2}{\tilde{\Lambda}^2}\right)^m$ non-perturbative effect of the same form as terms in the modified OPE (Eq.(4.43)).

6.3 Two-loop results for $A_{m,n}(m_\tau^2)$

Moving on from the one-loop case to the realistic case of full QCD we replace the 't Hooft scheme used in our treatment of $R_{e^+e^-}$ with the beta function

$$\mu \frac{da}{d\mu} = -\frac{ba^2}{1 - ca} \,, \tag{6.28}$$

This choice is made as it leads to a simple expression for $\mathcal{R}_\tau$, whereas the 't Hooft scheme does not.

Following the one-loop approach we now solve Eq.(6.28), and obtain an expression for the coupling

$$a(s) = -\frac{1}{cW(A(s))} , \tag{6.29}$$

where

$$A(s) = -\left(\frac{xs}{\tilde{\Lambda}^2}\right)^{-b/2c} , \tag{6.30}$$

and W is the Lambert W-function. $\tilde{\Lambda}$ is the dimensionful parameter chosen using the convention of Eq.(2.32). The choice of renormalisation scale is $\mu^2 = xs$.

Looking at this it is clear that to relate this to the two-loop coupling $a_{2-loop}(s)$ of Eq.(4.23) one has the relation

$$a_{2-loop}(se^{-2c/b}) = \frac{a(s)}{1-ca(s)} = a(s) + ca^2(s) + c^2a^3(s) + \cdots . \tag{6.31}$$

Using the integral in Eq.(6.3) with the change of variable to $w = W(A(t))$ gives $\mathcal{R}_\tau$ as a combination of integrals of the form

$$-\frac{c}{\pi bi}\left(\frac{\tilde{\Lambda}^2}{xm_\tau^2}\right)^m \int_{W_1(A(-m_\tau^2-i\epsilon))}^{W_{-1}(A(-m_\tau^2+i\epsilon))} \left(-\frac{1}{cw}\right)^n (-w)^{-2cm/b} \exp(-2cmw/b)\left(1+\frac{1}{w}\right) dw . \tag{6.32}$$

The subscript of 1 or -1 denotes the correct branch of the Lambert W function chosen by demanding asymptotic freedom, as demonstrated in section 4.2. Again this integral is ambiguous, and if m is non-zero then we cannot fix its value through asymptotic freedom. Choosing the path of integration that corresponds to the θ integral from $-\pi \to \pi$, and repeating the one-loop approach gives Eq.(6.4) for $\mathcal{R}_\tau(s)$, with different $A_n(s)$ and $A_{m,n}(s)$. These functions are now

$$\begin{aligned}
A_1(s) &= \left(\frac{2}{\pi b}\right) Im \left[\ln(-cW_{-1}(A(se^{i\pi}))) + \frac{c}{W_{-1}(A(se^{i\pi}))}\right] \\
A_n(s) &= (-1)^n \left(\frac{2}{\pi b c^{n-1}}\right) Im \left[\frac{1}{n}\left(\frac{1}{W_{-1}(A(se^{i\pi}))}\right)^n\right. \\
&+ \left.\frac{1}{n-1}\left(\frac{1}{W_{-1}(A(se^{i\pi}))}\right)^{n-1}\right] \; (n>1) \; . \qquad (6.33)
\end{aligned}$$

In this case the integral that goes straight from $W_1(A(-m_\tau^2 - i\epsilon))$ to its complex conjugate $W_{-1}(A(-m_\tau^2 + i\epsilon))$, yields functions $A_{m,n}(s)$ that are not infrared finite.

$$\begin{aligned}
A_{m,n}(s) = (-1)^n \left(\frac{\tilde{\Lambda}^2}{x m_\tau^2}\right)^m \left(\frac{2}{\pi b c^{n-1}}\right) Im \left[\exp(-2\pi i c m/b)\left(\frac{2mc}{b}\right)^{n+2mc/b}\right. \\
\left.\left(\Gamma(-n-2mc/b, W_{-1}(A(se^{i\pi}))) + \frac{b}{2mc}\Gamma(-n+1-2mc/b, W_{-1}(A(se^{i\pi})))\right)\right] \\
- \lim_{\alpha\to 0^+}(-1)^n \left(\frac{\tilde{\Lambda}^2}{x m_\tau^2}\right)^m \left(\frac{2}{\pi b c^{n-1}}\right) Im \left[\exp(-2\pi i c m/b)\left(\frac{2mc}{b}\right)^{n+2mc/b}\right. \\
\left.\left(\Gamma(-n-2mc/b, -1-i\alpha) + \frac{b}{2mc}\Gamma(-n+1-2mc/b, -1-i\alpha)\right)\right] \; . \; (6.34)
\end{aligned}$$

The limit is taken due to a branch cut in the Γ-function.

The infrared finite result for the $A_{m,n}(m_\tau^2)$ is

$$\begin{aligned}
A_{m,n}(s) = (-1)^n \left(\frac{\tilde{\Lambda}^2}{x m_\tau^2}\right)^m \left(\frac{2}{\pi b c^{n-1}}\right) \\
Im \left[\exp(-2\pi i c m/b)\left(\frac{2mc}{b}\right)^{n+2mc/b} \left\{\Gamma(-n-2mc/b, W_{-1}(A(se^{i\pi})))\right.\right. \\
\left.\left. + b/2mc\, \Gamma(-n+1-2mc/b, W_{-1}(A(se^{i\pi})))\right\}\right] \; . \qquad (6.35)
\end{aligned}$$

These functions and the $A_n(s)$ are displayed in figures 6.4 to 6.7. The integrals for each of the functions $A_{m,n}(s)$ have been solved in terms of an incomplete gamma function. If the 't Hooft scheme had been used then the $(-1/cw)^n$ term in those integrals would be replaced by $(-1/c(1+w))^n$. The 't Hooft scheme would lead to an infinite series of incomplete gamma functions.

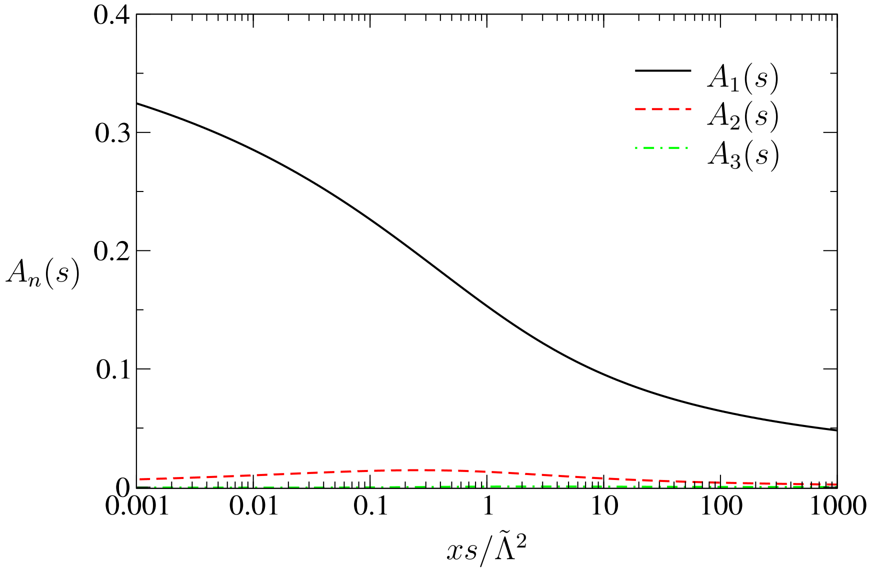

Figure 6.4: $A_n(s)$ from beta function in Eq.(6.28)

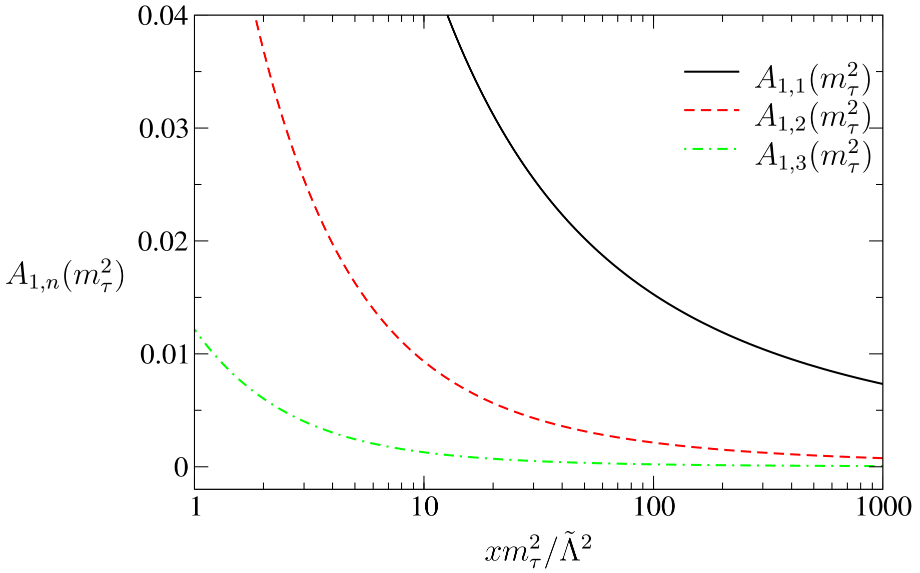

Figure 6.5: $A_{1,n}$ from beta function in Eq.(6.28)

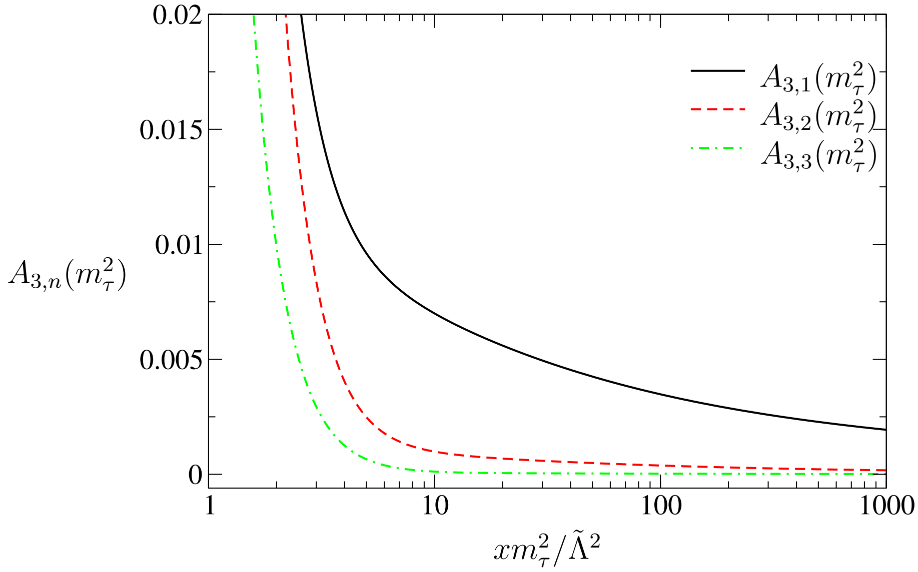

Figure 6.6: $A_{3,n}$ from beta function in Eq.(6.28)

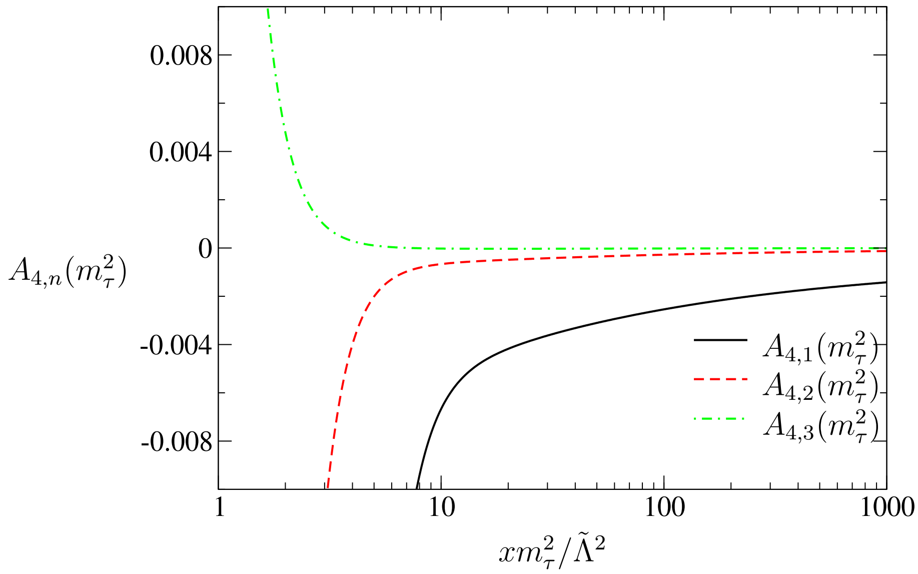

Figure 6.7: $A_{4,n}$ from beta function in Eq.(6.28)

In the limit where the second beta function coefficient, $c \to 0$, Eqs.(6.35, 6.34) become the same functions of the coupling as Eqs.(6.8, 6.6) respectively. One can see this numerically: taking $xs/\tilde{\Lambda}^2 = 100$ and three flavours of quark the one-loop coupling has the values $a(s) = 0.096510$, $a(se^{i\pi}) = 0.065860 + 0.044929I$. Eqs.(6.8, 6.6) for $A_{1,2(s)}$ take the values 0.0045445 and 0.0025692 respectively. Using the relation $W_{-1}(A(se^{i\pi})) = -1/ca(se^{i\pi})$ to insert the value of $a(se^{i\pi})$ into Eqs.(6.35, 6.34), one finds for $c = 0.001$ the values 0.0045261, 0.0025584 for Eqs.(6.35, 6.34) respectively. For $c = 0.000001$ one finds 0.0045444, 0.0025691.

For vanishing c Eq.(6.34) matches Eq.(6.6) and so for sufficiently large values of $s = m_\tau^2$ Eq.(6.34) will correspond to the perturbative sub-series returned by the Borel integral. Similarly Eq.(6.35) gives the perturbative sub-series from the alternative Borel integral for sufficiently low values of $s = m_\tau^2$.

All that remains is to isolate where the change in the form of the Borel integral takes place.

The choice of beta function used in Eq.(6.28) will return results similar to the previous two-loop beta-function, however this form of beta-function can be used to obtain the simple expressions for the functions $A_{m,n}(m_\tau^2)$ as shown earlier.

Proceeding as for the 't Hooft scheme, the integrals I_m from Eqs.(6.10, 6.11) can be expressed as integrals in the value of the Lambert W-function that gives the value of the coupling.

$$I_m = \frac{-c}{b\pi i} \int_{W_1(\bar{A}(-m_\tau^2 - i\epsilon))}^{W_{-1}(\bar{A}(-m_\tau^2 + i\epsilon))} \left(\frac{xm_\tau^2}{\tilde{\Lambda}^2} \right)^{-m} (-we^w)^{-2mc/b} e^{zcw} \frac{1+w}{w} dw \ . \quad (6.36)$$

Again the integrals I_m can be expressed as incomplete gamma functions,

$$\begin{aligned}
I_m = & \frac{2c}{\pi b} e^{-2m/ba(m_\tau^2)} \left(ca(m_\tau^2)\right)^{-2cm/b} \\
Im & \left[\Gamma\left(\frac{-2mc}{b}, \frac{1}{ca(-m_\tau^2+i\epsilon)}\left(zc-\frac{2mc}{b}\right)\right)\left(zc-\frac{2mc}{b}\right)^{2mc/b} \right. \\
-\Gamma & \left(\frac{-2mc}{b}+1, \frac{1}{ca(-m_\tau^2+i\epsilon)}\left(zc-\frac{2mc}{b}\right)\right) \\
& \left. \left(zc-\frac{2mc}{b}\right)^{2mc/b-1} \right] . \qquad (6.37)
\end{aligned}$$

The point at which the I_m diverge for large positive z and no longer diverge for large $-z$ is the point of the Landau divergence introduced in section 4.3. This change occurs at the point where $Re(a(-m_\tau^2 + i\epsilon)) = 0$. This s_L is different from the $R_{e^+e^-}$ case as a different beta function is used. It should be noted of course that m_τ^2 is large enough that the choice of Eq.(6.34) should be used to evaluate $\mathcal{R}_\tau$ itself.

6.4 Phenomenology

Previous use of expressing $\mathcal{R}_\tau$ as the integral of a perturbation series (in Eq.(6.3)) as opposed to using the said integral to obtain a perturbation series can be found in [46, 65].

In calculating the all-orders CORGI resummation for the R-ratio, the circular contour that determined $\mathcal{R}(s)$ at high energy could use the NNLO contour-improved CORGI result, for a sufficiently high value of s. However, due to the $(t/m_\tau^2)^m$ factors in the integrand of Eq.(6.3) the difference that is negligible in $\mathcal{R}(s)$ for the calculation of such a circular contour will be enhanced by a factor of $(t_0/m_\tau^2)^m$ where t_0 is the radius of the circular contour for the t integral. This enhancement of the difference between the calculation and the desired result is a problem considering the relatively small value of m_τ.

This means that the choice of prescription for integrating around the IR renormalons used in Eq.(4.62) cannot be used, as the $Ei(1, -z_j/a(t))$ term forbids a continuous circular contour of integration. Using the NNLO result

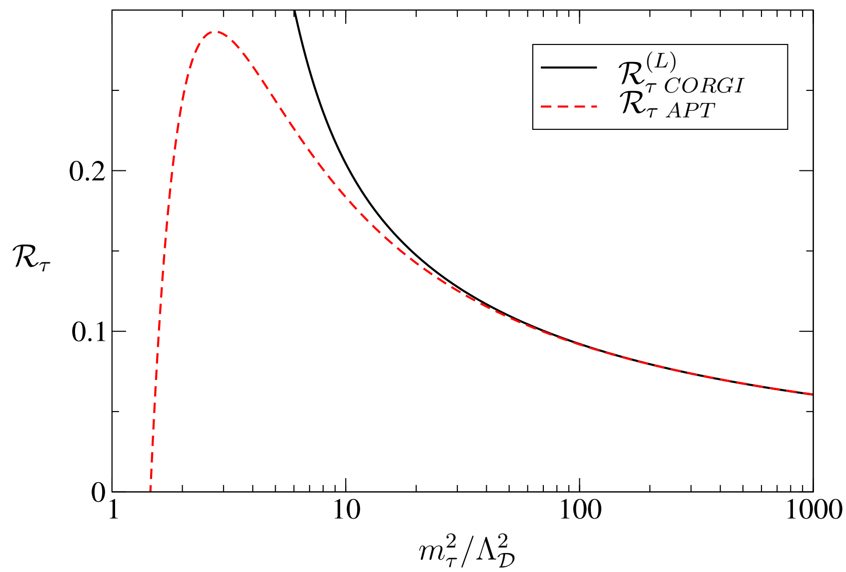

Figure 6.8: Comparison of fixed-order and all-orders calculations for $\mathcal{R}_\tau$.

or calculating the two semi-circular contours separately will lead to a negligible difference to the circular contour but will cause a massive difference to the result for $\mathcal{R}_\tau$.

In this case, in defining the Borel integral we are forced to use the principal value prescription used by [36, 46, 65] to deal with the renormalons. This prescription will not give a result that is finite for all values of m_τ; however, it will allow a comparison with the series using the $A_{m,n}$.

The choice of beta function in Eq.(6.28) will still lead to a CORGI series for $\mathcal{D}_{PT}$. In this case instead of zero the scheme-dependent parameters will be set to the scheme invariants $r_1 = 0$, $c_n = c^n$. The coupling will be obtained from the new beta function and the X_n will be replaced by different scheme invariants $\tilde{X}_n$ which are still obtained from Eq.(2.50) with $r_1 = 0$, $c_n = c^n$ instead of $r_1 = 0$, $c_n = 0$.

In figure 6.8 the all-orders calculation $\mathcal{R}^{(L)}_{\tau\ CORGI}$ and $\mathcal{R}_{\tau\ APT}$ are compared, where

$$\mathcal{R}_{\tau\ APT} = A_1(m_\tau^2) + \tilde{X}_2 A_3(m_\tau^2) + \sum_{m=1,3,4} \left(A_{m,1}(m_\tau^2) + \tilde{X}_2 A_{m,3}(m_\tau^2) \right) \ . \quad (6.38)$$

The $A_{m,n}(m_\tau^2)$ are those of Eq.(6.34).

The all-orders leading-b result has been calculated with the same procedure as was used for $\mathcal{R}$ but with a principal-value prescription for the IR renormalons.

From figure 6.8 it is possible to calculate the strength of the QCD coupling. Using [70] to provide the value of R_τ one finds

$$R_\tau = \frac{1 - B(\tau^- \to \nu_\tau e^- \bar{\nu}_e) - B(\tau^- \to \nu_\tau \mu^- \bar{\nu}_\mu)}{B(\tau^- \to \nu_\tau e^- \bar{\nu}_e)} = 3.6314 \pm 0.0193 \;, \quad (6.39)$$

where B represents the branching ratio for a decay channel. Using electroweak theory at leading order gives the QCD part to be $\mathcal{R}_\tau = 0.1944 \pm 0.0077$. For the fixed-order result $m_\tau^2/\Lambda_{\mathcal{D}}^2 = 8.658^{+0.916}_{-0.786}$, and for the all-orders result $m_\tau^2/\Lambda_{\mathcal{D}}^2 = 10.915^{+0.850}_{-0.720}$

From [70] $m_\tau = 1776.99^{+0.29}_{-0.26}$MeV. This value can be used to obtain the standard definition of the QCD Λ parameter for three flavours of quark using Eqs.(2.31,2.42). For the fixed-order result $\Lambda_{\overline{MS}}^{N_f=3} = 382^{+18}_{-20}$ MeV, and for the all-orders result $\Lambda_{\overline{MS}}^{N_f=3} = 340^{+12}_{-13}$ MeV.

6.5 Summary

The ratio of the hadronic decay to semi-leptonic decay rate for the tau lepton, $\mathcal{R}_\tau$, can be related to the Adler D-function through a similar relation as is used for the R-ratio. Again at one-loop order the θ integral of Eq.(4.18) is used. This time, however, there is an added complication: terms of the form $e^{im\theta}$ mean that the pole in the θ-plane has a non-zero asymptotically free residue. The functions that then make up the series for $\mathcal{R}_\tau$ are not exactly defined by the integral as, there is an ambiguity resulting from the pole's residue.

To solve this apparent ambiguity the Borel integral is used to resum the series in the coupling that makes up the θ integral. This series is convergent for a sufficiently small coupling, and the Borel integral returns the series for the integral. This then can be used to identify the correct choice of integration path for the θ integral.

For the more realistic two-loop case an ambiguity again arises when the integral for $\mathcal{R}_\tau$ is calculated. By taking the second beta function coefficient to zero, one can equate the one-loop function that corresponds to the Borel resummation to the equivalent two-loop expression. The two-loop function that is the resummation of the integral's sub-series is then identified.

In both the one-loop and two-loop cases the function that corresponds to the Borel integral changes for a low enough value of m_τ^2; the relevant function in the limit where $m_\tau^2 \to 0$ is IR finite.

With the two-loop $A_{m,n}$ determined it is possible to obtain a result using CORGI. The fixed-order and the all-orders Borel resummation results for $\mathcal{R}_{PT}$ can be compared.

The QCD contribution $\mathcal{R}_\tau$ can be related to the physical ratio itself (R_τ) to obtain a value for the QCD parameter $\Lambda_{\mathcal{D}}$ in terms of the mass m_τ, giving the parameter $\Lambda_{\overline{MS}}$.

Chapter 7

Conclusions

The work presented in this thesis attempts to make sense of a couple of problems that arise when one tries to relate an experimentally measurable quantity to a perturbation series when using the theory of QCD. These problems are the Landau pole that appears in the coupling, and factorial growth of the coefficients of the QCD perturbation series.

In chapter 1 the theory of QCD was introduced, and the method with which to obtain a perturbation series that would predict the likelihood of some physical process occurring was outlined. The perturbation series is a power expansion in the QCD coupling with the series coefficients obtained from the QCD Feynman rules.

Chapter 2 introduced the problem that the calculations required for the higher-order parts of a perturbation series appear to contain infinities. The method of renormalisation to remove these was introduced, and this in turn led to the scale dependence of a QCD coupling, leading to the first problem addressed in this thesis. The scale dependence of a QCD perturbation series is such that at very high energies QCD effects vanish (asymptotic freedom) but at a low enough energy scale there is an apparent Landau singularity in the coupling, and hence the perturbation series.

Chapter 3 introduced the further problem that QCD perturbation series have zero radii of convergence due to the factorial growth of the series coefficients. The series, although divergent, may be asymptotic to some function of the coupling. The standard approach of Borel summation is demonstrated on various examples; this technique evaluates a perturbation series in terms of the Borel integral acting upon the Borel transform. In QFT the poles in the Borel plane of integration known as renormalons are present, with those arising from the infrared part of a loop integral shown to give ambiguous results for the Borel integral. The cancellation of the infrared renormalon ambiguities with unknown OPE non-perturbative ambiguities is assumed, leading to a well defined QCD prediction.

The expansion in the leading-b approximation is introduced; the factorial divergence obtained from this approximation is known in the V-scheme, and the renormalon structure for the Adler D-function is known in the leading-b approximation.

If a method is introduced that solves the problem of the Landau pole arising from scale dependence, then this solution will still have to deal with the factorial growth of the series coefficients.

The ratio of hadron to muon production from electron positron annihilation R has a QCD perturbation series. This series can be related using the optical theorem to the perturbation series for the Adler D-function D. These two perturbation series are related through a dispersion integral in the complex energy plane. If each part of the QCD series for D is transformed in order to obtain the QCD part of R, one will have a power series in the coupling that is convergent for a small enough coupling. Such a series is then equated with a function which will evaluate the series through analytical continuation for all values of the coupling, and give a finite result for all energy values. A series for R is then obtained in terms of these functions and the perturbative coefficients of D. Such a series is given for the one-loop and two-loop coupling.

These new functions multiplied by the series coefficients for D make up the perturbation series for R, this new series for R is then finite for all energies, and in fact all but the first term will vanish in the infrared limit, leaving a result that smoothly approaches a constant value in terms of the first beta function coefficient $2/b$ as the physical scale goes to zero. As this is shown to happen for a two-loop coupling, a 't Hooft renormalisation scheme is shown to give a finite full perturbation series for R.

It should be noted that there exist non-perturbative corrections to the perturbation series and so the $2/b$ result does not apply to the full QCD quantity.

The series of finite terms still has the factorially growing coefficients which give the series a zero radius of convergence. A method of finding what the series is asymptotic to is then still required. The Borel integral, if it is to be used to evaluate the series at all energies, must be considered in the low energy limit.

As the energy is reduced we saw that the Borel integral will inevitably become divergent when the real part of the coupling becomes negative. We referred to this as the "Landau divergence" and showed that the energy at which this occurs is scheme independent. Below this energy we needed to switch to the alternative Borel representation of Eq.(4.42) which is valid for when the real part of the coupling is negative.

A Borel integral can be applied to the factorially growing part of D for all energies The modified form still has renormalons, only now the ultraviolet renormalons are the cause of ambiguities from the Borel integral for the perturbation series. The non-perturbative operator product expansion can, for a toy model, be shown to become a power series in terms that match the form of the ultraviolet renormalon ambiguity from the modified Borel transform. Again it is assumed that such ambiguities cancel to give a well defined quantity. Using these two forms for the Borel integral and the OPE, each part separately can remain well-defined for all energies.

Now that the leading-b Adler D-function is well defined for all energies one can evaluate the leading-b part of the R-ratio. The results for factorial growth from the known leading-b approximation were shown to give a small correction to the NNLO calculation for R.

For a comparison with experimental data there is the added complication of unknown non-perturbative effects. The contribution from these can be disregarded if a smearing procedure is used. A good agreement was found between low energy $R_{e^+e^-}$ data and theoretical prediction when both had been smeared. In addition an inverse transform was used to obtain the Adler D-function was used, again returning good agreement between data and theory.

The hadronic branching fraction of the τ lepton is also a quantity that can be related to the Adler D-function in a way similar to R. One again can try to obtain a finite series by transforming individual parts of the perturbation series for D. However, this time infrared finiteness is not immediately obvious due to ambiguous terms that demonstrate the asymptotic freedom expected of QCD, but become infinite in the infrared limit.

The ambiguity is resolved by relating the functions that will make up the new series to the Borel integral of their sub-series in the coupling. This is then used to find the function that the sub-series will converge to for a small enough coupling. Having made the choice for the hadronic branching fraction, the strength of the QCD coupling given by the Λ-parameter can be calculated in a ratio with the τ mass. The standard $\Lambda_{\overline{MS}}$ has then been calculated for three flavours of quark to be 382^{+18}_{-20} MeV from the fixed-order NNLO calculation and 340^{+12}_{-13} MeV from the all-orders calculation.

Bibliography

[1] M.E. Peskin and D.V. Schroeder, *An Introduction to Quantum Field Theory*, Perseus Books, (1995) ;
T. Muta *Foundations of Quantum Chromodynamics* (Second Edition), World Scientific, (1998).

[2] F. Halzen and A.D. Martin, *Quarks and Leptons*, John Wiley and Sons, (1984).

[3] H .Lehmann, K. Symanzik and W. Zimmermann, Nuovo. Cim. **1** (1955) 205.

[4] R.P. Feynman, Rev. Mod. Phys. **20** (1948) 367.

[5] L.D. Faddeev and V.N. Popov, Phys. Lett **25B** (1967) 29.

[6] K.G. Wilson, Phys. Rev **179** (1969) 1499.

[7] B. Naroska, Phys. Rept **148** (1987) 67.

[8] R.K. Ellis, W.J. Stirling and B.R. Webber, *QCD and Collider Physics*, Cambridge University Press, (1996).

[9] G. 't Hooft, and M. Veltman, Nucl. Phys. **B44** (1972) 189.

[10] G. 't Hooft, Nucl. Phys. **B61** (1973) 455.

[11] G. 't Hooft, Nucl. Phys. **B33** (1971) 173.

[12] E. C. G. Stuckelberg and A. Petermann, Helv. Phys. Acta. **26** (1953) 499.

[13] D.R.T. Jones, Nucl. Phys **B75** (1974) 537;
W.E. Caswell Phys. Lett. **33** (1974) 244.

[14] O.V. Tarasov, A.A. Vladimirov and A.Y. Zharkov, Phys. Lett. **93B** (1980) 429;
S.A. Larin and J.A.M. Vermaseren, Phys. Lett. **B303** (1993) 334;
S.A. Larin, T. Van Ritbergen and J.A.M Vermaseren, Phys. Lett. **B400** (1997) 379.

[15] P.M. Stevenson, Phys. Rev. **D23** (1981) 2916.

[16] A.J. Buras, E.G. Floratos, D.A. Ross and C.T. Sachrajda, Nucl. Phys. **B131** (1977) 308;
W.A. Bardeen, A.J. Buras, D.W.Duke and T.Muta, Phys. Rev. **D18** (1978) 3998.

[17] P.M. Stevenson, Ann. Phys. **152** (1981) 383;
D.T. Barclay, M.T. Reader and C.J. Maxwell, Phys. Rev **D49** (1994) 3480;

[18] S.J. Burby and C.J. Maxwell, Nucl. Phys. **B609** (2001) 193.

[19] G. Grunberg, Phys. Lett. **B95** (1980) 70.

[20] G. Grunberg, Phys. Rev. **D29** (1984) 2315.

[21] C.J. Maxwell and A. Mirjalili, Nucl. Phys. **B577** (2000) 209.

[22] M. Beneke, Phys. Rep. **317** (1999) 1.

[23] F. Dyson, Phys. Rev. **85** (1952) 631.

[24] F. David, Nucl. Phys. **B234** (1984) 237; *ibid* **B263** (1986) 637.

[25] M. Beneke, V.M. Braun and N. Kivel, Phys. Lett. **B443** (1998) 308.

[26] G. Parisi, Nucl. Phys. **B150** (1979) 163.

[27] A.H. Mueller, Nucl. Phys. **B250** (1985) 327.

[28] B. Lautrup, Phys. Lett. **69B** (1977) 109.

[29] G. 't Hooft, "Can we make sense out of Quantum Chromodynamics?", Proceedings of the Erice Summer School (1977) 943.

[30] M. Neubert, Phys. Rev. **D51** (1995) 5924.

[31] A. Denner, S. Dittmaier and G. Weiglein, Phys. Lett. **B333** (1994) 420;
S. Hashimoto, J. Kodaira, Y. Yashui and K. Sasaki, Phys. Rev. **D50** (1994) 7066;
J. Papavassiliou, Phys. Rev. **D51** (1995) 856.

[32] M. Beneke, Nucl. Phys. **B405** (1993) 424.

[33] D.J. Broadhurst, Z. Phys. **C58** (1993) 339.

[34] D.J. Broadhurst and A.L. Kataev, Phys. Lett. **B315** (1979) 179.

[35] S.J. Brodsky, G.P. Lepage and P.B. Mackenzie, Phys. Rev. **D28** (1983) 228.

[36] C.N. Lovett-Turner and C.J. Maxwell, Nucl. Phys. **B452** (1995) 188.

[37] I.I. Balitsky, Phys. Lett. **B273** (1991) 282.

[38] G. Grunberg, Phys. Lett. **B325** (1994) 441.

[39] L.R. Surguladze and M.A. Samuel, Phys. Rev. Lett. **66**, (1990) 560;
S.G. Gorishny, A.L. Kataev and S.A. Larin, Phys. Lett. **B259** (1991) 144.

[40] H. Jones and I.L. Solovtsov, Phys. Lett **B349** (1995) 519.

[41] D.V. Shirkov and I.L. Solovtsov, Phys. Rev. Lett **79** (1977) 1209;
K.A. Milton, I.L. Solovtsov and O.P. Solovtsova, Phys. Rev. **D65** (2002) 076009;
K.A. Milton, I.L. Solovtsov and O.P. Solovtsova, Eur. Phys. J. **C13** (2000) 497.

[42] D.A. Shirkov and I. Solovtsov, hep-ph/9906495; published in "Proceedings of the International Workshop on e^+e^- collisions", Eds. G. Fedotovich and S. Redin, Novosibirsk 2000, pp. 122-124.

[43] For a review see: M. Beneke and V.M. Braun, hep-ph/0010208, published in "The Boris Ioffe Festschrift- At the Frontier of Particle Physics/Handbook of QCD", edited by M. Shifman (World Scientific, Singapore, 2001).

[44] E.C. Poggio, H.R. Quinn and S. Weinberg, Phys. Rev. D**13** (1976) 1958.

[45] For a review of the APT approach see : D.V. Shirkov, Eur. Phys.**J.22** (2001) 331.

[46] C.J. Maxwell and A. Mirjalili, Nucl. Phys. **B611** (2001) 423.

[47] B.A. Magradze, “The QCD coupling up to third order in standard and analytic perturbation theories.”, hep-ph/0010070; D.S. Kourashev and B.A. Magradze, “Explicit expressions for Euclidean and Minkowskian observables in analytic perturbation theory” hep-ph/0104142 (to appear in Theor. Math. Phys.).

[48] A.C. Mattingly and P.M. Stevenson, Phys. Rev. D**49** (1994) 437.

[49] J. Chyla, A. Kataev and S. Larin, Phys. Lett. **B267** (1991) 269.

[50] A.A. Pivovarov, Sov. J. Nucl. Phys. **54** (1991) 676; A.A. Pivovarov, Z. Phys. C**53** (1992) 461.

[51] F. Le Diberder and A. Pich, Phys. Lett. **B289** (1992) 165.

[52] D.M. Howe and C.J. Maxwell, Phys. Lett. **B541**, 129 (2002).

[53] G ’t Hooft, in Deeper Pathways in High Energy Physics, proceedings of Orbis Scientiae, 1977, Coral Gables, Florida, edited by A. Perlmutter and L.F. Scott (Plenum, New York, 1977).

[54] E. Gardi, G. Grunberg and M. Karliner, JHEP **07** (1998) 007.

[55] R.M. Corless, G.H. Gonnet, D.E.G Hare, D.J. Jeffrey and D.E. Knuth, “On the Lambert *W* function”, Advances in Computational Mathematics **5** (1996) 329, available from `http://www.apmaths.uwo.ca/~djeffrey/offprints.html.`

[56] A.J. Buras, E.G. Floratos, D.A. Ross and C.T. Sachrajda, Nucl. Phys. **B131** (1977) 308.

[57] D.J. Braodhurst and A.G. Grozin, Phys. Rev. **D52** (1995) 4082.

[58] M. Beneke and V.M. Braun, Phys. Lett. **B348** (1995) 513.

[59] P. Ball, M. Beneke and V.M. Braun, Nucl. Phys. **B452** (1995) 563.

[60] Stanley J. Brodsky, Einan Gardi, Georges Grunberg and Johann Rathsman, hep-ph/0002065.

[61] S. Peris and E. de Rafael, Nucl. Phys. **B500** (1997) 325.

[62] Handbook of Mathematical Functions, eds. Milton Abramowitz and Irene A. Stegan, Section 5.1, p228. (ninth edition) Dover (1964).

[63] M. Beneke, V.M. Braun and N. Kivel, Phys. Lett. **B404** (1997) 315.

[64] C.J. Maxwell and D.G. Tonge, Nucl. Phys. **B481** (1996) 681.

[65] C.J. Maxwell and D.G. Tonge, Nucl. Phys. **B535** (1998) 19.

[66] A.V. Nesterenko, hep-ph/9912351 v2.

[67] P.M. Brooks and C.J. Maxwell (in preparation).

[68] K.A. Milton, I.L. Solovtsov and O.P. Solovtsova, Phys. Rev. **D60** (1999) 016001;
K.A. Milton, I.L. Solovtsov and O.P. Solovtsova, Phys. Lett. **B439** (1998) 421.

[69] E. Gardi and M. Karliner, Nucl. Phys. **B529** (1998) 383.

[70] S. Eidelman *et al*, Phys. Lett **B592** (2004) 1.

[71] Particle Data Group: K. Hagiwara et al, Phys. Rev. **D66** (2002) 010001.

[72] A.D. Martin, J. Outhwaite and M.G. Ryskin, Eur. Phys. J. **C19** (2001) 681

[73] $\gamma\gamma 2$ Collaboration: C. Bacci et al., Phys. Lett. **B86** (1979) 234.

[74] MEA Collaboration: B. Esposito et al., Lett. Nuovo Cim. **30** (1981) 65.

[75] BES Collaboration: J.Z. Bai et al., Phys. Rev. Lett. **88** (2002) 101802.

[76] MARK I Collaboration: J.Siegrist et al., Phys. Rev. **D26** (1982) 969.

[77] Crystal Ball Collaboration: C.Edwards et al., SLAC-PUB-5160, Jan 1990.

[78] MD-1 Collaboration: A.E. Blinov et al., Z. Phys. **C70** (1996) 31.

[79] CLEO Collaboration: R. Ammar et al., Phys. Rev. **D57** (1998) 1350.

[80] OLYA, CMD Collaboration: L.M. Barkov et al., Nucl. Phys. **B256** (1985) 365;
CMD2 Collaboration: R.R. Akhmetshin et al., hep-ex/9904027;
DM2 Collaboration: D. Bisello et al. Phys. Lett. **B220** (1989) 321;
ND Collaboration: S.I. Dolinsky et al., Phys. Rept. **202** (1991) 99;
CMD2 Collaboration: R.R. Akhmetshin et al., Phys. Lett. **B466** (1999) 392;
DM1 Collaboration: A. Cordier et al., Phys. Lett. **B81** (1979) 389;
CMD Collaboration: L.M. Barkov et al., Sov. J. Nucl. Phys. **47** (1988) 248;
DM2 Collaboration: A. Antonelli et al., Phys. Lett. **B212** (1988) 133;
OLYA Collaboration: P.M. Ivanov et al., Phys. Lett. **B107** (1981) 297;
DM2 Collaboration: D. Bisello et al., Z. Phys. **C39** (1988) 13;
DM2 Collaboration: A. Antonelli et al., Z. Phys. **C56** (1992) 15;
DM1 Collaboration: A. Cordier et al., Nucl. Phys. **B172** (1980) 13;
SND Collaboration: M.N. Achasov et al., Phys. Rev. **D66** (2002) 032001;
G. Cosme et al., Phys. Lett. **B48** (1974) 159.

[81] S.Eidelman, F. Jegerlehner, A.L.Kataev, O. Veretin, Phys. Lett. **B454** (1999) 369.

[82] A.N. Sissakian and I.L.Solovtsov, Phys. Lett. **A157** (1991) 261;
A.N. Sissakian and I.L.Solovtsov, Phys. Part. Nucl. **25** (1994) 478;
A.N. Sissakian, I.L.Solovtsov and O. Yu Shevchenko, Int. Mod. Phys. **A9** (1994) (1929).

[83] K.A. Milton, I.L. Solovtsov and O.P. Solovtsova, Eur. Phys. J. **C13** (2000) 497.

[84] E. Braaten and C.S. Liu, Phys. Rev. **D42** (1990) 3888.

[85] W.J. Marciano and A. Sirlin, Phys. Rev. Lett. **56** (1986) 22;
W.J. Marciano and A. Sirlin, Phys. Rev. Lett. **61** (1988) 1815.

[86] ALEPH collaboration, Eur. Phys. J. **C4** (1998) 409.

[87] K. Schilcher and M.D. Tran, Phys. Rev. **D29** (1984) 570.